

Non-Abelian Anyons and Non-Abelian Vortices in Topological Superconductors

Yusuke Masaki^{a,b}, Takeshi Mizushima^{c,*} and Muneto Nitta^{b,d,e,*}

^aDepartment of Physics, Tohoku University, Sendai, Miyagi 980-8578, Japan

^bResearch and Education Center for Natural Sciences, Keio University, Hiyoshi 4-1-1, Yokohama, Kanagawa 223-8521, Japan

^cDepartment of Materials Engineering Science, Osaka University, Toyonaka, Osaka 560-8531, Japan

^dDepartment of Physics, Keio University, Hiyoshi 4-1-1, Japan

^eInternational Institute for Sustainability with Knotted Chiral Meta Matter (SKCM²), Hiroshima University, Kagamiyama 1-3-2, Higashi-Hiroshima, Hiroshima 739-8511, Japan

ARTICLE INFO

Keywords:

Non-Abelian vortices, non-Abelian anyons, non-Abelian statistics, topological quantum computation, topological materials, topological superconductors, topological superfluids, superfluid ³He, spinor Bose-Einstein condensates, nematic liquid crystals, chiral liquid crystals, quark matter, nuclear matter, nuclear superfluids

ABSTRACT

Anyons are particles obeying statistics of neither bosons nor fermions. Non-Abelian anyons, whose exchanges are described by a non-Abelian group acting on a set of wave functions, are attracting a great attention because of possible applications to topological quantum computations. Braiding of non-Abelian anyons corresponds to quantum computations. The simplest non-Abelian anyons are Ising anyons which can be realized by Majorana fermions hosted by vortices or edges of topological superconductors, $\nu = 5/2$ quantum Hall states, spin liquids, and dense quark matter. While Ising anyons are insufficient for universal quantum computations, Fibonacci anyons present in $\nu = 12/5$ quantum Hall states can be used for universal quantum computations. Yang-Lee anyons are non-unitary counterparts of Fibonacci anyons. Another possibility of non-Abelian anyons (of bosonic origin) is given by vortex anyons, which are constructed from non-Abelian vortices supported by a non-Abelian first homotopy group, relevant for certain nematic liquid crystals, superfluid ³He, spinor Bose-Einstein condensates, and high density quark matter. Finally, there is a unique system admitting two types of non-Abelian anyons, Majorana fermions (Ising anyons) and non-Abelian vortex anyons. That is ³P₂ superfluids (spin-triplet, *p*-wave pairing of neutrons), expected to exist in neutron star interiors as the largest topological quantum matter in our universe.

Key points/objectives

- Unlike fermions and bosons, the exchange of non-Abelian anyons is described by unitary transformations that operate on topologically protected degenerate ground states. The adiabatic exchanges of two or more non-Abelian anyons manipulate quantum information stored in a set of degenerate ground states, leading to topological quantum computations.
- The simplest non-Abelian anyons are Ising anyons which are predicted to exist as Majorana zero modes in topological superconductors, fractional quantum Hall states, Kitaev materials, and dense quark matter.
- Another non-Abelian anyons are vortex anyons, which are constructed from non-Abelian vortices supported by a non-Abelian first homotopy group. Such vortex anyons exist in liquid crystals, superfluid ³He, spinor Bose-Einstein condensates, and high density quark matter.
- ³P₂ superfluids, which are expected to be realized in neutron stars, provide unique systems simultaneously admitting two kinds of non-Abelian anyons, i.e., Ising anyons and vortex anyons.

1. Introduction

In three spatial dimensions, all particles are either bosons or fermions in quantum physics, that is, a wave function of multi-particle states is symmetric (antisymmetric) under the exchanges of two bosons (fermions). On contrary, in two spatial dimensions, there exist exotic particles classified to neither bosons nor fermions, *anyons*. A wave function of two anyons receives a nontrivial phase factor under their exchanges Leinaas & Myrheim (1977), Wilczek (1982). Such exotic particles play essential roles in fractional quantum Hall states Halperin (1984), Arovas et al. (1984), and have been experimentally observed for $\nu = 1/3$ fractional quantum Hall states Bartolomei et al. (2020), Nakamura et al. (2020).

Recently, yet exotic particles attracted great attention, that is, *non-Abelian anyons*. Non-Abelian anyons are described by a set of multiple wave functions, and the exchanges of two non-Abelian anyons lead to unitary matrix operations on a set of wave functions. They have been theoretically predicted to exist in $\nu = 5/2$ fractional quantum Hall states Moore & Read (1991), Nayak & Wilczek (1996), topological superconductors (SCs) and superfluids (SFs) Read & Green (2000), Ivanov (2001), Kitaev (2001), and spin liquids Kitaev (2006), Motome & Nasu (2020), and experimental observation is pursued. Non-Abelian anyons are attracting significant interests owing to the possibility to offer a platform of topologically protected quantum computations realized by braiding of non-Abelian anyons Kitaev (2003), Kitaev & Laumann (2008), Nayak

*Corresponding author

mizushima@mp.es.osaka-u.ac.jp (T. Mizushima);

nitta@phys-h.keio.ac.jp (M. Nitta)

ORCID(s): 0000-0001-6891-7008 (Y. Masaki); 0000-0002-7313-6094 (T. Mizushima); 0000-0002-3851-9305 (M. Nitta)

et al. (2008), Pachos (2012), Sarma et al. (2015), Field & Simula (2018). Since the Hilbert space and braiding operations are topologically protected, they are robust against noises in contrast to the conventional quantum computation methods. Recently, it has been reported that non-Abelian braiding and fusions has been experimentally realised in a superconducting quantum processor, where the fusion and braiding protocols are implemented using a quantum circuit on a superconducting quantum processor Andersen et al. (2022), thereby opening a significant step to realize topological quantum computations.

One of the main routes to realize non-Abelian anyons is based on Majorana fermions in topological SCs Ivanov (2001), Kitaev (2001), Alicea (2012), Leijnse & Flensberg (2012), Beenakker (2013), Silaev & Volovik (2014), Elliott & Franz (2015), Sato & Fujimoto (2016), Mizushima et al. (2016), Sato & Ando (2017), Beenakker (2020), Marra (2022). Majorana fermions were originally proposed in high energy physics to explain neutrinos; they are particles that coincide with their own anti-particles Majorana (1937). In condensed matter physics, Majorana fermions are localized at vortices or edge of materials for which several protocols of non-Abelian braiding were proposed. Non-Abelian anyons constructed from Majorana fermions are so-called Ising anyons. They are not enough for universal quantum computations, and thus some non-topological process should be included Nayak et al. (2008). In contrast, another type of anyons called Fibonacci anyons Trebst et al. (2008) can offer a promising platform for universal topological quantum computation that all quantum gates are implemented by braiding manipulation in a topologically protected way Preskill (2004), Bonesteel et al. (2005), Hormozi et al. (2007). Such Fibonacci anyons are proposed to exist in $\nu = 12/5$ quantum Hall states, a junction made of a conventional SC and a $\nu = 2/3$ fractional quantum Hall state Mong et al. (2014), interacting Majorana fermions realized in a septuple-layer structure of topological SCs Hu & Kane (2018), and Rydberg atoms in a lattice Lesanovsky & Katsura (2012). Yang-Lee anyons are also proposed as non-unitary counterparts of Fibonacci anyons, obeying nonunitary non-Abelian statistics Ardonne et al. (2011), Freedman et al. (2012), Sanno et al. (2022).

The aforementioned anyons are all quasiparticle excitations composed of fermions. On the other hand, a different type of non-Abelian anyons can be composed of bosons in certain ordered states accompanied with symmetry breakings $G \rightarrow H$. They are called non-Abelian vortex anyons, whose exchange statistics are non-Abelian due to non-Abelian vortices, that is quantum vortices supported by a non-Abelian first homotopy (fundamental) group of order parameter manifolds, $\pi_1(G/H)$ Bais (1980), Wilczek & Wu (1990), Bucher (1991), Brekke et al. (1993), Lo & Preskill (1993), Lee (1994), Brekke et al. (1997).¹ Such non-Abelian

vortices exist in liquid crystals Poenaru & Toulouse (1977), Volovik & Mineev (1977), Mermin (1979), Lavrentovich & Kleman (2001), ³He SFs Balachandran et al. (1984), Salomaa & Volovik (1987), Volovik (2003), spinor Bose-Einstein condensates (BECs) Semenoff & Zhou (2007), Kobayashi et al. (2009, 2012), Borgh & Ruostekoski (2016), and high density quark (QCD) matter Fujimoto & Nitta (2021a,b,c), Eto & Nitta (2021). Non-Abelian braiding of vortex anyons in spinor BECs and its application to quantum computations were proposed Mawson et al. (2019).

In addition to these systems admitting one type of non-Abelian anyons, there is the unique system simultaneously admitting two kinds of non-Abelian anyons, Ising anyons based on Majorana fermions and non-Abelian vortex anyons. It is a ³P₂ SF, spin-triplet and *p*-wave pairing with the total angular momentum two Hoffberg et al. (1970), Tamagaki (1970), Takatsuka & Tamagaki (1971), Takatsuka (1972), Richardson (1972). Such ³P₂ SFs are expected to be realized by neutrons, relevant for neutron star interiors Sedrakian & Clark (2018). ³P₂ SFs are the largest topological SFs in our universe Mizushima et al. (2017) and admit non-Abelian vortices Masuda & Nitta (2020). Non-Abelian vortices host Majorana fermions in their cores Masaki et al. (2022), thus behaving as non-Abelian anyons.

The purpose of this article is to summarise these non-Abelian anyons of various types. After introducing basics of non-Abelian anyons in Sec. 2, we describe non-Abelian anyons in fermionic and bosonic systems, based on Majorana fermions and non-Abelian first homotopy group in Secs.3 and 4, respectively. In Sec. 5, we introduce ³P₂ SFs as the unique system simultaneously admitting two kinds of non-Abelian anyons. We summarize this article in Sec. 6

2. Non-Abelian anyons

2.1. Braid group and quantum statistics

Here we consider pointlike topological defects (e.g., vortices in two-dimensional *spinless* SCs) which behave as identical particles in a two-dimensional plane. The exchange of *n* particles in three or higher dimension is described by the symmetric group S_n Leinaas & Myrheim (1977). There are two one-dimensional representations of S_n , ± 1 , due to even/odd permutation and $+1$ (-1) corresponds the Bose (Fermi) statistics. Two dimension is special and the exchange of particles is given by the braid group B_n Wu (1984). The braid of particles is expressed as a set of operators T_k ($1 \leq k \leq n-1$) that exchange the neighboring *k*th and (*k* + 1)th particles in an anticlockwise direction. The operators obey the relations (see Fig. 1)

$$T_i T_j T_i = T_j T_i T_j, \quad \text{for } |i - j| = 1, \quad (1)$$

$$T_i T_j = T_j T_i, \quad \text{for } |i - j| \geq 2. \quad (2)$$

¹Hanany & Tong (2003), Auzzi et al. (2003), Eto et al. (2006), Shifman & Yung (2007), Eto et al. (2014). In condensed matter physics, vortices with Majorana fermions in their cores are also sometimes called non-Abelian vortices (because they are non-Abelian anyons). In this article, the term “non-Abelian” on vortices is used only for vortices with non-Abelian first homotopy group π_1 .

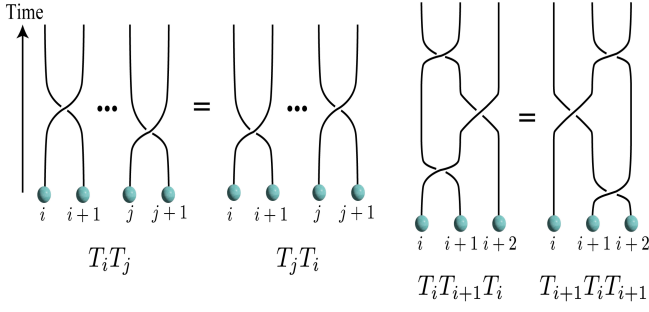


Figure 1: Schematic of the braid relations in Eqs. (1) and (2): $T_i T_j = T_j T_i$ for $|i - j| \geq 2$ (left) and $T_i T_j T_i = T_j T_i T_j$ for $|i - j| = 1$ (right).

The exotic statistics of particles represented by the braid group stems from the relation $T_i^{-1} \neq T_i$. In the one dimensional representation, the generator of T_i is given by a phase factor that a wave function under the exchange of particles acquires, $\tau_j \equiv \tau(T_j) = e^{i\theta_j}$ ($0 \leq \theta_j < 2\pi$). The relation in Eq. (1) implies that the exchange operation of any two particles induces the same phase factor $\tau_1 = \tau_2 = \dots = \tau_{n-1} = e^{i\theta}$. The phase factor characterizes the quantum statistics of particles Wu (1984), and the absence of the relation $T_i^2 = 1$ allows for the fractional (anyon) statistics with neither $\theta = 0$ (bosons) nor $\theta = \pi$ (fermions). In addition to the one-dimensional representation, the braid group has non-Abelian representations. In Sec. 3, we will show that the generators of the braid of Majorana zero modes are noncommutative as $[\tau_i, \tau_j] \neq 0$ for $|i - j| = 1$ and the pointlike defects hosting Majorana modes behave as non-Abelian anyons.

Although the braid group is trivial in three dimensions, a three-dimensional model with pointlike topological defects which host Majorana modes and obey the non-Abelian statistics has been proposed Teo & Kane (2010a). The non-Abelian statistics of the defects, which behave as hedgehogs, can be interpreted as the projective ribbon permutation statistics Freedman, Hastings, Nayak, Qi, Walker & Wang (2011), Freedman, Hastings, Nayak & Qi (2011). Such non-Abelian statistics enables to construct three-dimensional networks of topological superconducting wires supporting Majorana modes.

2.2. Non-Abelian anyons

In three spatial dimensions, the statistics of particles is determined by their intrinsic spins. According to the spin statistics theorem, all particles with integer (half-integer) spin are bosons (fermions). A pair formed by two fermions with the spin $1/2$ behaves as a boson, and the spin of the composite particle obeys the ‘‘fusion rule’’ $\frac{1}{2} \otimes \frac{1}{2} = 0 \oplus 1$, where 0 and 1 denote the spin singlet and triplet states, respectively. When particles are trapped in a two dimensional plane, however, there is another possibility that is neither fermions nor bosons, i.e., anyons. In general, anyons can be characterized by the topological charge, the fusion rule (N_{ab}^c), the associative law (the F -matrix), and the braiding operation (the R -matrix) Preskill (2004), Nayak

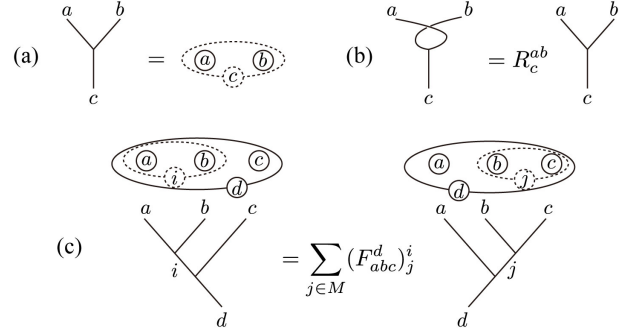


Figure 2: (a) Diagram of the fusion of two anyons a and b to an anyon c . Diagrammatic expressions of the R -matrix (b) and the F -matrix (c).

et al. (2008), Pachos (2012).

Let $\mathbf{1}$ and $\{a, b, \dots\}$ be the vacuum and the different species of particles, respectively. Consider the anyon model spanned by $M = \{\mathbf{1}, a, b, \dots\}$ and bring two anyons a and b together. The fused particle also belongs to M . The fusion rule is represented by

$$a \otimes b = \sum_{c \in M} N_{ab}^c c, \quad (3)$$

where fusion coefficients N_{ab}^c are non-negative integers. Figure 2(a) shows the diagrammatic expression of the fusion of two anyons with topological charges a and b to an anyon with charge c . When N_{ab}^c is not zero for only one value of c , the fusion of paired a and b anyons is uniquely determined and the anyon is called the Abelian anyon. The non-Abelian anyons are characterized by two or more coefficients that satisfy $N_{ab}^c \neq 0$. In the context of quantum computation, the fusion rule determines the Hilbert space that encodes quantum information, and quantum computation is implemented by the braiding manipulation of non-Abelian anyons in a topologically protected way. Figure 2(b) shows the diagrammatic expression of the R -matrix. When one anyon moves around the other, the pairwise anyons acquire a phase. As mentioned below, the R -matrix describes a phase resulting from the exchange of anyons a and b which fuse to a anyon c . Let us also consider the fusion of three anyons a , b , and c into an anyon d . The outcome of the fusion process is independent of order in which the anyons are to be fused. This implies that the fusion process obeys the associative law, $(a \otimes b) \otimes c = a \otimes (b \otimes c)$, which is characterized by the F -matrix. The F matrix represents the transformation between different fusion bases or the choice of order of fusion, which is expressed as shown in Fig. 2(c). The R -matrix and the F -matrix are the building-blocks for constructing the braid group in multiple anyon systems Preskill (2004).

Ising anyons. An example of the non-Abelian anyons is the Ising anyon Kitaev (2006), Nayak et al. (2008), Pachos (2012). The Ising anyon model consists of the vacuum $\mathbf{1}$, Ising anyons σ , and Dirac (complex) fermions ψ , which obey the fusion rules

$$\sigma \otimes \sigma = \mathbf{1} \oplus \psi, \quad \sigma \otimes \psi = \sigma, \quad \psi \otimes \psi = \mathbf{1}, \quad \mathbf{1} \otimes x = x, \quad (4)$$

where $x \in \{\mathbf{1}, \sigma, \psi\}$. Consider three Ising anyons, where the two left-most anyons fusing into either $\mathbf{1}$ or ψ (see Fig. 2(c) with $(a, b, c) \rightarrow \sigma$ and $i, j = \{\mathbf{1}, \psi\}$). The R -matrix and the F -matrix are given, respectively, by

$$R = \begin{pmatrix} R_1^{\sigma\sigma} & 0 \\ 0 & R_\psi^{\sigma\sigma} \end{pmatrix} = e^{-i\pi/8} \begin{pmatrix} 1 & 0 \\ 0 & i \end{pmatrix}, \quad (5)$$

$$F_{\sigma\sigma\sigma}^\sigma = \frac{1}{\sqrt{2}} \begin{pmatrix} 1 & 1 \\ 1 & -1 \end{pmatrix}. \quad (6)$$

The diagonal components of the R -matrix are the phases resulting from the counterclockwise exchange of two left-most Ising anyons (σ) fusing to $\mathbf{1}$ or ψ , while the twice exchange operation of two right-most Ising anyons is represented by the unitary matrix, $F^{-1}R^2F = e^{-i\pi/4}\sigma_x$. Hence, braiding two anyons corresponds to the implementation of the quantum gates acting on the quantum states spanned by $\mathbf{1}$ and ψ .

In general, the anyons are described by conformal field theory, corresponding to gapless edge states residing in the boundary of two-dimensional gapped topological phases. For Ising anyons, the theory is the conformal field theory with the central charge $c = 1/2$, which describes critical Ising models such as the two-dimensional Ising model at the point of second-order phase transition Di Francesco et al. (1997).

The Moore-Read state in the fractional quantum Hall state at the filling factor $\nu = 5/2$ supports this type of non-Abelian anyons Nayak et al. (2008). The Ising anyons can also be realized in the Kitaev's honeycomb model, which is an exactly solvable model of quantum spin liquid states Kitaev (2006). In this model, the spins are fractionalized to Majorana fermions coupled to \mathbb{Z}_2 gauge fields. The Ising anyons appear as Majorana zero modes bound to the \mathbb{Z}_2 flux. Materials including $4d$ or $5d$ atoms with a strong spin-orbit coupling have been proposed as candidates of Kitaev magnets, and the half-integer thermal Hall effect was reported in α -RuCl₃ Kasahara et al. (2018), Yamashita et al. (2020), Yokoi et al. (2021), Bruin et al. (2022), which is a signature of Majorana fermions in the chiral quantum spin liquid phase Vinkler-Aviv & Rosch (2018), Ye et al. (2018). Apart from materials, Google team reported the demonstration of fusion and braiding rules of non-Abelian Ising anyons on a superconducting quantum processor, where the fusion and braiding protocols are implemented using a quantum circuit on a superconducting quantum processor Andersen et al. (2022). Another platform to realize Ising anyons is a topological SC. In the context of topological SCs, the Ising anyons (σ) appear as Majorana zero modes bound at their boundaries or topological defects, such as the surface, interface, and vortices Read & Green (2000), Kitaev (2001), Nayak et al. (2008), Alicea (2012), Sato & Fujimoto (2016), Mizushima et al. (2016). Pairwise Majorana zero modes form a complex fermion that can define either the unoccupied state ($\mathbf{1}$) or the occupied state (ψ) of the zero energy eigenstate, implying $\sigma \otimes \sigma = \mathbf{1} \oplus \psi$. The vacuum $\mathbf{1}$ corresponds to a condensate of Cooper pairs, while ψ represents a Bogoliubov quasiparticle which can pair into a condensate,

i.e., $\psi \otimes \psi = \mathbf{1}$. The detailed properties and realization of Majorana zero modes in topological SCs are described in Secs. 3.1 and 3.2.

Fibonacci anyons. Another example is the Fibonacci anyons Trebst et al. (2008). The Fibonacci anyon model consists of the vacuum $\mathbf{1}$ and the non-trivial anyon τ , which obey the fusion rules

$$\tau \otimes \tau = \mathbf{1} \oplus \tau, \quad \mathbf{1} \otimes x = x, \quad (7)$$

where $x = \mathbf{1}, \tau$. The first rule implies that the fusion of two anyons may result in either annihilation or creation of a new anyon, and thus the Fibonacci anyon may be its own anti-particle. Repeated fusions of the $n + 1$ τ -anyons result in either the vacuum or the τ anyon as $\tau \otimes \tau \otimes \dots \otimes \tau = a_n \cdot \mathbf{1} \oplus b_n \tau$, where $a_n = 1$ for $n = 2$ and $a_n = n - 2$ for $n \geq 3$. The coefficient b_n grows as the Fibonacci series, and the first few values in the sequence are $b_2 = 1, b_3 = 2, b_4 = 3, b_5 = 5, \dots$. The R -matrix and the F -matrix are given, respectively, by

$$R = \begin{pmatrix} R_1^{\tau\tau} & 0 \\ 0 & R_\tau^{\tau\tau} \end{pmatrix} = \begin{pmatrix} e^{i4\pi/5} & 0 \\ 0 & -e^{i2\pi/5} \end{pmatrix}, \quad (8)$$

$$F_{\tau\tau\tau}^\tau = \begin{pmatrix} \phi^{-1} & \phi^{-1/2} \\ \phi^{-1/2} & -\phi^{-1} \end{pmatrix}, \quad (9)$$

where $\phi = (1 + \sqrt{5})/2$ is the golden ratio. The Fibonacci anyons are described by the level-1 G_2 Wess-Zumino-Witten theory with the central charge $c = 14/5$ Mong et al. (2014), where G_2 is the simplest exceptional Lie group. While Ising anyons are not sufficient for universal quantum computation, the Fibonacci anyon systems can offer a promising platform for universal topological quantum computation that all quantum gates are implemented by braiding manipulation in a topologically protected way Preskill (2004), Bonesteel et al. (2005), Hormozi et al. (2007).

The existence of the Fibonacci anyons is predicted in the $\nu = 12/5$ fractional quantum Hall state that is described by the Read-Rezayi state Read & Rezayi (1999). It is also proposed that a junction made of a conventional SC and the $\nu = 2/3$ fractional quantum Hall state supports the Fibonacci anyons Mong et al. (2014). Fibonacci anyons can also be made from interacting Majorana fermions realized in a septuple-layer structure of topological SCs Hu & Kane (2018) and from Rydberg atoms in a lattice Lesanovsky & Katsura (2012).

Yang-Lee anyons. There are nonunitary counterparts of Fibonacci anyons, which are referred to as Yang-Lee anyons. The conformal field theory corresponding to Yang-Lee anyons is nonunitary and Galois conjugate to the Fibonacci conformal field theory Ardonne et al. (2011), Freedman et al. (2012). Because of nonunitarity, the central charge and the scaling dimension for the one nontrivial primary field are negative, $c = -22/5$ and $\Delta = -2/5$, respectively. As shown in Eq. (9), the F -matrix for Fibonacci anyons is given by the golden ratio ϕ , i.e., one solution of the equation $x^2 = 1 + x$, which is an algebraic analogue of the fusion rule. The F -matrix for Yang-Lee anyons is

obtained from Eq. (9) by replacing $\phi \rightarrow -1/\phi$ as

$$F_{\tau\tau\tau}^\tau = \begin{pmatrix} -\phi & i\sqrt{\phi} \\ i\sqrt{\phi} & \phi \end{pmatrix}, \quad (10)$$

as $-1/\phi$ is the other solution of the equation $x^2 = 1 + x$. In Eq. (10), the bases of the F -matrix are spanned by the vacuum state $\mathbf{1}$ and a Yang-Lee anyon τ . The R -matrix are given by

$$R = \begin{pmatrix} R_1^{\tau\tau} & 0 \\ 0 & R_\tau^{\tau\tau} \end{pmatrix} = \begin{pmatrix} e^{i2\pi/5} & 0 \\ 0 & e^{i\pi/5} \end{pmatrix}. \quad (11)$$

Unlike the Fibonacci anyons, braiding two Yang-Lee anyons is represented by a combination of the R -matrix and the nonunitary matrix, $F^{-1}RF$. While Yang-Lee anyons obey the same fusion rule as that of Fibonacci anyons given by Eq. (7), the F -matrix in Eq. (10) is the nonunitary and the Yang-Lee anyons obey the nonunitary non-Abelian statistics.

The nonunitary conformal field theory with $c = -22/5$ describes the nonunitary critical phenomenon known as the Yang-Lee edge singularity Cardy (1985). Let us consider the Ising model with an imaginary magnetic field ih ($h \in \mathbb{R}$). For temperatures above the critical temperature, the zeros of the partition function in the thermodynamic limit, which are referred to as the Lee-Yang zeros, accumulate on the line $h > h_c$ and the edge of the Lee-Yang zeros corresponds to the critical point h_c Lee & Yang (1952). As $h (> h_c)$ approaches the edge, the density of zeros has a power-law behavior as $|h - h_c|^\sigma$, which characterizes the critical phenomenon Kortman & Griffiths (1971), Fisher (1978). For instance, the magnetization exhibits singular behavior with the same critical exponent σ . The Yang-Lee edge singularity is also realized by the quantum Ising model with a real transverse field and a pure-imaginary longitudinal field von Gehlen (1991).

The quantum Ising model with an imaginary longitudinal field, which supports the Yang-Lee anyons, can be constructed from Majorana zero modes in a network of topological superconducting wires coupled with dissipative electron baths Sanno et al. (2022). The Majorana modes bound at the end points of one-dimensional topological SCs constitute spin 1/2 operators. A coupling of Majorana zero modes with electrons in a metallic substrate plays an role of the pure-imaginary longitudinal field, while the tunneling of Majorana zero modes between neighboring superconducting wires induces a transverse magnetic field. Schemes for the fusion, measurement, and braiding of Yang-Lee anyons are also proposed in Ref. Sanno et al. (2022). As mentioned above, the Yang-Lee anyons obey the nonunitary non-Abelian statistics. The nonunitary evolution of quantum states has been discussed in connection with measurement-based quantum computation Terashima & Ueda (2005), Usher et al. (2017), Piroli & Cirac (2020), Zheng (2021). Although the Yang-Lee anyons with the nonunitary F -matrix are not suitable for application to unitary quantum computation, they can be the building-blocks for the construction of measurement-based quantum

computation. In addition, as the nonunitary quantum gates can be implemented by braiding manipulations, the Yang-Lee anyon systems may offer a quantum simulator for nonunitary time evolution of open quantum systems in a controllable way.

Vortex anyons. In this article, we also discuss non-Abelian anyons made of bosonic (topological) excitations in ordered states. The nontrivial structure of the order parameter manifold appears in the liquid crystals, spin-2 BECs, the A phase of SF ^3He , dense QCD matter, and 3P_2 SFs. The line defects in such ordered systems, such as vortices, are represented by non-Abelian first homotopy group and their topological charges are noncommutative. Such topological defects with noncommutative topological charges behave as non-Abelian anyons, called the non-Abelian vortex anyons. In Sec. 4, we demonstrate that order parameter manifolds in nematic liquid crystals and spin-2 BECs admit the existence of non-Abelian vortices and show the fusion rules of such non-Abelian vortex anyons.

3. Non-Abelian anyons in topological SCs

3.1. Majorana zero modes as Ising anyons

Majorana zero modes. An elementary excitation from superconducting ground states is a Bogoliubov quasiparticle that is a superposition of the electron and hole. The quasiparticle excitations are described by the Bogoliubov-de Gennes (BdG) Hamiltonian

$$H = \sum_{ij} (\psi_i^\dagger, \psi_i) \mathcal{H}_{ij} \begin{pmatrix} \psi_j \\ \psi_j^\dagger \end{pmatrix}, \quad (12)$$

$$\mathcal{H}_{ij} = \begin{pmatrix} h_{ij} & \Delta_{ij} \\ \Delta_{ij}^\dagger & -h_{ij}^* \end{pmatrix}. \quad (13)$$

Here, ψ_j is the N -component vector of the electron field operator and \mathcal{H} is the $2N \times 2N$ hermitian matrix, where N is the sum of the spin degrees of freedom and the number of the lattice sites and so on. The $N \times N$ hermitian matrix h describes the normal state Hamiltonian and the superconducting pair potential Δ obeys $\Delta^\dagger = -\Delta$ because of the Fermi statistics, where a^\dagger denotes the transpose of a matrix a . The BdG Hamiltonian naturally holds the particle-hole symmetry

$$CHC^{-1} = -H, \quad (14)$$

where the particle-hole operator $C = \Theta K$ is an antiunitary operator composed of the unitary operator Θ and the complex conjugation operator K . The self-conjugate Dirac fermions are called Majorana fermions, where the quantized field $\Psi \equiv (\psi, \psi^\dagger)^\dagger$ obeys

$$\Psi = C\Psi, \quad C^2 = +1. \quad (15)$$

We expand the quantized field Ψ in terms of the energy eigenstates. The energy eigenstates are obtained from the BdG equation,

$$\sum_j \mathcal{H}_{ij}(\varphi_E)_j = E(\varphi_E)_i, \quad (16)$$

which describes the quasiparticle with the energy E and the wave function φ_E . Equation (14) guarantees that the quasiparticle state with $E > 0$ and φ_E is accompanied by the negative energy state with $-E$ and $\varphi_{-E} = C\varphi_E$. Thus, the negative energy states are redundant as long as the particle-hole symmetry is maintained. Let η_E be the quasiparticle operator which satisfies the anticommutation relations, $\{\eta_E, \eta_{E'}^\dagger\} = \delta_{E,E'}$ and $\{\eta_E, \eta_{E'}\} = \{\eta_E^\dagger, \eta_{E'}^\dagger\} = 0$ ($E, E' > 0$). The self-charge conjugation relation (15) then implies that the quasiparticle annihilation operator with a positive energy is equivalent to the creation with a negative energy as $\eta_E = \eta_{-E}^\dagger$, and Ψ is expanded only in terms of positive energy states as $\Psi(\mathbf{r}) = \sum_{E>0} [\varphi_E \eta_E + C\varphi_E \eta_E^\dagger]$. The condition (15) can be fulfilled by odd-parity SCs. In the absence of spin-orbit coupling, the spin-singlet pair potential is always invariant under the spin rotation, and the particle-hole exchange operator is given by $C^2 = -1$ in each spin sector. Hence, spin-singlet SCs cannot satisfy Eq. (15). Spin-orbit coupling, however, enables even spin singlet SCs to host Majorana fermions Sato & Ando (2017), Alicea (2012), Sato & Fujimoto (2016).

Now, let us suppose that a single zero-energy state exists, and φ_0 is its wave function. Then, we can rewrite the quantized field to

$$\Psi = \varphi_0 \gamma + \sum_{E>0} \left[\varphi_E \eta_E + C\varphi_E \eta_E^\dagger \right]. \quad (17)$$

We have introduced γ , instead of $\eta_{E=0}$, to distinguish the zero mode from other energy eigenstates. Owing to Eq. (14), the zero-energy quasiparticle is composed of equal contributions from the particle-like and hole-like components of quasiparticles, i.e., $C\varphi_0 = \varphi_0$. The self-conjugate constraint in Eq. (15) imposes the following relations:

$$\gamma^\dagger = \gamma, \quad (18)$$

and $(\gamma)^2 = 1$ and $\{\gamma, \eta_{E>0}\} = \{\gamma, \eta_{E>0}^\dagger\} = 0$. The quasiparticle obeying this relation is called the Majorana zero mode. The zero energy states appear in a topological defect of topological SCs, such as chiral SCs. In Fig. 3(a), we show the spectrum of Andreev bound states bound at a vortex in a chiral SC, where the level spacing between the zero mode and the lowest excitation state is $\Delta E \sim \Delta_0^2/\varepsilon_F$ Kopnin & Salomaa (1991), Volovik (1999), Read & Green (2000), Matsumoto & Heeb (2001). In many vortices, the hybridization between neighboring Majorana modes gives rise to the formation of the band structure with the width $\Delta E_M \sim e^{-D/\xi}$ Cheng et al. (2009), Mizushima & Machida (2010), where D and ξ is the mean distance of neighboring vortices and superconducting coherence length, respectively (see Fig. 3(b)).

The Majorana zero modes exhibit the non-Abelian anyonic behaviors Ivanov (2001). To clarify this, we start with two Majorana zero modes residing in a SC. Using two Majorana operators, γ^1 and γ^2 , we define the new fermion operators c and c^\dagger as

$$c = \frac{1}{2}(\gamma^1 + i\gamma^2), \quad c^\dagger = \frac{1}{2}(\gamma^1 - i\gamma^2), \quad (19)$$

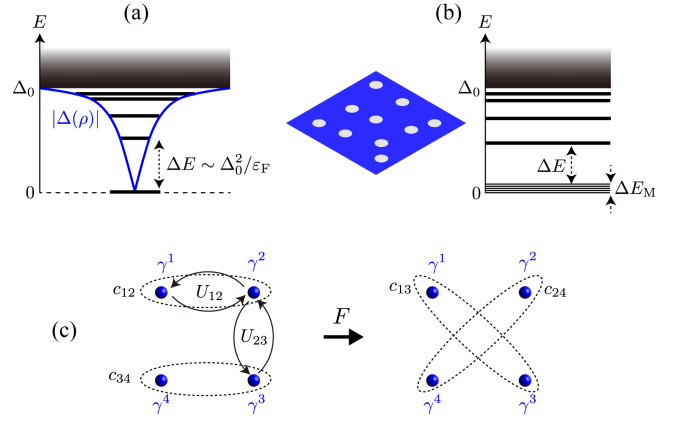


Figure 3: Schematic of the quasiparticle states bound at a single vortex (a) and energy spectrum of many vortices (b) in a *spinless* SC, where the level spacing of vortex bound states is $\Delta E \sim \Delta_0^2/\varepsilon_F$ and ΔE_M denotes the band width of Majorana states bound at each core. (c) Operations of the braiding matrices U_{12} and U_{23} and the F -matrix in four Majorana modes.

which obey the anticommutation relations, $\{c, c^\dagger\} = 1$ and $\{c, c\} = \{c^\dagger, c^\dagger\} = 0$. The two degenerate ground states are defined as the vacuum $|0\rangle$ and the occupied state of the zero energy state $|1\rangle = c^\dagger|0\rangle$, respectively, where the former (latter) state is the even (odd) fermion parity. We note that as the BdG Hamiltonian for superconducting states is generally commutable with the parity operator, the fermion parity remains as a good quantum number. For the even (odd) parity sector, the Hilbert space is spanned by using $|0\rangle$ ($|1\rangle$) and excited states that are constructed as $\eta_E^\dagger \eta_{E'}^\dagger \eta_{E''}^\dagger \cdots |0\rangle$ ($\eta_E^\dagger \eta_{E'}^\dagger \eta_{E''}^\dagger \cdots |1\rangle$). The Majorana operators, γ^1 , γ^2 , and $i\gamma^1\gamma^2$, act on the Hilbert space as the Pauli matrices σ_x , σ_y , and σ_z , respectively. The eigenstates of the Majorana operators γ^1 and γ^2 are given by the superposition of the degenerate states with different fermion parity, $|0\rangle$ and $|1\rangle$. Hence, the eigenstate of a single Majorana zero mode cannot be a physical state.

Consider $2N$ Majorana zero modes denoted by γ^j ($j = 1, \dots, 2N$), where N complex fermions are constructed by the fusion of i th and j th Majorana zero modes as $c_{ij} = (\gamma^i + i\gamma^j)/2$. We define the occupation number operator of the complex fermion,

$$n_{ij} \equiv c_{ij}^\dagger c_{ij} = \frac{1}{2}(1 + i\gamma^i\gamma^j). \quad (20)$$

In a basis that diagonalizes paired Majorana modes $i\gamma^i\gamma^j$, two eigenvalues of the complex fermion, $n_{ij} = 0$ and 1 , correspond to the fusion channels $\mathbf{1}$ and ψ , respectively. Hence, the Majorana zero mode is referred to as the Ising anyon. 2^N degenerate ground states are expressed in terms of the occupation numbers as $|n_{12}, n_{34}, \dots\rangle$, which are separated to the sectors of the even/odd fermion parity. Here we assume that the temperature of the system is much lower than the level spacing (ΔE) between the Majorana zero mode and the lowest excitation (non-Majorana) state. Then, the 2^{N-1}

degenerate ground states in each fermion parity sector can be utilized as topological qubits, where quantum information is stored in a topologically protected way.

Braiding Majorana zero modes. Here we discuss the braiding statistics of Majorana zero modes γ^i and γ^j and show the non-Abelian statistics of Majorana zero modes Ivanov (2001), Alicea et al. (2011), Clarke et al. (2011). While we consider the exchange of Majorana zero modes residing in vortices, the theory is also applicable to Majorana zero modes bound at the end points of one-dimensional topological SCs.

Let T_{ij} be the braid operators that satisfy Eqs. (1) and (2) and transform γ^i and γ^j to $e^{\theta_i}\gamma^j$ and $e^{i\theta_j}\gamma^i$, respectively. The unitary time-evolution of Majorana zero modes is governed by the Heisenberg equation, $i\frac{d}{dt}\gamma^j(t) = [\gamma^j(t), \mathcal{H}(t)]$. The positions of two Majorana modes are adiabatically exchanged in the time interval $[0, T]$. The adiabatic condition defines the lower bound for the time scale of the braiding operation, T , so that T is much longer than the inverse of the level spacing between the Majorana zero mode and the lowest excitation (non-Majorana) state, ΔE . In addition, the upper bound is associated with the band width of Majorana modes $\Delta E_M \sim e^{-D/\xi}$ (see Fig. 3(b)), i.e., $\Delta E^{-1} \ll T \ll \Delta E_M^{-1}$. Within the adiabatic condition, the braiding dynamics of Majorana zero modes can be regarded as the unitary time evolution, $\gamma^j(t) = U_{ij}^\dagger(t)\gamma^j(0)U_{ij}(t)$. After the braiding operation, γ^i (γ^j) changes to γ^j (γ^i) with an additional phase shift. Then, the braiding operation is represented by

$$U_{ij}^\dagger\gamma^i U_{ij} = e^{i\theta_i}\gamma^j, \quad U_{ij}^\dagger\gamma^j U_{ij} = e^{i\theta_j}\gamma^i, \quad (21)$$

where $U_{ij} \equiv U_{ij}(T)$ is the unitary operator which describes the exchange operation of two Majorana zero modes γ^i and γ^j , i.e., the representation of T_{ij} . According to the conditions, $(e^{i\theta_i}\gamma^j)^2 = (U_{ij}^\dagger\gamma^i U_{ij})^2 = 1$ and $(\gamma^j)^2 = 1$, the phase shifts obey $\theta_i = n\pi$ and $\theta_j = m\pi$, where $n, m \in \mathbb{Z}$. The braiding operations must not change the parity of the occupation number defined in Eq. (20) and thus satisfy $U_{ij}^\dagger n_{ij} U_{ij} = n_{ij}$, which imposes the condition, $\theta_1 + \theta_2 = (2n + 1)\pi$, on the phase shift. As a result, the exchange operation of two Majorana zero modes obtains the following braiding rules:

$$U_{ij}^\dagger\gamma^i U_{ij} = \gamma^j, \quad U_{ij}^\dagger\gamma^j U_{ij} = -\gamma^i. \quad (22)$$

Consider four Majorana zero modes denoted by γ^1 , γ^2 , γ^3 , and γ^4 , which form two complex fermions as $c_{12} \equiv (\gamma^1 + i\gamma^2)/\sqrt{2}$ and $c_{34} \equiv (\gamma^3 + i\gamma^4)/\sqrt{2}$ (Fig. 3(c)). When the Majorana mode “3” adiabatically encircles the Majorana mode “2”, both Majorana modes operators acquire the π phase shift, $\gamma^2 \mapsto -\gamma^2$ and $\gamma^3 \mapsto -\gamma^3$, corresponding to the twice operation of Eq. (22). Therefore, the braiding operation changes the occupation numbers of the complex fermion $n_{12} \equiv c_{12}^\dagger c_{12}$ and $n_{34} \equiv c_{34}^\dagger c_{34}$. For example, the above braiding generates a pair of the complex fermions $|11\rangle$ from their vacuum $|00\rangle$. Here these two states are orthogonal, $\langle 11|00\rangle = 0$. The braiding rule can be generalized to $2N$ Majorana modes. The $2N$ Majorana modes are fused to N complex fermions, leading to the

2^{N-1} -fold degeneracy of ground states while preserving fermion parity. As discussed above, when the i th and j th Majorana modes are exchanged with each other, their operators behave as $\gamma_i \mapsto \gamma_j$ and $\gamma_j \mapsto -\gamma_i$. The representation of the braid operator T_{ij} that satisfies Eq. (22) is given in terms of the zero mode operators as Ivanov (2001)

$$U_{ij} = e^{i\theta} \exp\left(\frac{\pi}{4}\gamma_j\gamma_i\right) = e^{i\theta} \frac{1}{\sqrt{2}} (1 + \gamma_j\gamma_i). \quad (23)$$

From now on, we omit the overall Abelian phase factor $e^{i\theta}$ as it is not important for quantum computation. Equation (23) also holds in the case of the Moore-Read state Nayak & Wilczek (1996). For $N = 1$, there is only a single ground state in each sector with definite fermion parity, and the exchange of two vortices results in the global phase of the ground state by $e^{i\pi/4}$. One can easily find that for $N \geq 2$ the exchange operators U_{ij} and U_{jk} do not commute to each other, $[U_{ij}, U_{jk}] \neq 0$, implying the non-Abelian anyon statistics of the Majorana zero modes.

For four Majorana zero modes ($N = 2$), twofold degenerate ground states exist in each fermion-parity sector: $|00\rangle \equiv |\text{vac}\rangle$ and $|11\rangle = c_{12}^\dagger c_{34}^\dagger |\text{vac}\rangle$ in the sector of even fermion parity, and $|10\rangle = c_{12}^\dagger |\text{vac}\rangle$ and $|01\rangle = c_{34}^\dagger |\text{vac}\rangle$ in the sector of odd fermion parity. For the even-parity sector, the representation matrix for the exchange of $1 \leftrightarrow 2$ and $3 \leftrightarrow 4$ [Fig. 3(c)] is given by

$$U_{12} = U_{34} = e^{-i\frac{\pi}{4}} |00\rangle\langle 00| + e^{i\frac{\pi}{4}} |11\rangle\langle 11|. \quad (24)$$

This merely rotates the phase of the ground state as in the $N = 1$ case. In contrast, the representation matrix for the intervortex exchange [$2 \leftrightarrow 3$ in Fig. 3(c)] has the mixing terms of the two degenerate ground states $|00\rangle$ and $|11\rangle$,

$$U_{23} = \frac{1}{\sqrt{2}} [|00\rangle\langle 00| - i |00\rangle\langle 11| + |11\rangle\langle 11| - i |11\rangle\langle 00|]. \quad (25)$$

We note that the choice of the pairing to form the complex fermion is arbitrary. The change of the fused Majorana modes corresponds to the change of the basis from one which diagonalizes $i\gamma^1\gamma^2$ and $i\gamma^3\gamma^4$ to another which diagonalizes $i\gamma^1\gamma^3$ and $i\gamma^2\gamma^4$. The basis transformation is represented by the F -matrix as

$$F = \frac{1}{\sqrt{2}} \begin{pmatrix} 1 & 1 \\ 1 & -1 \end{pmatrix}. \quad (26)$$

The braiding matrix in Eq. (24) implies that the exchange of two Majorana zero modes fusing to ψ ($|11\rangle$) acquires an additional $\pi/2$ phase compared to the fusion channel to $\mathbb{1}$ ($|00\rangle$). Hence, Eq. (24) satisfies the property of the R -matrix in Eq. (5), i.e., $R_{\mathbb{1}}^{\psi\psi} = -iR_{\psi}^{\sigma\sigma}$.

3.2. Platforms for Majorana zero modes

The realization of non-Abelian anyons requires to freeze out the internal degrees of freedom of Majorana modes. The

simplest example is *spinless* p -wave SCs/SFs, which emerge from the low-energy part of spinful chiral p -wave SCs. To clarify this, we start with spin-triplet SCs, whose pair potential is given by a 2×2 spin matrix Leggett (1975)

$$\begin{aligned} \hat{\Delta}(\mathbf{k}) &= \begin{pmatrix} \Delta_{\uparrow\uparrow}(\mathbf{k}) & \Delta_{\uparrow\downarrow}(\mathbf{k}) \\ \Delta_{\downarrow\uparrow}(\mathbf{k}) & \Delta_{\downarrow\downarrow}(\mathbf{k}) \end{pmatrix} \\ &= i\sigma_\mu\sigma_y d_\mu(\mathbf{k}) = i\sigma_\mu\sigma_y A_{\mu i} \hat{k}_i, \end{aligned} \quad (27)$$

where $\hat{k}_i \equiv k_i/k_F$ is scaled with the Fermi momentum k_F , and the repeated Greek/Roman indices imply the sum over x, y, z . Here we omit the spin-singlet component. Owing to the Fermi statistics, the spin-triplet order parameter, $\mathbf{d}(\mathbf{k})$, obeys $\mathbf{d}(\mathbf{k}) = -\mathbf{d}(-\mathbf{k})$. For spin-triplet p -wave pairing, the most general form of the order parameter is given by a 3×3 complex matrix, $A_{\mu i} \in \mathbb{C}$, where the components are labelled by $\mu, i \in \{x, y, z\}$.

HQVs with Majorana zero modes in SF ^3He . We consider the Anderson-Brinkman-Morel (ABM) state Anderson & Morel (1961), Anderson & Brinkman (1973), as a prototypical example of chiral p -wave states hosting Majorana zero modes. The ABM state is realized in the A-phase of the SF ^3He , which appears in high pressures and high temperatures Vollhardt & Wölfle (1990), Volovik (2003). At temperatures above the SF transition temperature, $T > T_c \approx 1\text{--}2$ mK, the normal Fermi liquid ^3He maintains a high degree of symmetry

$$G = SO(3)_L \times SO(3)_S \times U(1), \quad (28)$$

where $SO(3)_L$, $SO(3)_S$, and $U(1)$ are the rotation symmetry in space, the rotational symmetry of the nuclear spin degrees of freedom, and the global gauge symmetry, respectively. The tensor $A_{\mu i}$ transforms as a vector with respect to index μ under spin rotations, and, separately, as a vector with respect to index i under orbital rotations. The order parameter of the ABM state is then given by the complex form

$$A_{\mu j} = \Delta e^{i\varphi} \hat{d}_\mu(\hat{m}_j + i\hat{n}_j). \quad (29)$$

The ABM state is the condensation of Cooper pairs with the ‘‘ferromagnetic’’ orbital, and spontaneously breaks the time-reversal symmetry. The orbital part of the order parameter is characterized by a set of three unit vectors forming the triad $(\hat{m}, \hat{n}, \hat{l})$, where $\hat{l} = \hat{m} \times \hat{n}$ denotes the orientation of the orbital angular momentum of Cooper pairs. The remaining symmetry in the ABM state is $H_A = SO(2)_{S_z} \times SO(2)_{L_z - \varphi} \times \mathbb{Z}_2$, where $SO(2)_{S_z}$ is the two-dimensional rotation symmetry in the spin space. The ABM state is also invariant under $SO(2)_{L_z - \varphi}$ which is the combined gauge-orbital symmetry, where the $U(1)$ phase rotation, $\varphi \rightarrow \varphi + \delta\varphi$, is compensated by the continuous rotation of the orbital part about \hat{l} , $\hat{m}_j + i\hat{n}_j \rightarrow e^{-i\delta\varphi}(\hat{m}'_j + i\hat{n}'_j)$. In addition, \mathbb{Z}_2 is the mod-2 discrete symmetry $(\hat{d}, \hat{m}, \hat{n}) \rightarrow (-\hat{d}, -\hat{m}, -\hat{n})$. The manifold of the order parameter degeneracy is then given by

$$R_A \simeq G/H_A \simeq S^2_S \times SO(3)_{L_z, \varphi} / \mathbb{Z}_2. \quad (30)$$

The two-sphere, S^2_S , is associated with the variation of \hat{d} . The degeneracy space has an extra \mathbb{Z}_2 symmetry that the

change from \hat{d} to $-\hat{d}$ can be compensated by the phase rotation $\varphi \rightarrow \varphi + \pi$.

The topologically stable linear defects in the ABM state are characterized by the group of the integers modulo 4 Vollhardt & Wölfle (1990), Volovik (1992), Salomaa & Volovik (1987), Volovik (2003),

$$\pi_1(R_A) \simeq \pi_1(SO(3)/\mathbb{Z}_2) \simeq \mathbb{Z}_4. \quad (31)$$

There exist four different classes of topologically protected linear defects in the dipole-free case. The four linear defects can be categorized by the fractional topological charge,

$$N_A = 0, \frac{1}{2}, 1, \frac{3}{2}, \quad (32)$$

where $N_A = 3/2$ is topologically identical to $N_A = -1/2$. The representatives of $N_A = 0$ and $N_A = 1/2$ classes include continuous vortex such as the Anderson-Toulouse vortex and half quantum vortex (HQV), respectively. Owing to $N_A = 2 = 0$, a pure phase vortex with winding number 2 is continuously deformed into a nonsingular vortex without a core, that is, the Anderson-Toulouse vortex Anderson & Toulouse (1977). The $N_A = 1/2$ vortex is a combination of the half-wound \mathbf{d} -disgyration with a half-integer value of the $U(1)$ phase winding (Fig. 4). The extra \mathbb{Z}_2 symmetry allows us to take the half-integer value of the topological charge, because the π -phase jump arising from the half-winding of the $U(1)$ phase ($\varphi = \theta/2$) can be canceled out by the change in the orientation of \hat{d} ($\hat{d} \rightarrow -\hat{d}$). The $N_A = 1$ class includes a pure phase vortex with odd winding number and the radial/tangential disgyrations without phase winding. The latter was originally introduced by de Gennes as l -textures with a singularity line De Gennes (1973), Ambegaokar et al. (1974).

The vortex with the fractional charge $N_A = 1/2$ is a harbor for spinless Majorana zero modes. We introduce the center-of-mass coordinate of Cooper pairs, $\mathbf{R} = (\rho, \theta, z)$, as $\hat{\Delta}(\mathbf{k}) \rightarrow \hat{\Delta}(\mathbf{k}, \mathbf{R})$, where $\rho = \sqrt{x^2 + y^2}$. The vortex core is located at $\rho = 0$. The vortex state is subject to the boundary condition at $\rho \rightarrow \infty$ where the orbital angular momentum of the Cooper pair is aligned to the z -axis ($\hat{l} \parallel \hat{z}$) and the $U(1)$ phase φ continuously changes from 0 to $2\pi\kappa$ along the azimuthal (θ) direction,

$$A_{\mu i}(\rho = \infty, \theta) = \Delta e^{i\kappa\theta} \hat{d}_\mu(\theta)(\hat{x}_j + i\hat{y}_j). \quad (33)$$

Owing to the spontaneous breaking of the gauge-orbital symmetry, there are two classes for the vorticity κ : Integer quantum vortices with $\kappa \in \mathbb{Z}$ and HQVs with $\kappa \in \mathbb{Z}/2$. In the HQVs, both the $U(1)$ phase and \hat{d} rotate by π about the vortex center (see Fig. 4). In general, the \hat{d} -texture for HQVs is obtained as

$$\hat{d}(\theta) = \cos(\kappa^{\text{sp}}\theta)\hat{x} + \sin(\kappa^{\text{sp}}\theta)\hat{y}, \quad (34)$$

where κ^{sp} denotes the winding of \hat{d} . The HQV is characterized by $(\kappa, \kappa^{\text{sp}}) = (1/2, \pm 1/2)$, while the integer quantum vortex has $(\kappa, \kappa^{\text{sp}}) = (1, 0)$. It is remarkable to notice that since the ABM state is the equal spin pairing state, the order

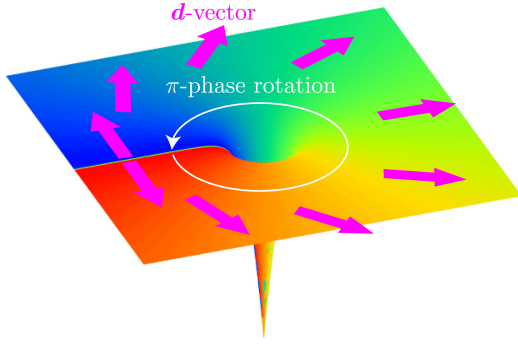


Figure 4: Schematic of the HQV realized in the ABM state. The color map shows the $U(1)$ phase winding from $\varphi = 0$ (red) at θ to π (blue) at $\theta = 2\pi$, and the arrows represent the texture of the $\hat{\mathbf{d}}$ -vectors shown in Eq. (34) with $\kappa^{\text{SP}} = 1/2$.

parameter for the HQV is recast into the representation in the spin basis as

$$\hat{\Delta} = \Delta \left[e^{i(\kappa - \kappa^{\text{SP}})\theta} |\uparrow\uparrow\rangle + e^{i(\kappa + \kappa^{\text{SP}})\theta} |\downarrow\downarrow\rangle \right]. \quad (35)$$

For the HQV with $(\kappa, \kappa^{\text{SP}}) = (1/2, 1/2)$ the $|\uparrow\uparrow\rangle$ Cooper pair possesses the spatially uniform phase, while the $|\downarrow\downarrow\rangle$ pair has the phase winding of 2π around the vortex as in a conventional singly quantized vortex. Thus, the vortex-free state in the \uparrow spin sector exhibits fully gapped quasiparticle excitations, while the low-lying structures in half quantum vortex are effectively describable with a singly quantized vortex in the \downarrow spin sector, i.e., the spin-polarized chiral p -wave SC. An odd-vorticity vortex in the spin-polarized chiral system hosts a single *spinless* Majorana zero mode that obeys non-Abelian statistics. The existence of non-Abelian anyonic zero modes in half quantum vortices was first revealed by Ivanov, who developed the non-Abelian braiding statistics of vortices with spinless Majorana zero modes Ivanov (2001).

In the bulk A-phase of the SF ^3He , an obstacle to realizing the HQVs is the formation of continuous vortices with the $\hat{\mathbf{l}}$ -texture, which are characterized by the topological charge $N = 0$. As the orientation of the $\hat{\mathbf{l}}$ -vector is associated with the orbital motion of the Cooper pair, the $\hat{\mathbf{l}}$ -texture can be uniformly aligned in a parallel plate geometry with thickness D . The motion of Cooper pairs is confined in the two-dimensional plane and $\hat{\mathbf{l}}$ is locked perpendicular to the plates. Applying a magnetic field further restricts the orientation of $\hat{\mathbf{d}}$ to the two-dimensional plane perpendicular to the applied field, which is a favorable situation to stabilize the HQVs. In the parallel plate geometry with $D = 12.5 \mu\text{m}$, the measurements of NMR frequency shift observed that the $\hat{\mathbf{d}}$ -vectors are confined to the two-dimensional plane perpendicular to $\hat{\mathbf{l}}$ Yamashita et al. (2008). The experiment was performed in a rotating cryostat at ISSP, University of Tokyo. The parallel plates are rotated at the angular velocity $\lesssim 12\text{rad/s}$ but no conclusive evidence of HQVs was observed Yamashita et al. (2008). Although

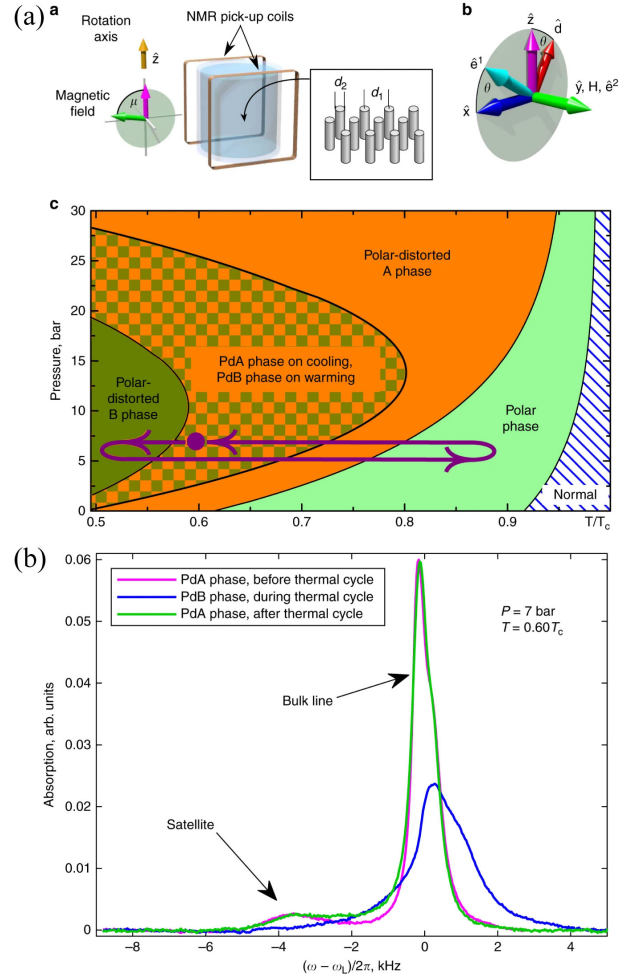


Figure 5: (a) The experimental setup and the phase diagram in the liquid ^3He with nematic disorders and (b) NMR spectra at pressure $P = 7 \text{ bar}$ and $T = 0.60T_c$ in the presence of a magnetic field perpendicular to the anisotropy direction of nematic disorders Mäkinen et al. (2019), where T_c is the critical temperature of the bulk SF ^3He without disorders. The disorders consist of nearly parallel Al_2O_3 strands, where the diameter and mean distance are $d_2 \approx 8 \text{ nm}$ and $d_1 \approx 50 \text{ nm}$, respectively. In (b), the main peaks with green and magenta colors correspond to the signal of the bulk PdA phase, while the satellite peaks originate from the spin excitation bound to the $\hat{\mathbf{d}}$ -solitons connecting pairs of HQVs. The satellite peak remains unchanged after the thermal cycling illustrated by purple arrows in (a). Both figures are taken from Ref. Mäkinen et al. (2019).

the SF ^3He -A thin film provides an ideal platform for HQVs with Majorana zero modes, the realization of HQVs remains as a challenging task. We also note that point-like solitons in a superfluid ^3He film, such as spin disclinations, were shown to behave as anyons with fractional charges Volovik & Yakovenko (1989).

Another promising route to realize HQVs with Majorana zero modes is to artificially introduce well-controlled disorders with high-porosity aerogel. In particular, the polar phase was observed in anisotropic aerogels consisting

of uniaxially ordered alumina strands, called the nematic aerogels Dmitriev et al. (2015), Halperin (2019) [See Fig. 5(a)]. The order parameter of the polar phase is given by $A_{\mu i} = \Delta e^{i\varphi} \hat{d}_\mu \hat{z}_i$, where the orbital state of the Cooper pair (\hat{z}_i) is confined by the uniaxially anisotropic disorders. As in the ABM state in the bulk ^3He , the texture of the \hat{d} -vector concomitant with the half-integer vorticity can realize HQVs in the polar phase. In the polar phase, HQVs are energetically preferable to integer quantum vortices at zero magnetic fields and magnetic fields applied along the uniaxial anisotropy Nagamura & Ikeda (2018), Mineev (2014), Regan et al. (2021). Indeed, the HQVs were experimentally observed in nematic aerogels under rotation Autti et al. (2016). The HQVs were also created by temperature quench via the Kibble-Zurek mechanism Rysti et al. (2021). As shown in Fig. 5(a), the superfluid phase diagram in nematic aerogels is drastically changed from that of the bulk ^3He without disorders, where the polar-distorted A and B (PdA and PdB) phases are stabilized in addition to the polar phase. The NMR measurements performed in Ref. Mäkinen et al. (2019) observed that the HQVs survive across the phase transition to the PdA phase. As shown in Fig. 4, the HQV is accompanied by the \hat{d} -soliton in which the \hat{d} orientation rotates. Figure 5(b) shows the observed NMR spectra which have satellite peaks in addition to the main peak around the Larmor frequency. The main peak is a signal of the bulk PdA phase. The satellite peak originates from the spin excitation localized at the \hat{d} -solitons connecting pairs of HQVs. The order parameter of the PdA phase is given by $A_{\mu i} = \Delta e^{i\varphi} \hat{d}_\mu (\hat{m} + i\varepsilon \hat{n})_i$, where \hat{m} is aligned along the axis of nematic aerogels and $\varepsilon \in (0, 1)$ is the temperature- and pressure-dependent parameter on the distortion of Eq. (29) by nematic aerogels. Although the HQVs in the polar phase host no Majorana zero modes, the low energy structure of the HQVs in the PdA phase is essentially same as that of HQVs in the ABM state and each core may support the existence of *spinless* Majorana zero modes Mäkinen et al. (2019), Mäkinen et al. (2022). Hence, the survival of the HQVs in the PdA phase is important as a potential platform for topological quantum computation. The elucidation of the nature of the fermionic excitations bound to the HQVs remains as a future problem.

HQVs in SCs. In contrast to the SF ^3He , it is difficult to stabilize HQVs in SCs. The difficulty is attributed to the fact that the mass (charge) current is screened exponentially in the length scale of the penetration depth λ , while such a screening effect is absent in the spin current Chung et al. (2007). The HQV is accompanied by the spin current in addition to the mass current, while in the integer quantum vortex, the integer vorticity ($\kappa \in \mathbb{Z}$) and uniform \hat{d} -texture in Eq. (33) induce no spin current. Therefore, the absence of the screening effect on the spin current is unfavorable for the stability of the HQVs relative to the integer quantum vortices, where the later may host spin-degenerate Majorana zero modes. It has also been proposed that configurational entropy at finite temperatures drives the fractionalization of the integer quantum vortices into pairwise HQVs Chung &

Kivelson (2010). However, no firm experimental evidence for HQVs has been reported in SCs.

Superconducting nanowires. Here we briefly mention recent progress on the search of Majorana zero modes bound at the end points of superconducting nanowires, although we mainly focus on non-Abelian anyons emergent in vortices in this article.

The first idea was proposed by Kitaev that a spinless one-dimensional SC is a platform to host a Majorana zero mode Kitaev (2001). Although it was initially thought to be a toy model, it was recognized that a system with the same topological properties can be realized by a semiconductor/SC heterostructure Alicea (2012), Sato & Ando (2017). The key ingredients are a semiconductor nanowire and a large Zeeman magnetic field in addition to the proximitized superconducting gap Δ Sato et al. (2009, 2010). Consider the Hamiltonian of the semiconductor nanowire under a magnetic field B , $h(p) = p^2/2m - \mu + \lambda p\sigma_y - B\sigma_z$, which appears in the diagonal part of Eq. (13), where m is the mass of an electron and λ is the strength of the spin-orbit coupling. The spin-orbit coupling is not only a source of nontrivial topology, but is also necessary to realize spinless electronic systems together with the large Zeeman field ($B > \mu$). In fact, if the proximitized superconducting gap is taken into account, a combination of spin-orbit coupling with the superconducting gap induces topological odd-parity superconductivity. The topological phase with the spinless Majorana zero mode appears in the higher magnetic field satisfying $B > B_c = \sqrt{\Delta^2 + \mu^2}$.

A direct signature of Majorana zero mode is the quantization of a zero-bias peak in differential conductance, where the height of the zero-bias peak stemming from the Majorana zero mode is predicted to be quantized to the universal conductance value of $2e^2/h$ at zero temperature Akhmerov et al. (2011), Fulga et al. (2011). Consider a charge-transfer process through a normal metal-SC junction. When an electron with the incident energy E enters from the normal metal to the SC, it forms the Cooper pair with an electron in the Fermi sea at the interface and a hole is created in the normal side as a consequence of momentum conservation. Such a process in which electrons are retroreflected as holes is called Andreev reflection. Let $\phi_E^{\text{in,out}} = [u_E, v_E]^t$ be the two-component wavefunctions of the incident and reflected particles, respectively, where u_E (v_E) accounts for the electron (hole) component. We now consider the scattering problem $\phi_E^{\text{out}}(\mathbf{x}) = S(E)\phi_E^{\text{in}}(\mathbf{x})$. The S -matrix is defined in the particle-hole space as

$$S(E) = \begin{pmatrix} r^{\text{ee}}(E) & r^{\text{eh}}(E) \\ r^{\text{he}}(E) & r^{\text{hh}}(E) \end{pmatrix}, \quad (36)$$

which is a unitary matrix $S \in U(2)$. The coefficient r^{ee} ($r^{\text{eh}}(E)$) is the amplitude of the normal (Andreev) reflection, and the others are the reflection coefficients of incident holes.

The conductance $G(E)$ at the normal/SC interface is obtained with the conductance quantum $G_0 = e^2/h$ per spin as $G(E) = 2G_0|r^{\text{eh}}(E)|^2$. The particle-hole symmetry imposes on the S matrix the constraint, $CS(E)C^{-1} = S(-E)$,

leading to $\det S(0) = |r^{\text{ec}}(0)|^2 - |r^{\text{eh}}(0)|^2$ at $E = 0$. Let V be the unitary matrix defined by $V\phi_0 = (\text{Re}u, \text{Im}u)$. In this basis, the scattering matrix $S(0)$ is transformed as $S'(0) = VS(0)V^\dagger$, where $S'(0) \in O(2)$ is an orthogonal matrix satisfying $S'^\dagger = S'^{-1} = S'^{\text{tr}}$ and $\det S(0) = \det S'(0) = \pm 1$. Hence, there are two different processes, a perfect normal reflection process ($\det S(0) = +1$) and a perfect Andreev reflection process ($\det S(0) = -1$). This discrete value, $\det S(0) = \pm 1$, is a topological invariant representing the parity of the number of Majorana zero modes residing at the interface. When $\det S(0) = -1$, there exists at least one Majorana zero mode, which involves the perfect Andreev reflection process and the quantized conductance,

$$G(0) = \frac{2e^2}{h}. \quad (37)$$

The analytical expression of the conductance is obtained by solving the BdG equation and quasiclassical Usadel equation at a interface of the normal metal and unconventional SCs (e.g., p - and d -wave SCs) Tanaka & Kashiwaya (1995), Kashiwaya & Tanaka (2000), Tanaka et al. (2004, 2005), where the the conductance per spin reaches $2e^2/h$. The quantized conductance is also related to the Atiyah-Singer index when the Hamiltonian holds the chiral symmetry Ikegaya et al. (2016).

The conductance has recently been measured in a junction system of InSb-Al hybrid semiconductor-SC nanowire devices. The differential conductance yields the plateau behavior where the peak height reaches values $2e^3/h$ Zhang et al. (2021). In the device used in the experiment, the tunnel barrier is controlled by applying a gate voltage to the narrow region between the electrode and the region where the proximity effect occurs in the semiconductor wire. In the vicinity of the barrier, the unintentionally formed quantum dot or nonuniform potential formed in the vicinity of the interface gives rise to the formation of nearly zero-energy Andreev bound states. Such Andreev bound states mimic the plateau of $G(0) = 2e^2/h$ even in the topologically trivial region of the magnetic field ($B < B_c$) Liu et al. (2017), Prada et al. (2020), Cayao & Bursset (2021), Yu et al. (2021), Valentini et al. (2021). From the plateau of $G(0)$, it is not possible to identify whether the observed $G(0) \sim 2e^2/h$ is due to Majorana zero mode or the effect of accidentally formed s bound states. Alternative experimental schemes to distinguish the trivial and topological bound states have been proposed Liu et al. (2018), Ricco et al. (2019), Yavilberg et al. (2019), Awoga et al. (2019), Zhang & Spånslätt (2020), Schulenburg & Flensberg (2020), Pan et al. (2021), Liu et al. (2021), Ricco et al. (2021), Thamm & Rosenow (2021), Chen et al. (2022), Sugeta et al. (2022).

Vortices in Fe(Se,Te). The iron-based SC Fe(Se,Te) is a candidate of topologically nontrivial superconducting state supporting Majorana zero modes. In the parent material FeSe, the $3d$ electrons of Fe near the Fermi level mainly contribute to superconductivity, and the p_z orbitals of Se appear on the higher energy. Substitution of Se with Te causes a band inversion between the p_z and $3d$ orbitals. As a result of the band inversion, the

normal state of $\text{FeTe}_{1-x}\text{Se}_x$ is topologically nontrivial, and accompanied by the surface Dirac fermions Zhang et al. (2018). Below the superconducting critical temperature, the superconducting gap is proximitized to the surface Dirac states. It was theoretically pointed out that the topological phase with a spinless Majorana zero mode can be realized when the superconducting proximity effect occurs in the Dirac fermion system Sato (2003), Fu & Kane (2008). Therefore, the surface state of Fe(Se,Te) is a topological superconducting state. When a magnetic field is applied to Fe(Se,Te), the vortex lines penetrate to the surface state and the zero energy state appears. The wave function of the zero mode is tightly bound at the intersection of the vortex line and the surface Hosur et al. (2011), Kawakami & Hu (2015).

When a magnetic field is applied to a SC, a quantized vortex penetrates. The magnetic flux is accompanied by the $2\pi m$ winding of the $U(1)$ phase and the superconducting gap vanishes. In other words, a quantized vortex can be regarded as a quantum well with a radius of ξ and a height of Δ . Hence, the Andreev bound states are formed and the level spacing between them is on the order of Δ^2/ϵ_F , where the level spacing is about 100–200 μeV in Fe(Se,Te). In the topological phase, the lowest level has the exact zero energy, and the quasiparticle behaves as Majorana fermion. Ultra-low temperature STM/STS with high energy resolution observed a pronounced zero-bias conductance peak Machida et al. (2019). If a Majorana zero mode is bound to the vortex, the conductance should be quantized to the universal value $2e^2/h$ independent of tunnel barriers. In the tunneling spectroscopy performed while changing the distance between the sample surface and the STM tip, the height of the zero-bias conductance peak is approximately 0.6 times as large as the universal value stemming from the Majorana zero mode Zhu et al. (2020). Although $2e^2/h$ has not been reached, this plateau structure strongly suggests the existence of Majorana zero modes because it cannot be explained by non-Majorana vortex bound states.

3.3. Topological quantum computation

Quantum computation based on the braiding of Majorana zero modes is basically along the two directions: implementation of quantum gates and measurement-based quantum computation. The unitary evolution of the qubits is controlled by a set of discrete unitary operations, i.e., quantum gates. The simple example of the quantum gates acting on a single qubit is the set of the Pauli gates, which are given by the three Pauli matrices $X \equiv \sigma_x$, $Y \equiv \sigma_y$, and $Z \equiv \sigma_z$. The multi-qubit gate operation can be implemented by a combination of a set of single-qubit gates and the controlled-NOT (CNOT) gate. According to the Solovay-Kitaev theorem Nielsen & Chuang (2010), an arbitrary single-qubit gate can be approximated by a sequence of the discrete gate operations (H, S, T), where $H = (X + Z)/\sqrt{2}$, $S = \sqrt{Z}$, and $T = \sqrt{S}$ are the Hadamard gate, the single-qubit 4π rotation, and the T -gate ($\pi/8$ -gate), respectively. Universal quantum computation can be implemented by a sequence of

the single-qubit gates (H, S, T) and the CNOT gate.

In Majorana qubits, the Pauli gates are expressed in terms of the braiding operations as $X = iU_{23}^2$, $Y = iU_{31}^2$, and $Z = iU_{12}^2$, and the Hadamard and S gates are implemented by a combination of such operations as $H = iU_{12}U_{23}U_{12}$ and $S = e^{i\pi/4}U_{12}$. In addition, the CNOT gate can be implemented by a combination of the measurement and braiding operations in two Majorana qubits (i.e., 8 Majorana zero modes) with a single ancilla Majorana qubit Bravyi (2006). All the Clifford gates (H, S, CNOT) are realized as a composition of braiding operators in a topologically protected way. According to the Gottesman-Knill theorem, however, quantum circuits only using the elements of Clifford group can be efficiently simulated in polynomial time on a classical computer Nielsen & Chuang (2010). Indeed, degenerate quantum states composed of multiple Ising anyons offer tolerant storage of quantum information and their braiding operations provide all necessary quantum gates in a topologically protected way, except for the non-Clifford T -gate. The T -gate can be implemented only in a topologically unprotected way. For instance, Karzig *et al.* proposed a scheme to implement the T -gate in a Y-shaped junction accompanied by 4 Majorana zero modes Karzig *et al.* (2016).

As mentioned in Sec. 2, Fibonacci anyon systems can offer a platform for universal topological quantum computation, where all the single-qubit gates (H, S, T) and the CNOT gate are implemented by the braiding manipulations of the anyons in a topologically protected way Preskill (2004), Bonesteel *et al.* (2005), Hormozi *et al.* (2007).

Another way to realize universal quantum computation in Majorana qubits is measurement-based quantum computation. It was realized that all braiding manipulations can be implemented in a topologically protected manner by the measurements of topological charges of pairwise anyons Bonderson *et al.* (2008, 2009). The process of the quantum information encoded to Majorana qubits can take place by a series of simple projective measurements without braiding Majorana modes. The building block is a Coulomb blockaded Majorana box which is made from even numbers of Majorana modes in a floating topological SC Plugge *et al.* (2017), Karzig *et al.* (2017), Oreg & von Oppen (2020).

3.4. Symmetry-protected non-Abelian anyons

Symmetry-protected non-Abelian anyons in spinful SCs and SFs were discussed for class D Ueno *et al.* (2013), Sato *et al.* (2014), Fang *et al.* (2014) and for class DIII Liu *et al.* (2014), Gao *et al.* (2016). In the former (latter) case, mirror reflection symmetry (time reversal symmetry) plays an essential role on the topological protection of non-Abelian nature. In addition, unitary symmetry-protected non-Abelian statistics has been theoretically proposed Hong *et al.* (2022). The non-Abelian statistics of vortices supporting multiple Majorana zero modes has also been discussed in Refs. Yasui *et al.* (2011) and Hirono *et al.* (2012) in the context of high-energy physics.

Mirror and unitary symmetries. As the simple example of symmetry-protected non-Abelian anyons, we consider integer quantum vortices in chiral p -wave SCs and $^3\text{He-A}$ Sato *et al.* (2014), where each vortex core supports spinful Majorana zero modes. Contrary to the standard wisdom, a pair of Majorana zero modes in integer quantum vortices can be protected by the mirror symmetry and obey the non-Abelian statistics Ueno *et al.* (2013), Sato *et al.* (2014).

Let us consider two-dimensional superconducting film and assume that the normal state holds the mirror symmetry with respect to the xy -plane, $M_{xy}h(\mathbf{k})M_{xy}^\dagger = h(\mathbf{k})$, where $\mathbf{k} = (k_x, k_y)$ is the two-dimensional momentum and the mirror operator is defined as $M_{xy} = i\sigma_z$. The nontrivial topological properties are characterized by the first Chern number in each mirror subsector. When $\Delta(\mathbf{k})$ obeys $M_{xy}\Delta(\mathbf{k})M_{xy}^\dagger = \eta\Delta(\mathbf{k})$ ($\eta = \pm$), the BdG Hamiltonian is commutable with the mirror reflection operator in the particle-hole space, \mathcal{M}^η , as

$$[\mathcal{M}^\eta, \mathcal{H}(\mathbf{k})] = 0, \quad \mathcal{M}^\eta = \begin{pmatrix} M_{xy} & 0 \\ 0 & \eta M_{xy}^* \end{pmatrix}. \quad (38)$$

Thus, the eigenstates of $\mathcal{H}(\mathbf{k})$ are the simultaneous eigenstates of \mathcal{M}^η . Let $|u_n^{(\lambda)}(\mathbf{k})\rangle$ and $E_n^{(\lambda)}$ be the wavefunction and eigenenergy of the Bogoliubov quasiparticles in each mirror subsector, where the $\lambda = \pm i$ are the eigenvalues of \mathcal{M}^η . Then, the first Chern number is defined in each mirror subsector,

$$\text{Ch}_1^{(\lambda)} = \frac{i}{2\pi} \int \mathcal{F}^{(\lambda)} \in \mathbb{Z}, \quad (39)$$

where $\mathcal{F}^{(\lambda)} = d\mathcal{A}^{(\lambda)}$ is the Berry curvature in each mirror subsector and $\mathcal{A}_\mu^{(\lambda)}(\mathbf{k}) = \sum_{E_n^{(\lambda)} < 0} \langle u_n^{(\lambda)}(\mathbf{k}) | \partial_{k_\mu} u_n^{(\lambda)}(\mathbf{k}) \rangle$. The nonzero value ensures the existence of the zero energy state in the λ subsector. For the $^3\text{He-A}$ thin film and chiral p -wave SCs, $|\text{Ch}_1^{(\lambda)}| = 1$ in each mirror subsector, implying that integer quantum vortices support two Majorana zero modes per each core.

Multiple Majorana zero modes behave as non-Abelian anyons only when the mirror subsector holds the particle-hole symmetry, which are referred to as mirror Majorana zero modes. The condition for each mirror subsector to maintain the particle-hole symmetry is given by Ueno *et al.* (2013), Sato *et al.* (2014)

$$\{C, \mathcal{M}^\eta\} = 0. \quad (40)$$

For integer quantum vortices, the condition depends on the orientation of the \mathbf{d} -vector. For $\hat{\mathbf{d}} \parallel \hat{\mathbf{z}}$, the mirror subsector supports its own particle-hole symmetry, but otherwise the subsector does not maintain the particle-hole symmetry and belongs to class A.

Now let us clarify the non-Abelian statistics of spin-degenerate Majorana modes. Consider $2N$ integer quantum vortices. Two Majorana zero modes bound at the i th vortex are denoted by γ_λ^i with mirror eigenvalues $\lambda = \pm i$. The Majorana zero modes satisfy the self-conjugate condition $\gamma_\lambda^i = (\gamma_\lambda^i)^\dagger$ and the anticommutation relation,

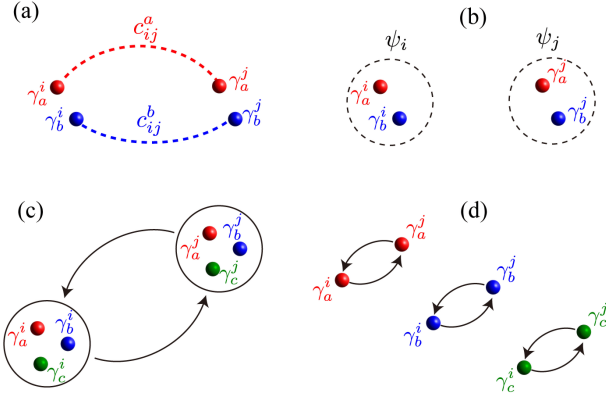


Figure 6: Complex fermions formed by intervortex pairs (a) and intravortex pairs (b), where γ_a^i denotes a Majorana zero mode with internal degrees of freedom a (e.g., spin) bound at the i th vortex. (c) Schematic of the exchange of two vortices with multiple Majorana zero modes. (d) When the system holds a unitary symmetry such as the mirror symmetry in Eq. (38), the operation (c) is equivalent to the exchange of two Majorana zero modes in each sector.

$\{\gamma_\lambda^i, \gamma_{\lambda'}^j\} = 2\delta_{i,j}\delta_{\lambda,\lambda'}$. In contrast to spinless Majorana zero modes, there are two possibilities to form a complex fermion: (i) intervortex pairs, $c_{ij}^\lambda \equiv (\gamma_\lambda^i + i\gamma_\lambda^j)/2$ and (ii) intravortex pairs, $\psi_i \equiv (\gamma_{\lambda=i}^i + i\gamma_{\lambda=-i}^i)/2$ [See Figs. 6(a,b)]. In the former case (i), the exchange operators of the i th and j th vortices are defined in a manner similar to that for spinless Majorana zero modes as

$$U_{ij}^{\lambda\dagger} \gamma_\lambda^i U_{ij}^\lambda = \gamma_\lambda^j, \quad U_{ij}^{\lambda\dagger} \gamma_\lambda^j U_{ij}^\lambda = -\gamma_\lambda^i. \quad (41)$$

The above transformation is realized by the unitary operator,

$$U_{ij}^\lambda = \exp\left(\frac{\pi}{4} \gamma_\lambda^j \gamma_\lambda^i\right) = \frac{1}{\sqrt{2}} \left(1 + \gamma_\lambda^j \gamma_\lambda^i\right), \quad (42)$$

Similarly to U_{ij} and U_{jk} in spinless Majorana zero modes, the exchange operators U_{ij}^λ and U_{jk}^λ defined in each mirror subsector do not commute to each other, which implies the non-Abelian anyon statistics of integer quantum vortices hosting mirror Majorana zero modes.

In the case (ii) [Fig. 6(b)], a complex fermion is formed as a local pair of two mirror Majorana modes, which also obeys the non-Abelian statistics Yasui et al. (2012), Sato et al. (2014). The expression of the exchange operator is obtained as $U_{ij} = 1 + \psi_j \psi_i^\dagger + \psi_i^\dagger \psi_j - \psi_i^\dagger \psi_i - \psi_j^\dagger \psi_j + 2\psi_j^\dagger \psi_j \psi_i^\dagger \psi_i$. In general, the exchange operators are not commutable with each other, $[U_{ij}, U_{jk}] \neq 0$. As the operator preserves the fermion number $N_f = \sum_i \psi_i^\dagger \psi_i$, the degenerate ground states are expressed in terms of the occupation number of the complex fermion in each vortex. For example, let us consider the four-vortex state $|1100\rangle$ where the first and second vortices are accompanied by the Dirac zero modes, while the third and fourth are not. Up to a phase factor, this state changes under U_{12} and U_{34} as $|1100\rangle \rightarrow |1100\rangle$

and $|1100\rangle \rightarrow |1010\rangle$, respectively. The complete representations of the exchange operators U_{ij} are presented in Ref. Yasui et al. (2012). The extension to non-Abelian statistics of multiple complex fermions was discussed in Ref. Yasui et al. (2013).

When the BdG Hamiltonian maintains the mirror symmetry in Eq. (38), as mentioned above, the braiding of vortices supporting spinful Majorana modes is decomposed into two individual exchanges between Majorana zero modes γ_λ^i and γ_λ^j in each mirror subsector [see also Figs. 6(c) and 6(d)] and the exchange matrices are represented by Eqs. (41) and (42). This argument is applicable for the systems hosting multiple Majorana modes protected by unitary symmetries Hong et al. (2022), where the couplings between Majorana zero modes in each core are excluded by the unitary symmetries. The braiding of two vortices with n unitary-symmetry-protected multiple Majorana modes generically reduces to the n independent braiding operations in each sector as

$$U_{ij} = \prod_a U_{ij}^a, \quad (43)$$

where a denotes the internal degrees of freedom of Majorana zero modes. The unitary time evolution representing the braiding process does not dynamically break the unitary symmetry, which prohibits the coupling between Majorana modes in different subsectors labeled by a . The mirror reflection symmetry in Eq. (38) is an example of such symmetry-protected non-Abelian anyons. Another example is the non-Abelian vortices in dense QCD matter which trap multiple Majorana zero modes in each core Yasui et al. (2010), Fujiwara et al. (2011). As discussed below, such vortices with multiple Majorana zero modes obey the non-Abelian statistics and the braiding matrices are identical with the elements in the Coxeter group Yasui et al. (2011), Hirono et al. (2012).

Contrary to unitary symmetries, the braiding process, characterized as a unitary evolution, may dynamically break antiunitary symmetry such as the time-reversal symmetry. We note that in contrast to time-reversal -broken topological SCs such as superconducting nanowires, topological superconductors with time-reversal symmetry do not require an external magnetic field for realizing the topological phase and can keep the topological gap close to the proximity-induced superconducting gap Haim & Oreg (2019), Wong & Law (2012), Zhang et al. (2013). Hence, the Majorana-Kramers pairs leads to longer decoherence time of the stored quantum information Liu et al. (2014). As mentioned above, however, the braiding process of the Majorana-Kramers pairs may dynamically break the antiunitary symmetry. Such dynamical symmetry breaking gives rise to the local mixing of the Majorana-Kramers pairs Wölms et al. (2014, 2016), Knapp et al. (2020). Gao et al. proposed the conditions to protect the non-Abelian statistics of the Majorana-Kramers pairs Gao et al. (2016). In addition, Tanaka et al. examined by numerical simulations the tolerance of non-Abelian braidings of

Majorana-Kramers pairs against two types of perturbations which may cause decoherence of Majorana-Kramers qubits Tanaka et al. (2022): (i) Applied magnetic fields, and (ii) the effect of a gate-induced inhomogeneous potential at junctions of superconducting nanowires. The former break time-reversal symmetry and generate the energy gap of Majorana states, while the latter gives rise to non-Majorana low-energy Andreev bound states Kells et al. (2012), Liu et al. (2017), Moore, Zeng, Stanescu & Tewari (2018), Moore, Stanescu & Tewari (2018), Pan et al. (2020), Pan & Das Sarma (2020). The numerical simulation revealed that the non-Abelian braiding is successful when the direction of the applied magnetic field preserves the chiral symmetry in the initial and final states of a braiding process, where the chiral symmetry is a combination of time-reversal symmetry and mirror symmetry Tanaka et al. (2022). Remarkably, this tolerance is preserved even when the intermediate states of the braiding process breaks this symmetry. As for (ii), non-Majorana bound states emergent in gate-induced inhomogeneous potentials make Majorana-Kramers qubits vulnerable to quasiparticle poisoning and disturb the braiding protocol. However, the influence can be ignored when the width of the gate-induced potential is sufficiently smaller than the superconducting coherence length.

Multiple Majorana zero modes and Coxeter group. It has been demonstrated that the non-Abelian statistics of vortices hosting three Majorana zero modes has a novel structure, when the Majorana modes have additional $SO(3)$ symmetry Yasui et al. (2011), Hirono et al. (2012). The representation of braiding operations in four vortices is given by a tensor product of two matrices, where one is identical to the matrix for the braiding of spinless Majorana zero modes, and the other is a generator of the Coxeter group.

Let γ_a^i ($a = 1, 2, 3$) be the operators of three Majorana zero modes in the i th vortex, belonging to the triplet of $SO(3)$. Consider four vortices hosting three Majorana zero modes in each core. The braiding of these vortices is decomposed into the three individual exchanges between Majorana zero modes γ_a^i and γ_a^j [see Figs. 6(c,d)]. For each component a , Majorana zero modes γ_a^i and γ_a^j under braiding manipulations transforms in the same way as Eq. (41) and the exchange matrices, U_{ij}^a , are obtained by $U_{ij}^\lambda \rightarrow U_{ij}^a$ in Eqs. (41) and (42). Then, the representations of U_{ij} for vortices with triplet Majorana zero modes are obtained by the 64×64 matrix, $U_{ij} = \prod_{a=1,2,3} U_{ij}^a$, as in Eq. (43).

We now introduce the complex fermion operators as the nonlocal pairs of Majorana zero modes, $c_{ij}^a = (\gamma_a^i + i\gamma_a^j)/2$. For two vortices (i.e., six Majorana modes), this leads to the 2^3 -fold degenerate ground states and the Hilbert space is spanned by the four basis sets: singlet-even $|1_0\rangle \equiv |0\rangle$ (vacuum) and triplet-even $|3_2\rangle \equiv \frac{1}{2!} e^{abc} c_{ij}^{b\dagger} c_{ij}^{c\dagger} |0\rangle$ (occupied by two fermions) for even fermion parity and singlet-odd $|1_3\rangle \equiv \frac{1}{3!} e^{abc} c_{ij}^{a\dagger} c_{ij}^{b\dagger} c_{ij}^{c\dagger} |0\rangle$ (occupied by three fermions) and triplet-odd $|3_1\rangle \equiv c_{ij}^{a\dagger} |0\rangle$ (occupied by single fermion). In the case of four vortices, the ground state degeneracy is

$2^6 = 64$ and the bases of the Hilbert space are singlet (**1**), triplet (**3**), and quintet (**5**) states, which are further divided in terms of the fermion parity. The exchange operator is expressed as a product of two $SO(3)$ invariant unitary operators,

$$U_{ij} = \prod_{a=1,2,3} U_{ij}^a = \sigma_{ij} h_{ij} \quad (44)$$

where both matrices are given in terms of γ_i^a as

$$\sigma_{ij} = \frac{1}{2} \left(1 - \gamma_j^1 \gamma_j^2 \gamma_i^1 \gamma_i^2 - \gamma_j^2 \gamma_j^3 \gamma_i^2 \gamma_i^3 - \gamma_j^3 \gamma_j^1 \gamma_i^3 \gamma_i^1 \right), \quad (45)$$

and

$$h_{ij} = \frac{1}{\sqrt{2}} \left(1 - \gamma_j^1 \gamma_j^2 \gamma_j^3 \gamma_i^1 \gamma_i^2 \gamma_i^3 \right). \quad (46)$$

While the matrices h_{ij} are a natural extension of that originally introduced in Ref. Ivanov (2001), the matrices σ_{ij} are proper to vortices with three or more Majorana zero modes. It was demonstrated that the matrices σ_{ij} are identified with the elements in the Coxeter group which satisfies the relations

$$(\sigma_{ij})^2 = 1, (\sigma_{ij}\sigma_{jk})^3 = 1, (\sigma_{ij}\sigma_{kl})^2 = 1. \quad (47)$$

The Coxeter group is a symmetry group of polytopes in high dimensions such as a triangle and a tetrahedron. The exchange operators acting on the singlet (**1**) and triplet (**3**) are identified with the elements in the Coxeter group, such as a 2-simplex (triangle) under the reflections for the singlet and a 3-simplex (tetrahedron) under the reflections for the triplet Yasui et al. (2011). The decomposition of the braiding operators U_{ij} in the $SO(3)$ triplet was generalized to the Majorana zero modes of arbitrary odd $n_M \geq 3$ with $SO(n_M)$ symmetry Hirono et al. (2012).

Such multiple Majorana zero modes were first found in Refs. Yasui et al. (2010), Fujiwara et al. (2011) inside the cores of color flux tubes (“non-Abelian” vortices) Balachandran et al. (2006), Nakano et al. (2008), Eto & Nitta (2009), Eto et al. (2014) in high density quark (QCD) matter Alford et al. (2008). They were also discussed in edges of a topological superconducting wire coupled to a normal lead Kashuba & Timm (2015).

4. Non-Abelian vortex anyons

Here we introduce non-Abelian anyons made of bosonic excitations, which are non-Abelian vortices obeying a non-Abelian statistics Bais (1980), Wilczek & Wu (1990), Bucher (1991), Brekke et al. (1993), Lo & Preskill (1993), Lee (1994), Brekke et al. (1997), Mawson et al. (2019). These non-Abelian vortices are sometime called fluxons.²

²Here, the term “flux” originally comes from the fact that they were proposed in gauge theory where non-Abelian symmetry is gauged in the context of high energy physics Bais (1980). In this article, we consider only global non-Abelian symmetry relevant for condensed matter physics and they do not carry non-Abelian fluxes.

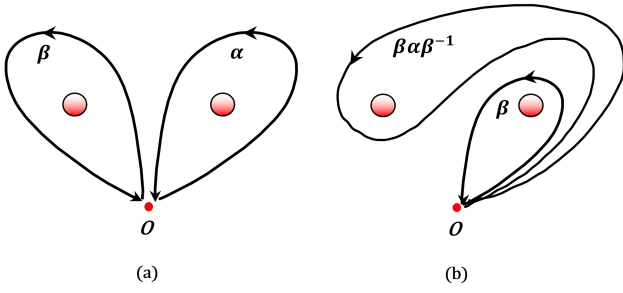


Figure 7: Exchange of two vortices. (a) Two closed paths α and β encircle two vortices. (b) Exchange them counterclockwise.

4.1. Non-Abelian vortices

When a symmetry G , that is either global or local, is spontaneously broken into its subgroup H , there appears an order parameter space

$$M \simeq G/H \quad (48)$$

parameterized by Nambu-Goldstone modes. The first homotopy group of the order parameter space

$$\pi_1(G/H) \simeq \pi_0(H) \quad (49)$$

is responsible for the existence of quantum vortices, where we have assumed that G is semisimple. We further have

$$\pi_0(H) \simeq H/H_0 (\simeq H \text{ for a discrete group } H) \quad (50)$$

with a normal subgroup H_0 of H . When $\pi_1(G/H)$ is Abelian (and thus H/H_0 (for semisimple G) is Abelian), vortices are Abelian, while when it is non-Abelian, vortices are non-Abelian Balachandran et al. (1984), Alford et al. (1990, 1991, 1992).

One of characteristic features of non-Abelian vortices is that H is not globally defined (or multi-valued): the unbroken symmetry H_θ depends on the azimuthal angle θ around a non-Abelian vortex as $H_\theta = g(\theta)H_{\theta=0}g^{-1}(\theta)$ with $g(\theta) \in G$, $g(0) = \mathbf{1}$ and $g(2\pi)$ taking a disconnected component of H/H_0 , see Eq. (50). Then, after an adiabatic transport along a loop encircling the non-Abelian vortex, the unbroken symmetry at $\theta = 2\pi$ does not have to come back: $H_{\theta=2\pi} \neq H_{\theta=0}$. This is called *topological obstruction*, and the symmetry H is topologically broken down to a subgroup $K \equiv \{h | [h, g(2\pi)] = 0, h \in H\}$ which is single-valued and globally defined Balachandran et al. (1984), Alford et al. (1990). This is also called *topological symmetry breaking*. When G and H are local gauge symmetries, it gives a non-Abelian Aharonov-Bohm effect Bais (1980), Wilczek & Wu (1990), Bucher (1991), Alford et al. (1990, 1991, 1992). Another related feature is the existence of non-local charges, called Cheshire charges, existing among separated vortices Preskill & Krauss (1990), Alford et al. (1990), Bucher et al. (1992).

Let $\alpha, \beta \in \pi_1(G/H)$ being closed passes enclosing two vortices. Then, if one adiabatically transports the vortex α

around the vortex β counterclockwise, the vortex α transforms as (see Fig. 7(b))

$$\alpha \rightarrow \beta\alpha\beta^{-1}. \quad (51)$$

Therefore, when one exchanges a pair (α, β) counterclockwise, they transform as

$$(\alpha, \beta) \rightarrow (\beta, \beta\alpha\beta^{-1}). \quad (52)$$

The first homotopy group π_1 is a based fundamental group for which every loop starts from a fixed point O . Instead of it, the conjugacy classes

$$[\alpha] = \beta\alpha\beta^{-1}, \quad \forall \beta \in \pi_1(G/H) \quad (53)$$

characterize individual vortices as can be seen from Eqs. (51) and (52). Two vortices corresponding to two different elements in the same conjugacy class are *indistinguishable* even though they are not the same.

Non-Abelian first homotopy groups significantly control the dynamics of vortices. In two spatial dimensions, scattering of such non-Abelian vortices was discussed in the case that G and H are local gauge symmetries Wilczek & Wu (1990), Bucher (1991), Lo & Preskill (1993). In three spatial dimensions, vortices are lines. When two vortex lines collide in three spatial dimensions, the fate is determined by corresponding elements of the first homotopy group. When these elements commute, the two vortices pass through or reconnect each other if these elements are identical. On the other hand, when these elements are non-commutative, the third vortex bridging them must be created Poenaru & Toulouse (1977), Mermin (1979), Kobayashi et al. (2009).

4.2. Examples of non-Abelian vortices

Nematic liquid crystals. Let us start from nematic liquid crystals focusing on uniaxial nematics (UNs), and D_2 - and D_4 -biaxial nematics (BNs).

UN liquid crystals. The order parameter of UNs is an unoriented rod. The rotational symmetry $G = SO(3)$ is spontaneously broken down to $H \simeq O(2)$, which implies the order parameter manifold

$$\frac{G}{H} = \frac{SO(3)}{O(2)} \simeq \frac{SU(2)}{Pin(2)} \simeq S^2/\mathbb{Z}_2 \simeq \mathbb{R}P^2, \quad (54)$$

which is a real projective space of two dimensions, where $SU(2)$ and $Pin(2)$ are double covering groups of $SO(3)$ and $O(2)$, respectively. Since the fundamental group $\pi_1(\mathbb{R}P^2) = \mathbb{Z}_2$ is Abelian, this does not admit non-Abelian vortices. These vortices are called Alice strings (when G and H are local gauge symmetries) Schwarz (1982). Around the Alice string, $SO(2) \subset H$ is not globally defined and H is topologically broken to $K \simeq \mathbb{Z}_2$.

D_2 -BN liquid crystals Poenaru & Toulouse (1977), Volovik & Mineev (1977), Mermin (1979), Balachandran et al. (1984).

Cholesteric liquid crystals (chiral nematic liquid crystals) can also have the same order parameter space with D_2 -BN liquid crystals Lavrentovich & Kleman (2001) and all the following discussions hold. The order parameter of BNs

$g(2\pi) \in \pi_1(G/H)$	$\mathbf{1}_2$	$-\mathbf{1}_2$	$\pm i\sigma_x$	$\pm i\sigma_y$	$\pm i\sigma_z$
$g(\theta)$	$\mathbf{1}_2$	$\exp\left(\pm i\frac{\theta}{2}\mathbf{n} \cdot \boldsymbol{\sigma}\right)$	$\exp\left(\pm i\frac{\theta}{4}\sigma_x\right)$	$\exp\left(\pm i\frac{\theta}{4}\sigma_y\right)$	$\exp\left(\pm i\frac{\theta}{4}\sigma_z\right)$
$O(2\pi)$	$\mathbf{1}_3$	$\mathbf{1}_3$	I_x	I_y	I_z
$O(\theta)$	$\mathbf{1}_3$	$\exp(i\theta\mathbf{n} \cdot \mathbf{L})$	$\exp\left(\pm i\frac{\theta}{2}L_x\right)$	$\exp\left(\pm i\frac{\theta}{2}L_y\right)$	$\exp\left(\pm i\frac{\theta}{2}L_z\right)$

Table 1

Asymptotic configurations of spin vortices in D_2 -BNs: the fundamental group elements $g(2\pi) \in \pi_1(G/H)$, the $SU(2)$ elements $g(\theta) \in SU(2)$, $O(2\pi)$, and the $SO(3)$ group elements $O(\theta) \in SO(3)$, acting on the order parameter A as Eq. (60). The group actions $O(\theta)$ and $g(\theta)$ for a spin vortex of 2π rotation ($-\mathbf{1}_2$) can be a rotation around any axis along the unit vector \mathbf{n} . L_i are 3×3 spin-1 matrices $[L_i]_{jk} = -i\epsilon_{ijk}$.

is a set of two unoriented rods of different lengths orthogonal to each other. The (unbroken) symmetry is the dihedral group D_2 keeping a rectangular invariant. Thus, the rotational symmetry $G = SO(3)$ is spontaneously broken down to

$$H \simeq D_2 = \left\{ \mathbf{1}_3, I_x = \begin{pmatrix} +1 & 0 & 0 \\ 0 & -1 & 0 \\ 0 & 0 & -1 \end{pmatrix}, \right. \\ \left. I_y = \begin{pmatrix} -1 & 0 & 0 \\ 0 & +1 & 0 \\ 0 & 0 & -1 \end{pmatrix}, I_z = \begin{pmatrix} -1 & 0 & 0 \\ 0 & -1 & 0 \\ 0 & 0 & +1 \end{pmatrix} \right\}. \quad (55)$$

Note that $D_2 \simeq \mathbb{Z}_2 \times \mathbb{Z}_2$ is Abelian. The order parameter manifold is

$$G/H = SO(3)/D_2 \simeq SU(2)/\mathbb{Q}, \quad (56)$$

where the quaternion group \mathbb{Q} are universal (double) covering group of D_2 :

$$\mathbb{Q} = \{ \pm \mathbf{1}_2, \pm i\sigma_x, \pm i\sigma_y, \pm i\sigma_z \}. \quad (57)$$

Note that $H^* \simeq \mathbb{Q}$ is a non-Abelian group while $H \simeq D_2$ is an Abelian group. This breaking can occur for instance by five real-scalar order-parameters belonging to spin-2 representation of $SO(3)$, which is a traceless symmetric 3×3 tensor A with real components, taking a form of

$$A = \text{diag}(1, r, -1 - r) \quad (58)$$

The first homotopy group is isomorphic to the quaternion group \mathbb{Q} in Eq. (57)

$$\pi_1(SU(2)/\mathbb{Q}) \simeq \mathbb{Q}. \quad (59)$$

The elements in Eq. (57) correspond to the ground state ($\mathbf{1}_2$), spin vortices of 2π rotation ($-\mathbf{1}_2$), and spin vortices of $\pm\pi$ rotation about the x, y, z -axes ($\pm i\sigma_{x,y,z}$). These vortex configurations at the large distance can be asymptotically written as

$$A \sim O(\theta)A_{\theta=0}O^T(\theta), \quad O(\theta) \in SO(3) \quad (60)$$

with the azimuthal angle θ . The concrete forms of $O(\theta)$'s are given in Table 1. Corresponding $SU(2)$ elements $g(\theta)$ can be defined as a double covering of $SO(3)$ with $g(2\pi) \in \pi_1(G/H)$. A spin vortex of 2π rotation ($-\mathbf{1}_2$) and a spin vortex of π rotation ($\pm i\sigma_a$) ($a = x, y, z$) are given by

$$g(\theta) = \exp\left(\pm i\frac{\theta}{2}\boldsymbol{\sigma} \cdot \mathbf{n}\right) = \cos\frac{\theta}{2}\mathbf{1}_2 \pm i\boldsymbol{\sigma} \cdot \mathbf{n} \sin\frac{\theta}{2}, \\ g(\theta) = \exp\left(\pm i\frac{\theta}{4}\sigma_a\right) = \cos\frac{\theta}{4}\mathbf{1}_2 \pm i\sigma_a \sin\frac{\theta}{4}, \quad (61)$$

respectively, with a unit three-vector \mathbf{n} , giving the elements of $\pi_1(G/H)$ at $\theta = 2\pi$: $g(2\pi) = -\mathbf{1}_2$ and $g(2\pi) = \pm i\sigma_a$, respectively. While the former is Abelian because $[g(2\pi), H^*] = 0$ (even though $g(2\pi) \neq g(0)$), the latter is non-Abelian because $[g(2\pi), H^*] \neq 0$ with the universal covering $H^* \simeq SU(2)$,³ and H^* is topologically broken to $K_a^* = \{ \pm \mathbf{1}_2, \pm i\sigma_a \}$.

The elements in Eq. (57) are grouped to the conjugacy classes, Eq. (53), consisting of five elements:

$$\{ \mathbf{1}_2 \}, \{ -\mathbf{1}_2 \}, \{ \pm i\sigma_x \}, \{ \pm i\sigma_y \}, \{ \pm i\sigma_z \}. \quad (62)$$

This follows for instance from $(i\sigma_y)^{-1}(i\sigma_x)(i\sigma_y) = -i\sigma_x$, implying that a vortex corresponding to $i\sigma_x$ becomes $-i\sigma_x$ when it travels around a vortex corresponding to $i\sigma_y$. Thus, the vortices corresponding to $i\sigma_x$ and $-i\sigma_x$ are *indistinguishable* although they are not the same. From $(i\sigma_a)(-i\sigma_a) = \mathbf{1}_2$ ($a = x, y, z$), vortices belonging to the same conjugacy class are anti-particles of each other, and thus they are similar to Majorana fermions discussed in the last section.

In three spatial dimensions, this phenomenon of non-commutativity appears as follows: when two vortex lines corresponding to $i\sigma_x$ and $i\sigma_y$ collide in three spatial dimensions, the third vortex bridging them is created Poenaru & Toulouse (1977), Mermin (1979).

D_4 -BN liquid crystals. The order parameter of D_4 BNs is a set of two unoriented indistinguishable rods of the *same* lengths orthogonal to each other. In this case, the (unbroken) symmetry is a dihedral group D_4 keeping a square invariant:

$$G/H = SO(3)/D_4 \simeq SU(2)/D_4^*, \quad (63)$$

³Note that $[O(2\pi), H] = 0$, and thus the criterion of non-Abelian property should be considered in the universal covering group H^* but not in H .

where M^* denotes a universal covering group of M . The fundamental group is given by

$$\pi_1(SU(2)/D_4^*) \simeq D_4^* \quad (64)$$

with the sixteen elements

$$\{\pm \mathbf{1}_2, \pm i\sigma_x, \pm i\sigma_y, \pm i\sigma_z, \pm C_4, \pm C_4^{-1}, \pm i\sigma_x C_4, \pm i\sigma_x C_4^{-1}\} \quad (65)$$

with $C_4 \equiv e^{i\frac{\pi}{4}\sigma_z} = (1/\sqrt{2})(\mathbf{1}_2 + i\sigma_z)$. Note $(C_4)^2 = i\sigma_z$ and $(C_4)^4 = -\mathbf{1}_2$. The conjugacy classes consist of the following seven elements

$$\{\mathbf{1}_2\}, \{-\mathbf{1}_2\}, \{\pm i\sigma_x, \pm i\sigma_y\}, \{\pm i\sigma_z\}, \\ \{C_4, C_4^{-1}\}, \{-C_4, -C_4^{-1}\}, \{\pm i\sigma_x C_4, \pm i\sigma_x C_4^{-1}\}. \quad (66)$$

Since $-C_4 = C_4^3$ ($-C_4^{-1} = C_4^{-3}$), vortices of these elements have more energy than those of C_4 and C_4^{-1} . This symmetry breaking of D_4 nematics can be realized by a higher rank tensor order parameter Mietke & Dunkel (2022), in which more generally D_n nematic liquid crystals were also discussed.

Spinor BECs. Next we provide examples of spinor BECs Kawaguchi & Ueda (2012). The order parameter of spin-2 BECs is a traceless symmetric 3×3 tensor A with complex components transforming under the symmetry $G = U(1) \times SO(3)$ as

$$A \rightarrow e^{i\theta} g A g^T, \quad e^{i\theta} \in U(1), \quad g \in SO(3). \quad (67)$$

Phases of condensations with total angular momentum two are classified by Mermin Mermin (1974). They are nematic, cyclic and ferromagnetic phases. All phases are theoretically possible in the case of spin-2 BECs. The spin-2 BECs are experimentally realized by ^{87}Rb atoms for which the phase is around the boundary between cyclic phase and ferromagnetic phase, see e.g. Ref. Tojo et al. (2009). Here, we discuss nematic and cyclic phases which host non-Abelian vortex anyons. In the next section, we discuss 3P_2 SF which is in the nematic phase.

BN phases in spin-2 BEC. Song et al. (2007), Uchino et al. (2010), Kobayashi et al. (2012), Borgh & Ruostekoski (2016). The nematic phase consists of three degenerate phases: the UN, D_2 - and D_4 -BN phases. The order parameters of the UN, D_2 - and D_4 -BN phases are given by

$$\begin{aligned} \text{UN} : A &\sim \text{diag}(1, -1/2, -1/2), \\ D_2\text{-BN} : A &\sim \text{diag}(1, r, -1 - r), \\ D_4\text{-BN} : A &\sim \text{diag}(1, -1, 0), \end{aligned} \quad (68)$$

respectively, where $r \in \mathbb{R}$ and $-1 < r < -1/2$. In the D_2 -BN phase, the limits $r \rightarrow -1/2, -1$ correspond to UN and D_4 -BN phases, respectively. The symmetry breaking patterns and the order parameter manifolds are

$$\begin{aligned} \text{UN} : \frac{G}{H} &= U(1) \times \frac{SO(3)}{O(2)} \simeq U(1) \times \mathbb{R}P^2, \\ D_2\text{-BN} : \frac{G}{H} &= U(1) \times \frac{SO(3)}{D_2} \simeq U(1) \times \frac{SU(2)}{\mathbb{Q}}, \\ D_4\text{-BN} : \frac{G}{H} &= \frac{U(1) \times SO(3)}{D_4} \simeq \frac{U(1) \times SU(2)}{D_4^*}. \end{aligned}$$

These phases are continuously connected by the parameter r interpreted as a quasi-Nambu-Goldstone mode. The degeneracy is lifted by quantum effects and either of these phases remains as the ground state Uchino et al. (2010).

The D_2 -BN and D_4 -BN admit non-Abelian vortices. The order parameters of the UN and D_2 -BN phases of spin-2 BECs are merely products of the $U(1)$ phonon and the order parameters of the corresponding nematic liquids. Thus, we concentrate on the D_4 -BN phase hereafter. The fundamental group of the D_4 -BN phase is given by

$$\pi_1 \left(\frac{U(1) \times SU(2)}{D_4^*} \right) \simeq \mathbb{Z} \times_h D_4^* \quad (70)$$

where \times_h is defined in Ref. Kobayashi et al. (2012). This consists of the following sixteen elements

$$\begin{aligned} &\left\{ (N, \pm \mathbf{1}_2), (N, \pm i\sigma_x), (N, \pm i\sigma_y), (N, \pm i\sigma_z), \right. \\ &\quad \left(N + \frac{1}{2}, \pm C_4 \right), \left(N + \frac{1}{2}, \pm i\sigma_x C_4 \right), \\ &\quad \left. \left(N + \frac{1}{2}, \pm C_4^{-1} \right), \left(N + \frac{1}{2}, \pm i\sigma_x C_4^{-1} \right) \right\}, \end{aligned} \quad (71)$$

where the first and second elements of a pair (\cdot, \cdot) denote the circulation κ ($U(1)$ winding number) and an $SU(2)$ element, respectively with $N \in \mathbb{Z}$. Here $C_4 \equiv e^{i\frac{\pi}{4}\sigma_z} = (1/\sqrt{2})(\mathbf{1}_2 + i\sigma_z)$ satisfying $C_4^4 = -\mathbf{1}_2$. The conjugacy classes of Eq. (71) are composed of seven elements for each N :

$$\begin{aligned} \text{(I)} &\quad \{(N, \mathbf{1}_2)\}, \\ \text{(II)} &\quad \{(N, -\mathbf{1}_2)\}, \\ \text{(III)} &\quad \{(N, \pm i\sigma_x), (N, \pm i\sigma_y)\}, \\ \text{(IV)} &\quad \{(N, \pm i\sigma_z)\}, \\ \text{(V)} &\quad \left\{ \left(N + \frac{1}{2}, C_4 \right), \left(N + \frac{1}{2}, C_4^{-1} \right) \right\}, \\ \text{(VI)} &\quad \left\{ \left(N + \frac{1}{2}, -C_4 \right), \left(N + \frac{1}{2}, -C_4^{-1} \right) \right\}, \\ \text{(VII)} &\quad \left\{ \left(N + \frac{1}{2}, \pm i\sigma_x C_4 \right), \left(N + \frac{1}{2}, \pm i\sigma_x C_4^{-1} \right) \right\}. \end{aligned} \quad (72)$$

They describe (I) integer vortices ($N = 0$ corresponds to the vacuum), (II) spin vortices of 2π rotation, (III),(IV) spin vortices of π rotation around the x , y , and z axes, and (V) – (VII) non-Abelian HQVs.

In Sec. 5, we see that 3P_2 SFs are in the D_4 -BN phase in a strong magnetic field. There, a singly quantized vortex $(1, \mathbf{1})$ splits into two HQVs $(1/2, C_4)$ and $(1/2, C_4^{-1})$ both in the conjugacy class (V)⁴. When they fuse, they go back to the singly quantized vortex $(1, \mathbf{1})$. However, one of them, e.g., $(1/2, C_4^{-1})$ can transform to the other $(1/2, C_4)$ once some other vortex passes through between them because they belong to the same conjugacy class. If they fuse after

⁴Topologically a decay into a pair $(1/2, -C_4)$ and $(1/2, -C_4^{-1})$ in the conjugacy class (VI) is also possible, but energetically disfavored.

that, they become $(1, i\sigma_z)$ because $C_4^2 = i\sigma_z$ which is a composite belonging to (IV), of a singly quantized vortex and a spin vortex of π rotation.

Cyclic phase in spin-2 BEC. Semenoff & Zhou (2007), Kobayashi et al. (2009, 2012). The order parameter of the cyclic phase is

$$A \sim \text{diag}(1, e^{2\pi i/3}, e^{4\pi i/3}), \quad (73)$$

yielding the symmetry breaking to the tetrahedral group $H \simeq T$ and the order parameter manifold, given by

$$\frac{G}{H} = \frac{U(1) \times SO(3)}{T} \simeq \frac{U(1) \times SU(2)}{T^*} \quad (74)$$

with the universal covering group T^* of T . The fundamental group in the cyclic phase is given by

$$\pi_1 \left(\frac{U(1) \times SU(2)}{T^*} \right) \cong \mathbb{Z} \times_h T^* \quad (75)$$

with the 24 elements

$$\left\{ (N, \pm \mathbf{1}_2), (N, \pm i\sigma_x), (N, \pm i\sigma_y), (N, \pm i\sigma_z), \right. \\ \left. \left(N + \frac{1}{3}, \pm C_3 \right), \left(N + \frac{1}{3}, \pm i\sigma_x C_3 \right), \right. \\ \left. \left(N + \frac{1}{3}, \pm i\sigma_y C_3 \right), \left(N + \frac{1}{3}, \pm i\sigma_z C_3 \right), \right. \\ \left. \left(N - \frac{1}{3}, \pm C_3^2 \right), \left(N - \frac{1}{3}, \pm i\sigma_x C_3^2 \right), \right. \\ \left. \left(N - \frac{1}{3}, \pm i\sigma_y C_3^2 \right), \left(N - \frac{1}{3}, \pm i\sigma_z C_3^2 \right) \right\} \quad (76)$$

with the same notation with Eq. (71). Here $C_3 \equiv (1/2)(\mathbf{1}_2 + i\sigma_x + i\sigma_y + i\sigma_z)$ satisfying $(C_3)^3 = -\mathbf{1}_2$. The conjugacy classes of Eq. (76) are composed of the following seven elements for each N Semenoff & Zhou (2007):

$$\begin{aligned} \text{(I)} & \quad \{(N, \mathbf{1}_2)\}, \\ \text{(II)} & \quad \{(N, -\mathbf{1}_2)\}, \\ \text{(III)} & \quad \{(N, \pm i\sigma_x), (N, \pm i\sigma_y), (N, \pm i\sigma_z)\}, \\ \text{(IV)} & \quad \left\{ \left(N + \frac{i}{3}, C_3 \right), \left(N + \frac{1}{3}, -i\sigma_x C_3 \right), \right. \\ & \quad \left. \left(N + \frac{1}{3}, -i\sigma_y C_3 \right), \left(N + \frac{1}{3}, -i\sigma_z C_3 \right) \right\}, \\ \text{(V)} & \quad \left\{ \left(N + \frac{i}{3}, -C_3 \right), \left(N + \frac{1}{3}, i\sigma_x C_3 \right), \right. \\ & \quad \left. \left(N + \frac{i}{3}, i\sigma_y C_3 \right), \left(N + \frac{1}{3}, i\sigma_z C_3 \right) \right\}, \\ \text{(VI)} & \quad \left\{ \left(N - \frac{1}{3}, C_3^2 \right), \left(N - \frac{1}{3}, i\sigma_x C_3^2 \right), \right. \\ & \quad \left. \left(N - \frac{1}{3}, i\sigma_y C_3^2 \right), \left(N - \frac{1}{3}, i\sigma_z C_3^2 \right) \right\}, \\ \text{(VII)} & \quad \left\{ \left(N - \frac{1}{3}, -C_3^2 \right), \left(N - \frac{1}{3}, -i\sigma_x C_3^2 \right), \right. \\ & \quad \left. \left(N - \frac{1}{3}, -i\sigma_y C_3^2 \right), \left(N - \frac{1}{3}, -i\sigma_z C_3^2 \right) \right\}. \end{aligned} \quad (77)$$

They describe (I) integer vortices ($N = 0$ corresponds to the vacuum), (II) spin vortices of 2π rotation, (III) spin vortices

of π rotation around the x, y, z axes, and (IV) – (VII) 1/3-quantum vortices.

Other examples. Another example in condensed matter physics can be found in vortex lines in the dipole-free A-phase of SF ^3He Balachandran et al. (1984), Salomaa & Volovik (1987). An example in high energy physics can be found in color flux tubes (“non-Abelian” vortices) in high density QCD matter Fujimoto & Nitta (2021a,b,c), Eto & Nitta (2021).

4.3. Fusion rules for non-Abelian vortex anyons

Two non-Abelian vortices belonging to the same conjugacy class are indistinguishable even if they are not identical. For instance, a vortex $a \in \pi_1(G/H)$ and a vortex $b = cac^{-1}$ with $c \in \pi_1(G/H)$ are not the same and thus a and anti-vortex of b cannot pair annihilate. Nevertheless they are indistinguishable with a help of c . This leads a class of non-Abelian statistics Brekke et al. (1993), Lo & Preskill (1993), Lee (1994), Brekke et al. (1997). Such non-Abelian anyons are called non-Abelian vortex anyons.

In order to discuss non-Abelian vortex anyons, first we define anyons $\{\mathbf{1}, \sigma, \tau\}$ appropriately by conjugacy classes of non-Abelian vortices. Then, the fusion rule (3) for non-Abelian vortex anyons can be written as Mawson et al. (2019)

$$\begin{aligned} \tau \otimes \tau &= N_{\tau\tau}^{\mathbf{1}} \mathbf{1} \oplus N_{\tau\tau}^{\sigma} \sigma \oplus N_{\tau\tau}^{\tau} \tau, \\ \tau \otimes \sigma &= \tau, \quad \sigma \otimes \sigma = \mathbf{1}, \quad x \otimes \mathbf{1} = x, \end{aligned} \quad (78)$$

with $x \in \{\mathbf{1}, \sigma, \tau\}$.

Non-Abelian vortex anyons in D_2 -BN. Let us discuss the simplest case. For D_2 -BN liquid crystals or D_2 -BN phases of spin-2 BECs, the conjugacy class is given in Eq. (62). We then define

$$\mathbf{1} = \{+\mathbf{1}_2\}, \quad \sigma = \{-\mathbf{1}_2\}, \quad \tau = \{\pm i\sigma_a\} \quad (79)$$

with a being either $x, y, \text{ or } z$. The coefficient N_{ab}^c counts how many ways anyons a and b fuse to an anyon c . The relations $(-i\sigma_a)(+i\sigma_a) = (+i\sigma_a)(-i\sigma_a) = +\mathbf{1}_2$ and $(-i\sigma_a)(-i\sigma_a) = (+i\sigma_a)(+i\sigma_a) = -\mathbf{1}_2$ lead $N_{\tau\tau}^{\mathbf{1}} = 2$ and $N_{\tau\tau}^{\sigma} = 2$, respectively. Furthermore, τ anyons do not fuse to τ in this case and then $N_{\tau\tau}^{\tau} = 0$. We thus reach

$$\begin{aligned} \tau \otimes \tau &= 2\mathbf{1}_2 \oplus 2\sigma, \\ \tau \otimes \sigma &= \tau, \quad \sigma \otimes \sigma = \mathbf{1}, \quad x \otimes \mathbf{1} = x, \end{aligned} \quad (80)$$

with $x \in \{\mathbf{1}, \sigma, \tau\}$. Since two τ -anyons fuse to two different anyons $\mathbf{1}$ and σ , τ anyons are non-Abelian anyons. Comparing this fusion rule with that of the Ising anyons in Eq. (4), we find that these non-Abelian vortex anyons are similar to the Ising anyons. In fact, a τ anyon coincide with its anti-particle, and so similar to a Majorana fermion.

Gathering all $\tau_a = \{\pm i\sigma_a\}$ ($a = x, y, z$) together, we obtain the following fusion formula from the relation $(i\sigma_a)(i\sigma_b) = -\delta_{ab} + \epsilon_{abc}(-i\sigma_c)$:

$$\begin{aligned} \tau_a \otimes \tau_b &= 2\delta_{ab} \mathbf{1} \oplus 2\delta_{ab} \sigma \oplus 2\epsilon_{abc} \tau_c \\ \tau_a \otimes \sigma &= \tau_a, \quad \sigma \otimes \sigma = \mathbf{1}, \quad x \otimes \mathbf{1} = x, \end{aligned} \quad (81)$$

	I_0	II_0	III_0	IV_0	V_0	VI_{-1}	VII_{-1}
$\mathbf{1} = I_0$	I_0	II_0	III_0	IV_0	V_0	VI_{-1}	VII_{-1}
$\sigma = II_0$	I_0	I_0	III_0	V_0	IV_0	VII_{-1}	VI_{-1}
$\tau = III_0$	III_0	III_0	$6I_0 \oplus 6II_0 \oplus 4III_0$	$3IV_0 \oplus 3V_0$	$3IV_0 \oplus 3V_0$	$3VI_{-1} \oplus 3VII_{-1}$	$3VI_{-1} \oplus 3VII_{-1}$
IV_0	IV_0	V_0	$3IV_0 \oplus 3V_0$	$3VI_0 \oplus VII_0$	$VI_0 \oplus 3VII_0$	$4I_0 \oplus 3III_0$	$4II_0 \oplus 2III_0$
V_0	V_0	IV_0	$3IV_0 \oplus 3V_0$	$VI_0 \oplus 3VII_0$	$3VI_0 \oplus VII_0$	$4II_0 \oplus 2III_0$	$4I_0 \oplus 2III_0$
VI_{-1}	VI_{-1}	VII_{-1}	$3VI_{-1} \oplus 3VII_{-1}$	$4I_0 \oplus 2III_0$	$4II_0 \oplus 2III_0$	$3IV_{-1} \oplus V_{-1}$	$IV_{-1} \oplus 3V_{-1}$
VII_{-1}	VII_{-1}	VI_{-1}	$3IV_{-1} \oplus 3VII_{-1}$	$4II_0 \oplus 2III_0$	$4I_0 \oplus 2III_0$	$IV_{-1} \oplus 3V_{-1}$	$3IV_{-1} \oplus 2V_{-1}$

Table 2

Fusion rule for vortex anyons in a cyclic spin-2 BEC Mawson et al. (2019). The subscript on the conjugacy class denotes the $U(1)$ winding number N .

	I_0	II_0	III_0	IV_0	V_0	VI_0	VII_0
$\mathbf{1} = I_0$	I_0	II_0	III_0	IV_0	V_0	VI_0	VII_0
$\sigma = II_0$	II_0	I_0	III_0	IV_0	VI_0	V_0	VII_0
$\tau_1 = III_0$	III_0	III_0	$4I_0 \oplus 4II_0 \oplus 4IV_0$	$2III_0$	$2VII_0$	$2VII_0$	$4V_0 \oplus 4VI_0$
$\tau_2 = IV_0$	IV_0	IV_0	$2III_0$	$2I_0 \oplus 2II_0$	$V_0 \oplus VI_0$	$V_0 \oplus VI_0$	$2VII_0$
V_0	V_0	VI_0	$2VII_0$	$V_0 \oplus VI_0$	$2I_1 \oplus IV_1$	$2II_1 \oplus IV_1$	$2III_1$
VI_0	VI_0	V_0	$2VII_0$	$V_0 \oplus VI_0$	$2II_1 \oplus IV_1$	$2I_1 \oplus IV_1$	$2III_1$
VII_0	VII_0	VII_0	$4IV_0 \oplus 4V_0$	$2VII_0$	$2III_1$	$2III_1$	$4I_1 \oplus 4II_1 \oplus 4IV_1$

Table 3

Fusion rule for for vortex anyons in a D_4 -BN spin-2 BEC Mawson et al. (2019). The subscript on the conjugacy class denotes the $U(1)$ winding number N .

with $x \in \{\mathbf{1}, \sigma, \tau_x, \tau_y, \tau_z\}$. In this case, there are the three non-Abelian anyons τ_a coupled to each other.

Non-Abelian vortex anyons in spin-2 BECs.

Non-Abelian vortex anyons in spin-2 BECs were studied in Mawson et al. (2019). For the cyclic phase in a spin-2 BEC, $\{\mathbf{1}, \sigma, \tau\}$ are defined by the conjugacy classes (I), (II) and (III) with $N = 0$ in Eq. (77). Then, we have (see Table 2) $N_{\tau\tau}^{\mathbf{1}} = 6$, $N_{\tau\tau}^{\sigma} = 6$, $N_{\tau\tau}^{\tau} = 4$:

$$\begin{aligned} \tau \otimes \tau &= 6\mathbf{1} \oplus 6\sigma \oplus 4\tau, \\ \tau \otimes \sigma &= \tau, \quad \sigma \otimes \sigma = \mathbf{1}, \quad x \otimes \mathbf{1} = x, \end{aligned} \quad (82)$$

with $x \in \{\mathbf{1}, \sigma, \tau\}$. The non-Abelian $1/3$ -quantum vortices in (IV)–(VII) are also non-Abelian anyons but one cannot restrict to the $N = 0$ sector, and needs infinite numbers of anyons for a closed algebra.

The fusion rule for vortex anyons in the D_4 -BN phase of a spin-2 BEC was also obtained by the conjugacy classes (I)–(IV) in Eq. (72) Mawson et al. (2019). In this case, τ in the cyclic phase is split into $\tau_1 = III_0$ and $\tau_2 = IV_0$. Then, we have $N_{\tau_1\tau_1}^{\mathbf{1}} = 4$, $N_{\tau_1\tau_1}^{\sigma} = 4$, $N_{\tau_1\tau_1}^{\tau_1} = 4$, $N_{\tau_2\tau_2}^{\mathbf{1}} = 2$, $N_{\tau_2\tau_2}^{\sigma} = 2$ with the other components zero:

$$\begin{aligned} \tau_1 \otimes \tau_1 &= 4\mathbf{1} \oplus 4\sigma \oplus 4\tau_1, \\ \tau_2 \otimes \tau_2 &= 2\mathbf{1} \oplus 2\sigma, \\ \tau_i \otimes \sigma &= \tau_i, \quad \sigma \otimes \sigma = \mathbf{1}, \quad x \otimes \mathbf{1} = x, \end{aligned} \quad (83)$$

with $i = 1, 2$ and $x \in \{\mathbf{1}, \sigma, \tau_i\}$. See Table 3. The non-Abelian HQVs in (V)–(VII) are also non-Abelian anyons, but again infinite numbers of anyons are necessary for a closed algebra. The same fusion rule in Eq. (83) should hold for a D_4 -BN liquid crystal, as seen in Eq. (66).

Including Bogoliubov modes, the algebra of vortex anyons is extended to a quantum double Koornwinder et al.

(1999), Mawson et al. (2019). An application to quantum computation was also proposed in Ref. G en etay Johansen & Simula (2022).

5. 3P_2 topological SFs

Finally we discuss the two-fold non-Abelian object in a novel topological SF called a 3P_2 SF: The two-fold non-Abelian nature is attributed to the fermionic part (Sec. 3) and the vortex part (Sec. 4). The 3P_2 SF is a condensate of spin-triplet ($S = 1$) p -wave ($L = 2$) Cooper pairs with total angular momentum $J = 2$. In the following, we briefly review 3P_2 SFs in Sec. 5.1. In Sec. 5.2, the stability of a pair of HQVs compared with a singly quantized vortex is discussed. In Sec. 5.3, we show that a Majorana fermion, a non-Abelian Ising anyon, exists in the core of each HQV.

5.1. Overview of 3P_2 topological SFs

Study of 3P_2 SFs was initiated since 1970s Hoffberg et al. (1970), Tamagaki (1970), Takatsuka & Tamagaki (1971), Takatsuka (1972), Richardson (1972), Sedrakian & Clark (2018). On the basis of the analysis of the phase-shifts from nucleon-nucleon scattering in a free space, spin-singlet s -wave 1S_0 symmetry is a dominant attractive channel in the inner crust region ($\rho \lesssim 0.5\rho_0$, where $\rho_0 = 0.17\text{fm}^{-3}$ is called the nuclear density) Tamagaki (1970). The critical temperature was estimated as $10^8 - 10^{10}$ K, which is two orders of magnitude smaller than the Fermi energy. For further increase in density $0.7\rho_0 \lesssim \rho \lesssim 3\rho_0$ in the inner core region, the 1S_0 superfluidity is suppressed, and instead the attractive channel of the 3P_2 grows. Because of the attractively strong spin-orbit force, the 3P_2 Cooper pair channels with high angular momentum become more attractive than other 3P pairing symmetry in contrast to the atomic physics where

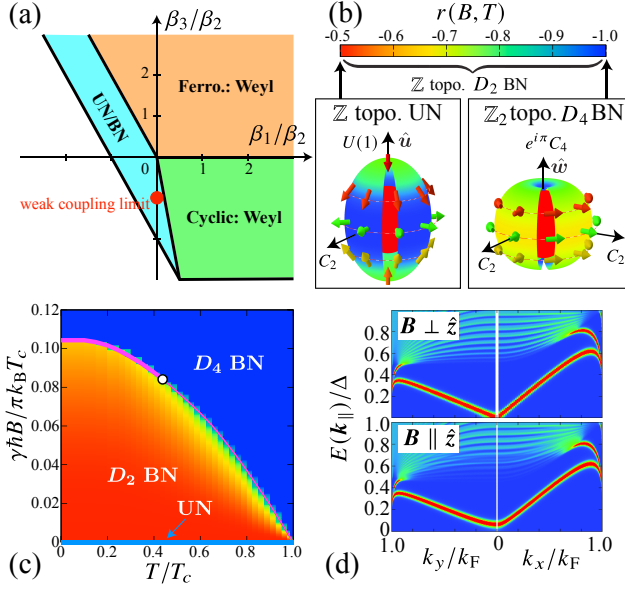


Figure 8: (a) Phase diagram without magnetic field based on the GL theory. (b) Gap structure of the nematic state. (c) Phase diagram with magnetic field in the weak coupling limit. (d) The momentum resolved local density state at the surface perpendicular to the \hat{z} axis. The magnetic field is applied parallel (perpendicular) to the surface [top (bottom) panel]. Figures are adapted from Ref. Mizushima et al. (2017) ©2022 American Physical Society.

the lower total angular momentum state is favored as in the SF $^3\text{He-B}$ phase. The anisotropic form of the Cooper pair is thought to affect the Cooling rate of neutron stars. Extreme conditions of neutron stars are not only high density, but also rapid rotation, and a strong magnetic field. Especially, neutron stars accompanied by magnetic field ranging from 10^{15} – 10^{18} G are called magnetars. Rich structures of exotic condensates and vortices explained below may be the origin of the observed *pulsar glitches*, that is, the sudden increase of the angular momentum of neutron stars. Among them, the existence of non-Abelian HQVs in high magnetic fields is responsible for the scaling law of the glitches without any fitting parameters Marmorini et al. (2020).

In terms of the symmetry point of view, $^3\text{P}_2$ SFs spontaneously break the global gauge symmetry $U(1)_\varphi$ and the simultaneous rotational symmetry in the spin-momentum space $SO(3)_J$ which originally exist in the normal state inside neutron stars. The order parameter of $^3\text{P}_2$ SFs is spanned by 3 by 3 traceless symmetric tensor $A_{\mu i}$, where the 2 by 2 gap function in momentum space can be given by $\hat{\Delta}(\mathbf{k}) = A_{\mu i} \hat{k}_i \hat{\sigma}_\mu i \hat{\sigma}_y$. For later convenience, we introduce a representation based on the total angular momentum along the quantization axis, $M = -2, \dots, 2$:

$$A_{\mu i} = \sum_{M=-2}^2 \gamma_M [\Gamma_M]_{\mu i}, \quad (84)$$

where γ_M is a complex wave function of the Cooper pair in the angular momentum sector M . A basis set Γ_M is given

for the quantization axis \hat{w} by

$$[\Gamma_{\pm 2}]_{\mu i} = \frac{(\hat{u} \pm i\hat{v})_\mu (\hat{u} \pm i\hat{v})_i}{2}, \quad (85)$$

$$[\Gamma_{\pm 1}]_{\mu i} = \mp \frac{(\hat{u} \pm i\hat{v})_\mu \hat{w}_i + \hat{w}_\mu (\hat{u} \pm i\hat{v})_i}{2}, \quad (86)$$

$$[\Gamma_0]_{\mu i} = \frac{-\hat{u}_\mu \hat{u}_i - \hat{v}_\mu \hat{v}_i + 2\hat{w}_\mu \hat{w}_i}{\sqrt{6}}, \quad (87)$$

where \hat{u} , \hat{v} , and \hat{w} constitute the orthonormal triad.

From a phenomenological aspect, the Ginzburg-Landau (GL) energy functional invariant under the $SO(3)_J$ and $U(1)_\varphi$ symmetry was obtained for $^3\text{P}_2$ SFs as Richardson (1972), Fujita & Tsuneto (1972), Sauls & Serene (1978), Muzikar et al. (1980), Sauls et al. (1982)

$$\mathcal{F} = \alpha \text{tr}[AA^*] + \beta_1 |\text{tr} A^2|^2 + \beta_2 (\text{tr}[AA^*])^2 + \beta_3 \text{tr}[A^2 A^{*2}]. \quad (88)$$

It should be remarked that spin-2 spinor BECs ($L = 0, S = 2$) and d -wave superconductivity ($L = 2, S = 0$) have similar order parameter structures. The GL functional for the $^3\text{P}_2$ Cooper pairs was minimized by Sauls and Serene by using the correspondence to the $L = 2$ GL functional which was solved by Mermin Sauls & Serene (1978), Mermin (1974). The ground state solutions are classified into three types of phases determined by $\beta_{i=1,2,3}$, as shown in Fig. 8(a): nematic phases with time reversal symmetry and the cyclic and ferromagnetic phases as non-unitary state. The microscopic derivation of the GL parameters clarifies that the ground state is the nematic phases in the weak coupling limit Sauls & Serene (1978), Sauls (1980). The order parameter tensor of a nematic phase is given by $A_{\mu i} = \Delta[\hat{u}_\mu \hat{u}_i + r \hat{v}_\mu \hat{v}_i - (1+r) \hat{w}_\mu \hat{w}_i]$ with a real number $r \in [-1, -1/2]$ [see also Eq. (68)]. The nematic phase has a continuous degeneracy which is lifted by either a magnetic field or sixth-order terms in the GL free energy. For the GL parameters derived from the microscopic model, the UN phase for $r = -1/2$ is favored at zero magnetic field while D_2 -BN ($-1 < r < -1/2$) and D_4 -BN $r = -1$ phases are favored for moderate and strong magnetic fields, respectively Masuda & Nitta (2016), relevant for magnetars. The schematic images of the gap structures for the UN and D_4 -BN states are shown in Fig. 8(b), where the arrows account for the momentum-dependent direction of the d -vector, defined by $d_\mu(\mathbf{k}) = \sum_i A_{\mu i} k_i$. We will discuss other possible states later in the context of the fermionic topology.

The microscopic model of $^3\text{P}_2$ SFs in terms of the fermion degrees of freedom was constructed by Richardson Richardson (1972) and Tamagaki and Takatsuka Tamagaki (1970), Takatsuka & Tamagaki (1971), Takatsuka (1972): The starting microscopic Hamiltonian is composed of the one-body term H_1 and the interaction term H_2 given, respectively, in the following forms:

$$H_1 = \int d\mathbf{r} \bar{\psi}^\dagger(\mathbf{r}) [\hat{h}_N(-i\nabla)] \bar{\psi}(\mathbf{r}), \quad (89)$$

$$H_2 = - \int d\mathbf{r} \sum_{\alpha\beta=x,y,z} \frac{g}{2} T_{\alpha\beta}^\dagger(\mathbf{r}) T_{\alpha\beta}(\mathbf{r}). \quad (90)$$

In the first line, $[\tilde{\psi}(\mathbf{r})]_\sigma = \psi_\sigma(\mathbf{r})$ and $[\hat{h}_N(-i\nabla)]_{\sigma,\sigma'}$ is the sum of the kinetic energy $h_0(-i\nabla)\delta_{\sigma,\sigma'} = (-\nabla^2/2m - \mu)\delta_{\sigma,\sigma'}$ measured from the chemical potential μ , and the Zeeman energy $-\mathbf{B} \cdot \hat{\sigma}$ for a magnetic field $\mathbf{B} = B\mathbf{n}$. The 3P_2 force with coupling strength $g > 0$ is represented by H_2 with the pair-annihilation operator T defined by $T_{\alpha\beta}(\mathbf{r}) = \sum_{\sigma\sigma'} [t_{\alpha\beta,\sigma\sigma'}(-i\nabla)\psi_{\sigma'}(\mathbf{r})\psi_\sigma(\mathbf{r})]$, where $\bar{\nabla} \equiv k_F^{-1}\nabla$. We have introduced a spin-momentum coupling in the pair force via the 2×2 matrix in spin space $\hat{t}_{\alpha\beta}$ defined by $\hat{t}_{\alpha\beta}(-i\nabla) = i\hat{\sigma}_y \left\{ [\hat{\sigma}_\alpha(-i\nabla_\beta) + \hat{\sigma}_\beta(-i\nabla_\alpha)] / 2\sqrt{2} - \delta_{\alpha\beta}\hat{\sigma} \cdot (-i\nabla) / 3\sqrt{2} \right\}$. Within the mean field approximation, the BdG equation is derived as,

$$\check{H}(-i\nabla, \mathbf{R})\vec{u}_v(\mathbf{R}) = \epsilon_v\vec{u}_v(\mathbf{R}), \quad (91)$$

$$\check{H}(-i\nabla, \mathbf{R}) = \begin{pmatrix} \hat{h}_N(-i\nabla) & \hat{\Delta}(-i\nabla, \mathbf{R}) \\ -[\hat{\Delta}(-i\nabla, \mathbf{R})]^* & -[\hat{h}_N(-i\nabla)]^* \end{pmatrix}, \quad (92)$$

where the gap matrix is given by $\hat{\Delta}(-i\nabla, \mathbf{R}) = \sum_{\alpha,\beta} \frac{i\hat{\sigma}_\alpha\hat{\sigma}_\beta}{2k_F} \{ 2A_{\alpha\beta}(\mathbf{R})(-i\nabla_\beta) + [(-i\nabla_\beta)A_{\alpha\beta}(\mathbf{R})] \}$. This model was also used to determine the aforementioned GL parameters in the weak coupling limit and was directly investigated within a quasiclassical approximation recently in Ref. Mizushima et al. (2017). Even in the presence of the magnetic field, the quasiclassical approximation where the size of the Fermi surface is treated as an infinite one, predicts that a nematic state is the most stable with parameter r determined by the strength of the magnetic field as in the GL theory. The T - B phase diagram is shown in Fig. 8(c). As explained later, the ferromagnetic state appears near T_c when the finite-size correction of the Fermi surface is taken into account. The microscopic analysis reveals the existence of the tricritical point on the phase boundary between the D_4 -BN and D_2 -BN states in the T - B phase diagram shown in Fig. 8(c): at temperatures below the tricritical point, the phase transition becomes discontinuous Mizushima et al. (2017). The existence of the tricritical point was later confirmed in Ref. Mizushima et al. (2020) also in the GL theory with higher order terms (up to the eighth order Yasui, Chatterjee, Kobayashi & Nitta (2019)). In addition to such drastic change in critical phenomena, the advantage of the microscopic model lies in studies of the fermionic topology of the superfluidity. In the following, we explain the fermionic topology of the possible phases of the 3P_2 SFs.

Nematic state. In the weak coupling limit without a magnetic field, the UN state is the ground state. The order parameter tensors of the UN state and the BN state under a magnetic field are already explained above. On the basis of the symmetry of the BdG Hamiltonian, the nematic state is revealed as a topological SF with time reversal symmetry (a class DIII in the classification of topological insulators and SCs). The analysis of the BdG equation in the presence of the boundary clarifies the existence of the gapless

surface bound Majorana fermion, the hallmark character of the topological states. The surface Majorana fermion has an Ising spin character Chung & Zhang (2009), Nagato et al. (2009), Volovik (2010), Mizushima & Machida (2011), that is, the only external field coupled to the Ising spin gives a mass gap to the Majorana fermion as shown in Fig. 8(d). The magnetic field direction giving the gap to the Majorana fermion is the direction perpendicular to the surface, denoted by \mathbf{n}_\perp . This is because the surface Majorana fermion is protected not only by the time reversal symmetry but also another key symmetry, which is the magnetic π -rotation symmetry about \mathbf{n}_\perp . The magnetic π -rotation symmetry is also called the \bar{P}_3 symmetry⁵. The magnetic π -rotation is the combined operation of the time-reversal and the π rotation. The chiral operator, defined by the combination of particle-hole operation C and the magnetic π -rotation \bar{P}_3 as $\Gamma = C\bar{P}_3$, commutes with the Hamiltonian $\mathcal{H}(\mathbf{k}_\perp)$ with magnetic field $\mathbf{B} \cdot \mathbf{n}_\perp = 0$ and the chiral symmetric momentum $\mathbf{k}_\perp = k_\perp \mathbf{n}_\perp$ such that $\Gamma : \mathbf{k}_\perp \rightarrow \mathbf{k}_\perp$. Using this commutation relation, a one-dimensional winding number can be introduced as $w_{1d} = -\frac{1}{4\pi i} \int dk_\perp \text{Tr}[\Gamma \mathcal{H}(\mathbf{k}_\perp) \partial_{k_\perp} \mathcal{H}(\mathbf{k}_\perp)] = 2$, which is unchanged unless the symmetry is broken or the bulk gap is closed. The P_3 symmetry and thus the chiral symmetry is broken by the magnetic field $\mathbf{B} \cdot \mathbf{n}_\perp \neq 0$ which gives a mass gap to the Majorana fermion (the bottom panel of Fig. 8(d), where $\mathbf{n}_\perp \parallel \hat{z}$).

Cyclic state. For $-6\beta_1 < \beta_3 < 0$ based on the basis of $SO(3)_J$ invariant GL functional, the cyclic state is the ground state. The order parameter tensor has a form of $A_{\mu i} = \Delta[\hat{u}_\mu \hat{u}_i + \omega \hat{v}_\mu \hat{v}_i + \omega^2 \hat{w}_\mu \hat{w}_i]$ with $\omega = e^{2\pi i/3}$ [see also Eq. (73)], which is unique except for trivial $SO(3)_J$ and $U(1)_\varphi$ rotations. In the absence of magnetic field, the quasiparticle excitation energy consists of two branches $E_\pm(\mathbf{k}) = [h_0(\mathbf{k})^2 + |\mathbf{d}(\mathbf{k})|^2 \pm |\mathbf{d}(\mathbf{k}) \times \mathbf{d}^*(\mathbf{k})|]^2$, where $E_+(\mathbf{k})$ is full gap and $E_-(\mathbf{k})$ has 8 nodal points $\pm \mathbf{k}_{\alpha=1,\dots,4}$, each of which is a Weyl point. The subscript α denotes the 4 vertices of a tetrahedron, and \pm represents the monopole charge of the Weyl point. Because of the topological nature of Weyl SCs/SFs, there exist surface zero energy states which connect two oppositely charged Weyl points on the projected momentum space normal to the surface direction.

Ferromagnetic state. For $|\beta_1| - \beta_1 < \beta_3$, the ferromagnetic state described by $A_{\mu i} = \Delta(\hat{u}_\mu + i\hat{v}_\mu)(\hat{u}_i + i\hat{v}_i)$ minimizes the GL functional. This non-unitary state is also unique except for trivial $SO(3)_J$ and $U(1)_\varphi$ rotations. The order parameter is equivalent to the A_1 state of the SF³He. The bulk quasiparticle spectrum consists of two parts: one is a normal fluid, and the other is a Weyl SF with a pair of oppositely charged Weyl fermions. The ferromagnetic state is also realized in the limit of a strong magnetic field or the vicinity of the critical temperature even in the weak coupling limit owing to the finite-size correction of the Fermi surface.

Magnetized nematic state. Recently, even in the weak coupling limit, non-unitary states are predicted in a magnetic field Mizushima et al. (2021). As mentioned above, quasi-

⁵Here we use the bar to distinguish the magnetic π -rotation about the x -axis introduced later.

classical approximation, which treats the size of the Fermi surface as infinity, allows only the nematic states, which is unitary. By contrast, in the presence of the finite-size correction of the Fermi surface, a magnetic field along the \hat{w} -direction induces the non-unitary component into the nematic state with $r \in (-1, -1/2)$ as $A_{\mu i} = \Delta[\hat{u}_\mu \hat{u}_i + r \hat{v}_\mu \hat{v}_i + i\kappa(\hat{u}_\mu \hat{v}_i + \hat{v}_\mu \hat{u}_i) - (1+r)\hat{w}_\mu \hat{w}_i]$ or equivalently

$$A_{\mu i} = \Delta \begin{pmatrix} 1 & i\kappa & 0 \\ i\kappa & r & 0 \\ 0 & 0 & -(1+r) \end{pmatrix}. \quad (93)$$

For simplicity, Ref. Mizushima et al. (2021) studies the case of $r = -1$, i.e., in a strong magnetic field. In the quasi-classical limit, $\kappa = 0$ and the D_4 -BN state is realized. The order parameter tensor in the angular momentum representation is reduced to $A_{\mu i} = \Delta[\Gamma_2 + \Gamma_{-2}]_{\mu i}$, which shows the same gap amplitudes for $M = \pm 2$. The finite size correction of the Fermi surface induces a finite κ . In the angular momentum representation, the order parameter tensor becomes $A_{\mu i} = \Delta[(1 + \kappa)\Gamma_2 + (1 - \kappa)\Gamma_{-2}]_{\mu i}$. Thus, κ represents the imbalance between the $M = \pm 2$ sectors. In terms of the gap matrix in the spin basis, the Cooper pairs are decomposed into two spin polarized sectors $|\uparrow\uparrow\rangle$ and $|\downarrow\downarrow\rangle$ with different gap amplitudes. Each spin sector has a polarized orbital angular momentum state, and thus, a pair of the Weyl fermions appears at the north pole and the south pole in each spin sector. The orbital angular momentum between these two spin states are opposite, which means that two Weyl fermions with opposite helicity at each pole. This is in contrast to the A_2 phase proposed for the SF ^3He . In the limit of a strong magnetic field or the vicinity of the critical temperature, $\kappa \rightarrow 1$, the ferromagnetic state is realized. However, we note that this imbalance originates from the finite size effect of the Fermi surface. The effect is parametrized by Δ/ε_F , which is usually small for conventional neutron stars, and thus the imbalance κ is also expected to be small.

Vortices in 3P_2 SFs. The vortices admitted in 3P_2 SFs are basically the same as those in spin-2 BECs, which are discussed in Sec. 4.2. Table 4 summarizes remaining symmetry, order parameter manifold, and fundamental group of the topological defects of the above-discussed possible phases. Non-Abelian vortex anyons are included in the D_2 - and D_4 -BN states and the cyclic state as discussed in Sec. 4.3. Non-Abelian vortex anyons in the D_2 -BN states are spin vortices of π rotation, as shown in Eq. (81). The D_4 -BN states admit HQVs (V)–(VII) in Eq. (72) in addition to spin vortices (III) and (IV) in Eq. (72) as non-Abelian vortex anyons (see also Table 3). The cyclic states admit 1/3-quantum vortices (IV)–(VII) in Eq. (77) as well as spin vortices (III) in Eq. (77) as non-Abelian vortex anyons (see also Table 2).

Especially, the non-Abelian vortex in the D_4 -BN state is the main target in the remaining part. We explain the vortices in the D_4 -BN state in the beginning of the next subsection.

5.2. Half quantum vortex in D_4 -BN state

Vortices in D_4 -BN state. The D_4 -BN state, which can

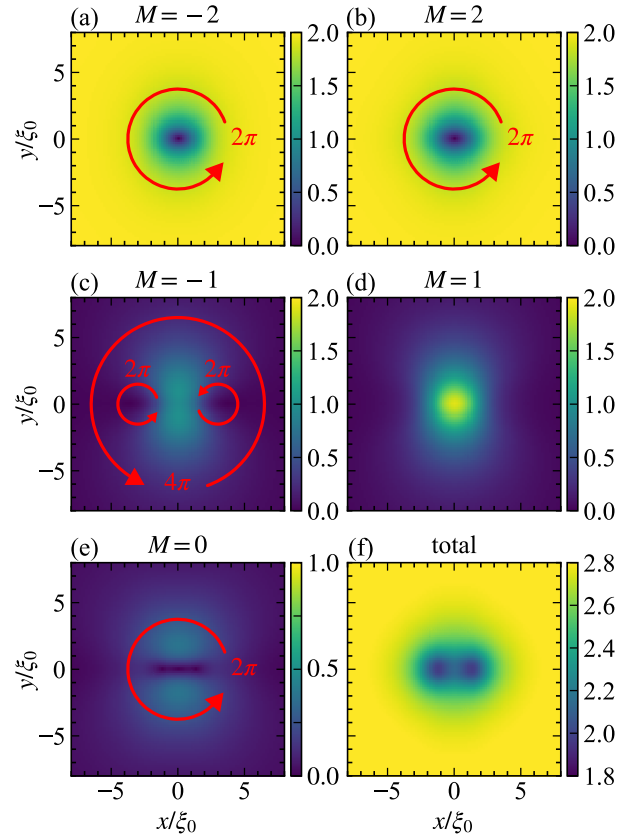


Figure 9: Gap structure of the d vortex in the D_4 -BN state ($T = 0.4T_c$ and $B = 0.5T_c$). (a)–(e) Amplitude of each angular momentum sector. Red arrows indicate the phase winding structures. (f) Total amplitude of the order parameter defined by $[\frac{3}{2}\text{Tr} \langle \hat{\Delta}^\dagger \hat{\Delta} \rangle_F]^{1/2}$.

be thermodynamically stabilized by a large magnetic field, has a pair of point nodes at the north and south poles along the direction of the magnetic field Masuda & Nitta (2016), Mizushima et al. (2017), Yasui, Chatterjee & Nitta (2019), Mizushima et al. (2020). Hereafter, we focus on the D_4 -BN state with a pair of point node along $\hat{w} = \hat{z}$. The homogeneous order parameter tensor has a diagonal form Sauls & Serene (1978): $A = \Delta \text{diag}(1, -1, 0)$ [Eq. (68)], which is invariant under a D_4 group. (A similar order parameter form is taken in the planar state of SF ^3He Makhlin et al. (2014), Silaev & Volovik (2014), but different topological defects are resulted from different order parameter manifolds.)

As already discussed in Sec. 4, the order parameter manifold in the D_4 -BN state is then characterized by the broken symmetry, $R \simeq [U(1) \times SO(3)]/D_4$, see Eq. (69). The topological charges of line defects are characterized by the first homotopy group, Eq. (75)

$$\pi_1(R) \simeq \mathbb{Z} \times_h D_4^* \quad (94)$$

where \times_h denotes a product defined in Ref. Kobayashi et al. (2012). This ensures two different classes of topological line defects: Vortices with commutative topological charges

Table 4

Summary of order parameters (r, κ in Eq. (93)), remaining symmetry (H), ($R \simeq G/H$), and topological vortices $\pi_1(R)$ in possible phases, taken from Ref. Mizushima et al. (2021). See also the references therein.

phase	r & κ in Eq. (93)	H	$R \simeq G/H$	$\pi_1(R)$
UN	$r = -1/2$ & $\kappa = 0$	$D_\infty \simeq O(2)$	$U(1) \times \mathbb{R}P^2$	$\mathbb{Z} \oplus \mathbb{Z}_2$
D_2 -BN	$r \in (-1, -1/2)$ & $\kappa = 0$	D_2	$[U(1) \times SO(3)]/D_4$	$\mathbb{Z} \oplus \mathbb{Q}$
D_4 -BN	$r = -1$ & $\kappa = 0$	D_4	$[U(1) \times SO(3)]/D_4$	$\mathbb{Z} \times_h D_4^*$
Cyclic	$r = e^{i2\pi/3}$ & $\kappa = 0$	T	$[U(1) \times SO(3)]/T$	$\mathbb{Z} \times_h T^*$
Mag. D_2 -BN	$r \in (-1, -1/2)$ & $\kappa \in (0, 1)$	0	$U(1) \times SO(3)$	$\mathbb{Z} \oplus \mathbb{Z}_2$
Mag. D_4 -BN	$r = -1$ & $\kappa = -1$	C_4	$[U(1) \times SO(3)]/Z_4$	$\mathbb{Z} \times_h C_4^*$
FM	$r = -1$ & $\kappa = 1$	$U(1)_{J_z+2\Phi}$	$SO(3)_{J_z-2\Phi}/\mathbb{Z}_2$	\mathbb{Z}_4

and vortices with non-commutative topological charges. The former includes integer vortices (I) in Eq. (72) with or without internal structures, while an example of the latter is the non-Abelian HQV, (V)–(VII) in Eq. (72). Integer vortices are characterized by vorticity quantized to an integer number because of the singlevaluedness of the order parameter. Fractionally quantized case such as a HQV usually has a phase jump (π -phase jump for a HQV) along the contour surrounding the vortex. In the D_4 -BN state, however, the phase discontinuity is compensated by the phase originating from the discrete rotation of the D_4 symmetry. Thereby HQVs are topologically allowed. Here, we particularly focus on the case where the vorticity is along the \hat{z} -direction accompanying the π -phase jump compensated by the C_4 rotation about the \hat{z} -axis, as indicated in Figs. 8(b), 10(a), 10(f), and 11(a). Such HQVs belong to the group (V) or (VI) in Eq. (72).

Hereafter, we review possible vortices when the vorticity and the point nodes of the D_4 -BN state are along the \hat{z} -direction. As a basis set of the order parameter tensor $A_{\mu i}$, the eigenstates of the z component of the total angular momentum, denoted by $J_z \Gamma_M = M \Gamma_M$, are convenient: $A_{\mu i}(\rho, \theta) = \sum_{M=-2}^2 \gamma_M(\rho, \theta) [\Gamma_M]_{\mu i}$, where the cylindrical coordinate system $\mathbf{R} = (\rho, \theta)$ is introduced with assumption of uniformity along the z -direction. In the region far from the vortex core $\rho \rightarrow \infty$, there is no radial dependence, and the order parameter modulation is described by the $U(1)$ phase rotation characterized by vorticity κ and the simultaneous rotation in the spin-orbit space of Cooper pairs. For the latter rotation by angle φ about the \hat{z} -axis, the other components of the triad, \hat{x} , and \hat{y} , are transformed as

$$R(\varphi) : \hat{x} \rightarrow \cos \varphi \hat{x} + \sin \varphi \hat{y}, \quad (95)$$

$$R(\varphi) : \hat{y} \rightarrow -\sin \varphi \hat{x} + \cos \varphi \hat{y}. \quad (96)$$

Using Γ_M , the $U(1)$ phase winding and the spin-orbit rotation for non-zero bulk components (i.e., $\rho \rightarrow \infty$) are expressed as

$$\begin{aligned} A_{\mu i}(\theta) &= \sum_{M=-2}^2 \gamma_{M,\infty} e^{i\kappa\theta - M\varphi} [\Gamma_M]_{\mu i} \\ &\equiv \sum_{M=-2}^2 \gamma_{M,\infty} e^{i(\kappa - nM)\theta} [\Gamma_M]_{\mu i}. \end{aligned} \quad (97)$$

Especially, in the D_4 -BN state with the point nodes along the \hat{z} -axis, $|\gamma_{2,\infty}| = |\gamma_{-2,\infty}|$ and $\gamma_{\pm 1,\infty} = \gamma_{0,\infty} = 0$. Here in the second line, we parametrize $\varphi = n\theta$ along the contour surrounding the vortex, where the spin-orbit rotation can be regarded as the n -fold J -disgyration⁶. Note that n is not necessarily an integer. The boundary condition of a vortex characterized by (κ, n) is given by Eq. (97).

Axisymmetric singly quantized vortex. The integer vortices belong to a class $\kappa \in \mathbb{Z}$. Even in the singly quantized case $\kappa = \pm 1$, however, there are many possibilities because of differences in the internal structure and the disgyration in the spin-orbit space. As a simple case, the axisymmetric vortex can be described as $A_{\mu i}(\rho, \theta) = \sum_{M=-2}^2 \gamma_M(\rho) e^{i(\kappa - M)\theta} [\Gamma_M]_{\mu i}$ in a whole region, which includes complex radial functions $\gamma_M(\rho)$ to be determined. The disgyration of the axisymmetric vortex is 1-fold ($n = 1$ in Eq. (97)), that is, the 2π rotation of the triad around the vortex. Thus, the axisymmetric vortex belongs to the conjugacy class (II) in Eq. (72)⁷. Although the loss in the kinetic energy becomes large because of the J -disgyration, there is a nice analogy with vortices in SF $^3\text{He-B}$ phase. As in the SF $^3\text{He-B}$ phase, the symmetry of the vortices can be characterized by three discrete symmetries called $P_{1,2,3}$ symmetries Salomaa & Volovik (1985b, 1987), which are discussed in the next subsection⁸. The internal structures $\gamma_{-1,0,1}(\rho)$ characterize a classification based on these discrete symmetries, which allows several vortices as summarized in Table 5.2. Within an axisymmetric condition, only o vortex or v vortex is realized as a self-consistent solution. The o vortex has a singular core and is the most symmetric one so that it meets all the discrete symmetries. By contrast, the core of the axisymmetric v vortex is occupied by the SF component $\gamma_{\pm 1}$ for $\kappa = \pm 1$, and it has the P_2 (magnetic mirror reflection) symmetry, but does not have the P_1 (inversion) or P_3 (magnetic π -rotation about the x axis) symmetries. Energetically, the v vortex is more stable than the o vortex because of a gain in the condensation energy in the core

⁶The term “ J -disgyration” accounts for a singularity in the spin-orbit space, i.e., the total angular momentum (J) space. Spin disgyrations and orbital disgyrations are introduced after Eq. (32).

⁷In Sec. 4.2, we discuss the spin vortex of 2π rotation in spin-2 BECs.

⁸The P_3 symmetry is already introduced when defining the one-dimensional winding number in the bulk nematic state.

vortex	$\gamma_{M=0}(\rho)$	$\gamma_{M=\pm 1}(\rho)$	core	symmetry
o vortex	real	zero	singular	P_1, P_2, P_3
u vortex	complex	zero	singular	P_1
v vortex	real	real	coreless	P_2
w vortex	real	imaginary	coreless	P_3
uvw vortex	complex	complex	coreless	-

Table 5

Internal structures of axisymmetric vortices. The second and third columns show order parameters of the core structure. The fourth column is coreless (singular) whether the vortex core is occupied (unoccupied) by some SF components. The last column accounts for the preserved symmetry.

region. However, the induced component of the v vortex which occupies the core is suppressed by a magnetic field.

Non-axisymmetric singly quantized vortex. Without the axisymmetric condition, the lower energy condition for a singly quantized vortex is given by $(\kappa, n) = (\pm 1, 0)$ to reduce the loss of the gradient energy. Such a vortex belongs to the conjugacy class (I) in Eq. (72). In this case, so called double-core vortex (d vortex) can be a self-consistent solution Masaki et al. (2022) as in the SF $^3\text{He-B}$ phase Thuneberg (1986), Salomaa & Volovik (1986). The d vortex is also called the non-axisymmetric v vortex because it has the P_2 symmetry but does not have the P_1 and P_3 symmetries Tsutsumi et al. (2015). Note that the axial symmetry is spontaneously broken for the d vortex in the SF $^3\text{He-B}$ phase, while the symmetry is broken by the boundary condition for the d vortex in a 3P_2 SF. Figure 9 shows the order parameter structure of the d vortex in the D_4 -BN state for $T = 0.4T_c$ and $B = 0.5T_c$ with critical temperature T_c . In the panels, the unit of length is the coherence length defined by $\xi_0 = v_F/2\pi T_c$ with Fermi velocity v_F , where $\langle \dots \rangle_F$ accounts for the Fermi surface average. The bulk components $\gamma_{\pm 2}$ have a conventional vortex structure with a single phase winding [see panels (a) and (b)]. The double core structure can be clearly observed in the total amplitude defined by $[\frac{3}{2}\text{Tr} \langle \hat{\Delta}^\dagger \hat{\Delta} \rangle_F]^{1/2}$ in panel (f). Such a structure is due to the occupations of the core by $\gamma_{M=\pm 1}$ as shown in panels (c) and (d). As can be seen below, the d vortex is not the lowest energy state among the vortex states with $(\kappa, n) = (\pm 1, 0)$ in the D_4 -BN state and it splits into two HQVs. The d vortex in the SF $^3\text{He-B}$ phase is the most stable vortex solution in the low pressure region Kasamatsu et al. (2019), Regan et al. (2019). A d vortex is realized as the lowest energy state in the UN and the D_2 -BN states.

HQVs. The HQVs can be characterized by $\kappa = \pm 1/2$. The possibility of the half-quantized vortex in the D_4 -BN state was pointed out long back in 1980 Sauls (1980) on the basis of the topological consideration of the form of $A_{\mu i}$. Since κ is a half odd integer, the $U(1)$ phase part gives the minus sign under the spatial rotation $\theta \rightarrow \theta + 2\pi$. By rotating the triad by angle $\pm\pi/2$ while going around the vortex, which is denoted by $n = \pm 1/4$ in Eq. (97), the above minus sign can be compensated by the other minus sign stemming from the disgyration. This topological consideration is represented by the boundary condition Eq. (97) with $(\kappa, n) =$

$(\pm 1/2, \pm 1/4)$, which belongs to the conjugacy class (V) or (VI) in Eq. (72). The gradient energy of an isolated HQV far from the core is a half of that of an singly quantized vortex described by $(\kappa, n) = (\pm 1, 0)$, namely, the energy of two HQVs is the same as that of the singly quantized vortex except for contributions from the vortex cores. In other words, whether the singly quantized vortex can split into two HQVs depends on the energy of their internal structures and the interaction energy between two HQVs.

Although the above topological consideration does not take into account the core structure, recently, the whole structures of isolated HQVs were studied using the phenomenological GL theory Masuda & Nitta (2020), Kobayashi & Nitta (2022a,b), and the microscopic quasi-classical theory Masaki et al. (2022). It is proposed that an integer vortex with $\kappa = 1$ can split into two HQVs with $(\kappa, n) = (1/2, 1/4)$ and $(\kappa, n) = (1/2, -1/4)$ Masuda & Nitta (2020). Here we assume that $\kappa > 0$ without loss of generality. The configuration of the two HQVs given as one for $n_1 = +1/4$ with its core at \mathbf{R}_1 and the other for $n_2 = -1/4$ with its core at \mathbf{R}_2 has the following boundary condition at \mathbf{R} :

$$A(\mathbf{R}) \sim \sum_{M=\pm 2} e^{i(\kappa-n_1 M)\theta_1 + i(\kappa-n_2 M)\theta_2} \gamma_M \Gamma_M, \quad (98)$$

where θ_1 (θ_2) is the angle of $\mathbf{R} - \mathbf{R}_1$ ($\mathbf{R} - \mathbf{R}_2$). Since the difference between θ_1 and θ_2 is negligible for $|\mathbf{R}| \rightarrow \infty$, the phase part behaves as $\exp(2i\kappa\theta)$ [$\theta \simeq (\theta_1 + \theta_2)/2$], which means the boundary conditions for the two HQVs and the singly quantized vortex are equivalent in the limit $\rho \rightarrow \infty$. In the following, we explain the internal structure of each HQV, and the interaction energy of the two HQV vortex through the comparison of the singly quantized vortex Masaki et al. (2022). Particularly, the non-axisymmetric internal structure of each HQV is important to the interaction energy.

Isolated HQV $(\kappa, n) = (1/2, +1/4)$. The two disgyrations of the triads, given by $n = \pm 1/4$, are inequivalent because one is parallel to the vorticity, while the other is antiparallel. Here we first explain the antiparallel case $(n, \kappa) = (1/2, 1/4)$. In the above notation, by setting $\mathbf{R}_1 = (0, 0)$ and $\mathbf{R}_2 = (-\infty, 0)$, and thus setting $\theta_2 \rightarrow 0$, the boundary condition is obtained from Eq. (98). In this case, the relative phase of $\gamma_{\pm 2}$ is zero, and the schematic image of the disgyration is drawn in Fig. 10(a). Each circular object shows the directions of d -vectors by colored arrows, whose color bar is the same as in panel (c). There are also the cyan and magenta lines, which represent the directions of the eigenvalues $+1$ and -1 of the order parameter A , respectively. This HQV is $(1/2, C_4)$ in the conjugacy class (V) in Eq. (72). The self-consistent solutions of the non-trivial components are shown in panels (b)–(e). Here γ_2 , not shown, is almost uniform without phase winding, as expected from the boundary condition $\kappa - n_1 M = 1/2 - 1/4 * 2 = 0$. The other bulk component γ_{-2} is a conventional singular vortex with the single phase winding shown in panel (c). The amplitude and the phase of the internal structure of γ_0 are, respectively, shown in panels (d) and (e). The phase of the internal

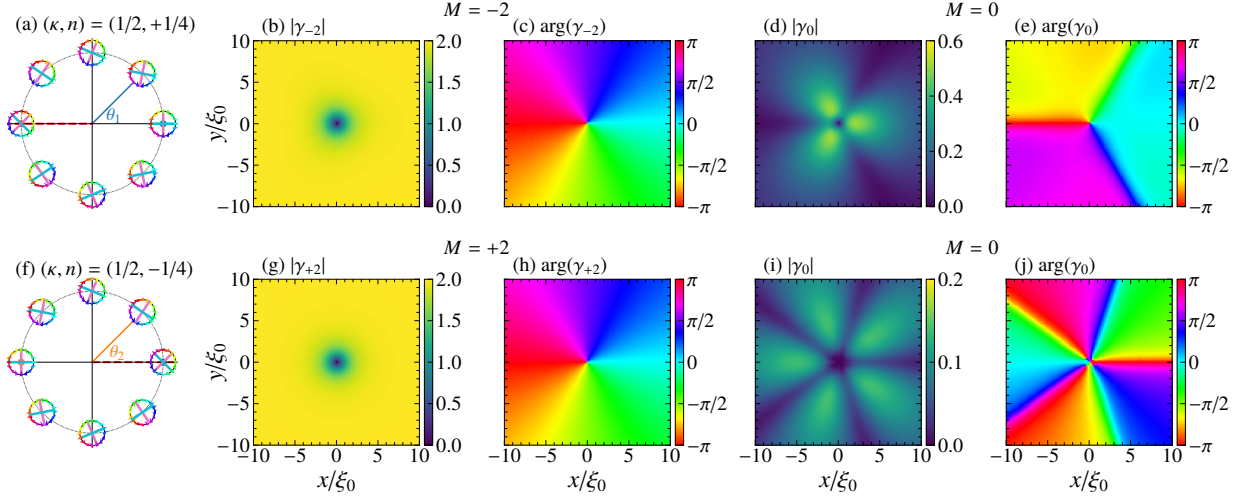


Figure 10: HQV with $(\kappa, n) = (1/2, +1/4)$ [(a) - (e)] and $(\kappa, n) = (1/2, -1/4)$ [(f) - (j)]. The boundary conditions are sketched in (a) and (f). The amplitudes of γ_M for $M = -2$ and 0 (+2 and 0) are shown in (b) and (d) [(g) and (i)], respectively. The phases of γ_M for $M = -2$ and 0 (+2 and 0) are shown in (c) and (e) [(h) and (j)], respectively. Figures are adapted from Ref. Masaki et al. (2022) ©2022 American Physical Society.

structure is oppositely winding against γ_{-2} , which can be understood by analogy with a vortex in a spinless chiral p -wave SC. We assume, for simplicity, $\bar{k}_z = 0$, and then write $\bar{k}_\chi = (k_x + i\chi k_y)/k_F = e^{i\chi\alpha}$ with the sign of the angular momentum $\chi = \pm$. With this notation, the gap function is written as

$$\hat{\Delta}(\mathbf{k}_F, \mathbf{R}) = [-\gamma_2(\mathbf{R})\bar{k}_+ + \gamma_0(\mathbf{R})/\sqrt{6}\bar{k}_-]|\uparrow\uparrow\rangle + [\gamma_{-2}(\mathbf{R})\bar{k}_- - \gamma_0(\mathbf{R})/\sqrt{6}\bar{k}_+]|\downarrow\downarrow\rangle. \quad (99)$$

In each spin sector, two opposite orbital-angular-momenta, \bar{k}_\pm , are mixed owing to the induced component γ_0 . In a spinless chiral p -wave SC, the induced component has the opposite angular momentum relative to the component which has a non-zero order parameter far from the vortex core, i.e., $\chi_i = -\chi_b$ Heeb & Agterberg (1999), Matsumoto & Heeb (2001). Here we call the latter component the *bulk component*, and χ_b (χ_i) represents the sign of the angular momentum for the bulk (induced) component. The vorticity of the induced component, κ_i , is given by $\kappa_i = \kappa_b + \chi_b - \chi_i$, where κ_b is the vorticity of the bulk component. Here the $\chi_b - \chi_i$ accounts for the angular momentum difference between the bulk and induced components, and is reduced to $2\chi_b$. For the $(1/2, +1/4)$ -HQV, the bulk component γ_{-2} has the vorticity $\kappa_b = \kappa - n(-2) = 1$, and $\chi_b = -1$. Thereby $\kappa_i = \kappa_b + 2\chi_b = -1$ successfully explains the vorticity of the induced component shown in panel (e). More striking feature is the three-fold symmetry in the amplitude of the induced component $|\gamma_0|$. Reflecting this discrete symmetry, the phase evolution of the induced component surrounding the vortex is non-linear. As seen from Eq. (99), the main structure of this HQV is in the spin-down sector.

Isolated HQV $(\kappa, n) = (1/2, -1/4)$. The other HQV, characterized by $(1/2, -1/4)$, at $\mathbf{R}_2 = (0, 0)$, is obtained by

$\mathbf{R}_1 \rightarrow (+\infty, 0)$, i.e., $\theta \rightarrow \pi$ in Eq. (98), in which the relative phase of $\gamma_{\pm 2}$ is opposite because of the phase factor $\exp[i(1/2 + M/4)\pi]$ from the $(1/2, +1/4)$ HQV. This HQV is $(1/2, C_4^{-1})$ in the conjugacy class (V) in Eq. (72), and its disgyration is schematically drawn in Fig. 10(f). In contrast to the previous case, a conventional vortex structure appears in the $M = +2$ sector shown in panels (g) and (h), while an almost uniform structure without phase winding is in the $M = -2$ sector. In panel (j) the phase winding of the induced component is $+3$, which can be understood as in the previous case: $\kappa_i = \kappa_b + 2\chi_b = 3$ for $\kappa_b = \kappa + M/4 = 1$ and $\chi_b = +1$. The phase evolution surrounding the vortex is again non-linear reflecting the discrete symmetry of the amplitude $|\gamma_0|$, which is five-fold as shown in panel (h). The major vortex structure of this HQV is in the spin-up sector.

Molecule of HQVs (stability). The two types of internal structures in the $M = 0$ component induced for the HQVs with $n = \pm 1/4$ are modulated by the connection of these two HQVs. This modulation causes an interaction between the two HQVs. The interaction energy of the two HQVs are defined by $\Delta\mathcal{J}_{\text{sn}}(d_v) = \mathcal{J}_{\text{sn}}(\mathbf{R}_1, \mathbf{R}_2) - \mathcal{J}_{\text{sn}}^+(\mathbf{R}_1) - \mathcal{J}_{\text{sn}}^-(\mathbf{R}_2)$ based on the Luttinger–Ward energy functional \mathcal{J}_{sn} Vorontsov & Sauls (2003). Here the two HQVs are at $\mathbf{R}_1 = (d_v/2, 0)$ and $\mathbf{R}_2 = (-d_v/2, 0)$, schematically shown in Fig. 11(a), whose energy is denoted by $\mathcal{J}_{\text{sn}}(\mathbf{R}_1, \mathbf{R}_2)$. The energies of the isolated HQVs $(\kappa, n) = (1/2, +1/4)$ at \mathbf{R}_1 and $(1/2, -1/4)$ at \mathbf{R}_2 are denoted by $\mathcal{J}_{\text{sn}}^+(\mathbf{R}_1)$ and $\mathcal{J}_{\text{sn}}^-(\mathbf{R}_2)$, respectively.

Figure 11(b) shows the interaction energies of the two HQVs as a function of intervortex distance d_v . When $d_v = 0$, the d vortex (the singly quantized vortex with double core structure) is realized. The gap structure is show in Fig. 9. Importantly, the positive energy of the d vortex means that two isolated HQVs ($d_v \rightarrow \infty$) are more stable than the d vortex. The actual interaction energy takes the minimum

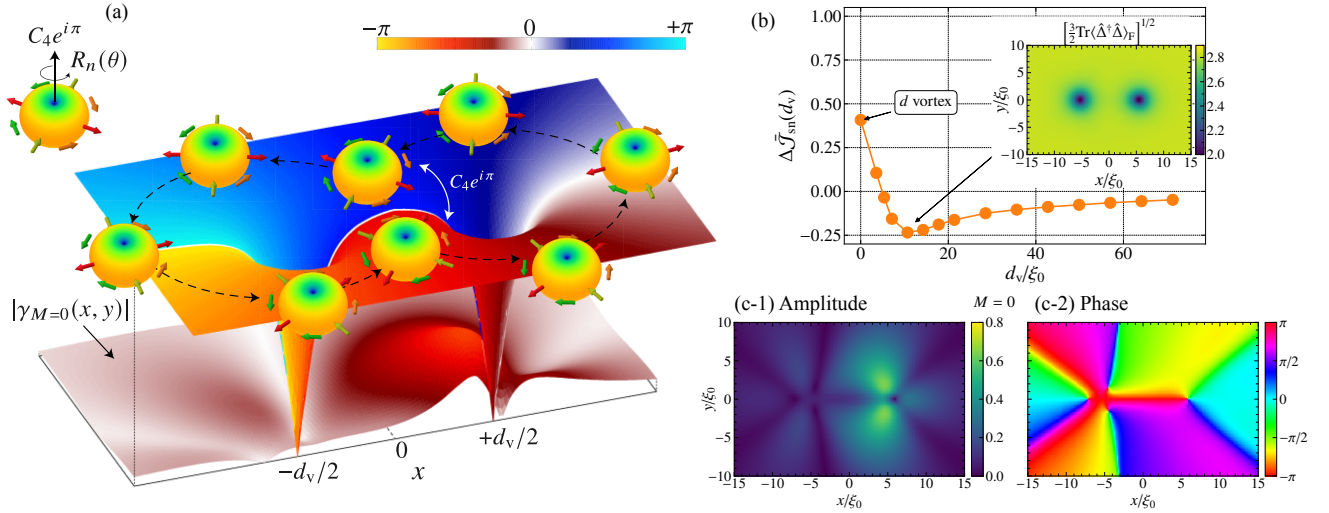


Figure 11: (a) Schematic image of a molecule of non-Abelian HQVs in a D_4 -BN state at a cross section perpendicular to the two parallel vortex lines, characterized by $(\kappa, n) = (1/2, +1/4)$ at $x = d_v/2$ and $(1/2, -1/4)$ at $x = -d_v/2$. Its spin-momentum structure is shown by objects with color arrows representing d vectors. The color map on the surface shows the $U(1)$ phase, and the bottom plot shows the induced component also shown in panel (c-1). (b) Interaction energy of two HQVs as a function of their separation d_v . The inset shows the total amplitude of the order parameter for the HQV molecule whose intervortex distance is indicated by the arrow. The free energy is scaled as $\bar{J}_{sn} = J_{sn}/(\nu_n T_c^2 \xi_0^2 \Omega_z)$, where Ω_z is the length of the system in the z direction, and ν_n is the density of states at the Fermi energy in the normal state. The energy at $d_v = 0$ is the free energy of the d vortex shown in Fig. 9. (c-1) and (c-2) The amplitude and the phase of the induced component γ_0 . The intervortex distance d_v is the same as that in the inset of panel (b). Figures are adapted from Ref. Masaki et al. (2022) ©2022 American Physical Society.

at finite d_v , indicating the instability of the d vortex into a bound state of the two HQVs like a molecule. As discussed in Sec. 4.2, a singly quantized vortex $(\kappa, n) = (1, 0)$ in the conjugacy class (I) in Eq. (72) splits into two HQVs $(1/2, +1/4)$ and $(1/2, -1/4)$ in the class (V).

The stabilization mechanism in this molecule state is a deformation in the non-axisymmetric induced component γ_0 , as shown in Figs. 11(c-1) and 11(c-2), realized in the strongly spin-orbit coupled Cooper pairs Masaki et al. (2022). This mechanism is purely intrinsic and possible even in the weak coupling limit, different from those in other systems such as the SF ^3He Salomaa & Volovik (1985a) and unconventional SCs Chung et al. (2007): In the SF ^3He -A phase, Volovik and Salomaa phenomenologically introduced some corrections in spin mass to stabilize the HQV Salomaa & Volovik (1985a); This correction might be regarded as a kind of strong coupling effect through the Fermi liquid correction, but another strong coupling effect is known to destabilize the HQV Kawakami et al. (2009, 2010, 2011), Mizushima et al. (2016). Vakaryuk and Leggett unveiled that the HQVs in equal spin pairing states, such as ^3He -A and D_4 -BN, are accompanied by a nonzero spin polarization even in the absence of external Zeeman coupling Vakaryuk & Leggett (2009). The coupling of such spin polarization to external magnetic fields may affect the stability of HQVs. Another example of the stabilization mechanism is an extrinsic one in the polar and

polar distorted phases of the SF ^3He because of strongly anisotropic impurities, as discussed in Sec. 3.2.

5.3. Non-Abelian anyon in non-Abelian vortex

In this section, first the zero energy bound states in above-discussed HQVs are demonstrated. Second we

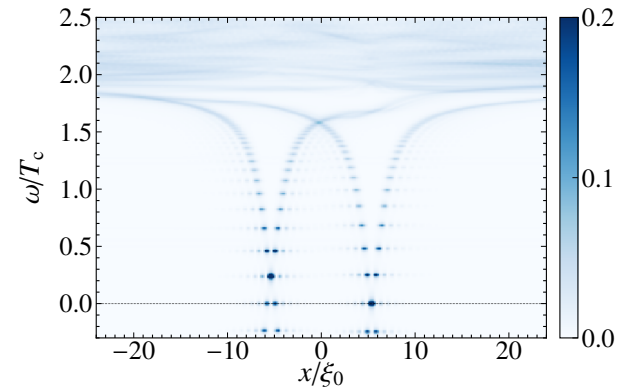


Figure 12: Local density of states $\nu_{k_z=0}(\mathbf{R}; \omega)$ at $k_z = 0$ and $y = 0$ for a pair of HQVs located at $(x, y) = (\pm d_v/2, 0)$ with $d_v \approx 10.7\xi_0$. The spatial distributions of the two zero energy states are different. Figures are adapted from Ref. Masaki et al. (2022) ©2022 American Physical Society.

summarize the discrete symmetries in the presence of vortices, and finally discuss the topological protection of the zero energy states and their non-Abelian nature.

Existence of zero energy states. To investigate fermionic bound states at discrete energy levels, it is necessary to solve the BdG equation (92). By assuming the spatial uniformity along the z -direction, the quantum number is labeled as $\nu = (\alpha, k_z)$, and only the $k_z = 0$ sector is focused on to seek for zero energy bound states. The direct numerical calculation gives us a spectral function including the discrete bound states around the HQV-cores, as shown in Fig. 12(a). There are two zero energy states localized in both of the cores. Here, the molecule state of the two HQVs with $d_\nu \simeq 10.7\xi_0$ is used for a gap function in the BdG equation, and the spectral function, also known as the local density of state, is defined as $\nu_{k_z=0}(\mathbf{R}; \omega) = \sum_{\alpha, \sigma} |u_{\alpha, k_z=0, \sigma}(\mathbf{R})|^2 \delta(\omega - \epsilon_{\alpha, k_z=0})$ along $\mathbf{R} = (x, 0)$, where $u_{\alpha, k_z, \sigma}(\mathbf{R})$ is the particle component with spin σ of the eigenfunction $\tilde{u}_{\alpha, k_z}(\mathbf{R})$. In the calculation, the parameter $k_F \xi_0$, characterizing the discreteness of the bound states, is set to 5. The Majorana condition, $u_{\alpha, k_z=0, \sigma}(\mathbf{R}) = [v_{\alpha, k_z=0, \sigma}(\mathbf{R})]^*$, for the wave functions of the zero energy state can be confirmed Masaki et al. (2022).

Discrete symmetry of vortices. We utilize the semiclassical approximation to clarify the symmetry and topology of vortices, following Refs. Tsutsumi et al. (2015), Mizushima et al. (2016), Shiozaki & Sato (2014). In the semiclassical approximation, the spatial modulation due to a vortex line is treated as adiabatic changes as a function of the real-space coordinate surrounding the defect with the angle θ . Then, the BdG Hamiltonian in the base space, (\mathbf{k}, θ) , is obtained from Eq. (92) as

$$\check{H}(\mathbf{k}, \theta) = \begin{pmatrix} \hat{h}_N(\mathbf{k}) & \hat{\Delta}(\mathbf{k}, \theta) \\ \hat{\Delta}^\dagger(\mathbf{k}, \theta) & -\hat{h}_N^*(\mathbf{k}) \end{pmatrix}, \quad (100)$$

where the 3P_2 pair potential within a semiclassical approximation is given by

$$\hat{\Delta}(\mathbf{k}, \theta) = i \hat{\sigma}_\mu A_{\mu i}(\theta) k_i / k_F \hat{\sigma}_y. \quad (101)$$

Let us now summarize the discrete symmetries of the BdG Hamiltonian in Eq. (100). In the presence of vortex, the BdG Hamiltonian breaks the time-reversal symmetry $\hat{T} = -i \hat{\sigma}_y K$, but holds the particle-hole symmetry

$$\check{C} \check{H}(\mathbf{k}, \theta) \check{C}^{-1} = -\check{H}(-\mathbf{k}, \theta), \quad (102)$$

where $\check{C} = \check{\tau}_x K$ and K is the complex conjugation operator. In addition to the particle-hole symmetry, three discrete symmetries, the $\{P_1, P_2, P_3\}$, are pointed out to be relevant to vortices of the SF ${}^3\text{He-B}$ phase Salomaa & Volovik (1985b, 1987). Their representations are given by

$$\hat{P}_1 = P U_\pi \hat{1}, \quad \hat{P}_3 = \hat{T} \hat{C}_{2,x}, \quad (103)$$

and $\hat{P}_2 = \hat{P}_1 \hat{P}_3$. Here, $P, U_\pi = e^{i(\kappa+1)\pi}$, $\hat{C}_{2,x} = e^{-i\hat{J}_x \pi}$ are the spatial inversion, the discrete phase rotation, and the π -rotation in the spin-orbit space about the x -axis. The physical meanings of P_1, P_2 , and P_3 symmetries are, the inversion,

magnetic reflection, and magnetic π -rotation symmetries respectively. From the definition, $P_1 P_2 P_3 = 1$. Under these symmetry operations, a momentum \mathbf{k} and a spin σ are transformed as

$$P_1 : \mathbf{k} \rightarrow (-k_x, -k_y, -k_z), \quad \sigma \rightarrow (\sigma_x, \sigma_y, \sigma_z), \quad (104)$$

$$P_2 : \mathbf{k} \rightarrow (k_x, -k_y, -k_z), \quad \sigma \rightarrow (-\sigma_x, \sigma_y, \sigma_z), \quad (105)$$

$$P_3 : \mathbf{k} \rightarrow (-k_x, k_y, k_z), \quad \sigma \rightarrow (-\sigma_x, \sigma_y, \sigma_z). \quad (106)$$

Under these transformation, the order parameters are transformed as

$$P_1 : \gamma_M(\rho, \theta) \rightarrow -\gamma_M(\rho, \theta + \pi), \quad (107)$$

$$P_2 : \gamma_M(\rho, \theta) \rightarrow (-1)^{\kappa+M} [\gamma_M(\rho, \pi - \theta)]^*, \quad (108)$$

$$P_3 : \gamma_M(\rho, \theta) \rightarrow (-1)^M [\gamma_M(\rho, -\theta)]^*. \quad (109)$$

For axisymmetric vortices, we confirm the non-zero components of $\gamma_M(\rho)$ summarized in Table. 5.2 by using the relation $\gamma_M(\rho, \theta) = \gamma_M(\rho) e^{i(\kappa-M)\theta}$. For example, $P_2 : \gamma_M(\rho) e^{i(\kappa-M)\theta} \rightarrow \gamma_M^*(\rho) e^{i(\kappa-M)\theta}$, and when the P_2 symmetry is preserved, $\gamma_M(\rho) = \gamma_M^*(\rho)$ can be obtained. In the case of the d vortex, the P_3 symmetry is broken because of the non-zero $\gamma_{\pm 1}$ components, and the P_2 symmetry is the only preserved symmetry among these three. In the case of isolated HQVs, even though $\gamma_{\pm 1} = 0$, because of the three-fold, and five-fold symmetry in the gap amplitude of γ_0 , the P_1 and P_2 symmetries are broken, but the P_3 symmetry is preserved.

Another discrete symmetry is the mirror reflection symmetry about the plane perpendicular to the vortex line, that is, the xy -plane, which is already discussed in Sec. 3.4. The mirror reflection symmetry M_{xy} transforms the momentum and the spin as

$$M_{xy} : \mathbf{k} \rightarrow (k_x, k_y, -k_z), \quad \sigma \rightarrow (-\sigma_x, -\sigma_y, \sigma_z), \quad (110)$$

and thus the order parameter is transformed as

$$M_{xy} : \gamma_M(\rho, \theta) \rightarrow (-1)^{M+1} \gamma_M(\rho, \theta). \quad (111)$$

Therefore, in the presence of M_{xy} , even M and odd M cannot be mixed. In the case of the D_4 -BN state with the point nodes along the z -direction, $\gamma_{M=\pm 2} \neq 0$, and the only possible mirror operation that commutes with the BdG Hamiltonian at the mirror invariant momentum $\mathbf{k}_M = (k_x, k_y, 0)$ is $\eta = -$ in Eq. (38) when $\gamma_{\pm 1} = 0$. The above-discussed vortices of a 3P_2 SF which preserve the M_{xy} symmetry are the axisymmetric o and u vortices, and the HQVs.

Topology of the vortex bound states. On the basis of the above-discussed discrete symmetries, the zero energy state of each HQV is shown to be protected by two topological number: one based on the chiral symmetry, a combined symmetry between the particle-hole symmetry and the P_3 symmetry, and the other based on the mirror reflection symmetry.

When the P_3 symmetry is preserved, the semiclassical BdG Hamiltonian is transformed under the combined symmetry operation $\Gamma = C P_3$ with $\Gamma^2 = +1$ as

$$\check{\Gamma} \check{H}(\mathbf{k}, \theta) \check{\Gamma}^{-1} = -\check{H}(k_x, -k_y, -k_z, -\theta). \quad (112)$$

Particularly, for $k_y = k_z = 0$ and $\theta = 0$ or π , the BdG Hamiltonian anticommutes with Γ , which can be regarded as chiral symmetry Sato et al. (2011), Mizushima et al. (2012), Tsutsumi et al. (2013), Shiozaki & Sato (2014), Tsutsumi et al. (2015), Masaki et al. (2020), Mizushima et al. (2016). As in the bulk nematic state, as long as the chiral symmetry is preserved, one can define the one-dimensional winding number for $\mathbf{k}_x = (k_x, 0, 0)$ and $\theta = 0$ or π as

$$w_{1d}(\theta) = -\frac{1}{4\pi i} \int dk_x \text{tr} \left[\tilde{\Gamma} \tilde{\mathcal{H}}^{-1}(\mathbf{k}_x, \theta) \partial_{k_x} \tilde{\mathcal{H}}(\mathbf{k}_x, \theta) \right]. \quad (113)$$

The vortices which preserve the P_3 symmetry are o , and w vortices and the non-Abelian HQVs. Among them, the winding numbers $(w_{1d}(0), w_{1d}(\pi))$ of o and w vortices are $(2, -2)$, and thus the topological invariant $w_{1d} = (w_{1d}(0) - w_{1d}(\pi))/2 = 2$ ensures the existence of two zero energy states. In the case of non-Abelian HQVs, $(w_{1d}(0), w_{1d}(\pi))$ is $(2, 0)$ for $(\kappa, n) = (1/2, +1/4)$ and $(0, -2)$ for $(1/2, -1/4)$ ⁹. In both cases, the topological invariant w_{1d} becomes 1, which ensures the existence of one zero energy state in each HQV core.

Next we explain the topological invariant based on the mirror reflection symmetry M_{xy} . As discussed above, the BdG Hamiltonian $\tilde{\mathcal{H}}(\mathbf{k}_M, \theta)$ for the mirror invariant momentum \mathbf{k}_M commutes with the mirror operator $\tilde{\mathcal{M}}^\eta$ for $\eta = -$ in Eq. (38). Thus, $\tilde{\mathcal{H}}(\mathbf{k}_M, \theta)$ can be block diagonalized with respect to the mirror eigenstates with eigenvalues $\lambda = \pm i$ as

$$\tilde{\mathcal{H}}(\mathbf{k}_M, \theta) = \bigoplus_{\lambda} \tilde{\mathcal{H}}_{\lambda}(\mathbf{k}_M, \theta). \quad (114)$$

Significantly, even for the BdG Hamiltonian in each mirror subsector, $\tilde{\mathcal{H}}_{\lambda}$, the reduced particle-hole symmetry $\tilde{\mathcal{C}}$ is preserved, though it is not for the other mirror symmetry operator $\tilde{\mathcal{M}}^{\eta=\pm}$. Therefore, $\tilde{\mathcal{H}}_{\lambda}$ belongs to the class D as well as spinless chiral SCs Schnyder et al. (2008), and the \mathbb{Z}_2 invariant, ν_{λ} can be constructed in each mirror subsector Teo & Kane (2010b), Qi et al. (2008). Non-trivial (odd) value of ν_{λ} ensures that the vortex has a single Majorana zero mode which behaves as a non-Abelian (Ising) anyon Ueno et al. (2013), Sato et al. (2014), Tsutsumi et al. (2013).

The \mathbb{Z}_2 invariant ν_{λ} is defined on the base space $(S^2 \times S)$ composed of the two dimensional mirror invariant momentum space \mathbf{k}_M and the angle in the real space surrounding the vortex θ , and constructed by the dimensional reduction of the second Chern number defined in the four dimensional base space $(S^3 \times S)$ composed of \mathbf{k} and θ . The \mathbb{Z}_2 invariant in each mirror subsector is given by the integral of the Chern-Simons form:

$$\nu_{\lambda} = \left(\frac{i}{\pi} \right)^2 \int_{S^2 \times S^1} \tilde{\mathcal{Q}}_{3,\lambda} \quad \text{mod } 2, \quad (115)$$

$$\tilde{\mathcal{Q}}_{3,\lambda} = \text{tr}[\tilde{\mathcal{A}}_{\lambda} \wedge d\tilde{\mathcal{A}}_{\lambda} + \frac{2}{3}\tilde{\mathcal{A}}_{\lambda} \wedge \tilde{\mathcal{A}}_{\lambda} \wedge \tilde{\mathcal{A}}_{\lambda}]. \quad (116)$$

⁹The choice of the relative phase between $\gamma_{\pm 2}$ as π by $\theta_1 \rightarrow \pi$ leads to $(w_{1d}(0), w_{1d}(\pi)) = (0, -2)$ rather than $(2, 0)$ for the HQV of $(\kappa, n) = (1/2, -1/4)$.

A non-Abelian Berry connection $\tilde{\mathcal{A}}_{\lambda}$ is given by

$$i[\tilde{\mathcal{A}}_{\lambda}]_{nm} = \sum_{\alpha} \langle \tilde{u}_{\lambda,n}(\mathbf{k}_M, \theta) | \partial_{\alpha} \tilde{u}_{\lambda,m}(\mathbf{k}_M, \theta) \rangle d\alpha, \quad (117)$$

where α denotes (k_x, k_y, θ) , and $|\tilde{u}_{\lambda,m}(\mathbf{k}_M, \theta)\rangle$ is the m th eigenstate of $\tilde{\mathcal{H}}_{\lambda}(\mathbf{k}, \theta)$. Within the semiclassical approximation in the D_4 -BN state, the \mathbb{Z}_2 invariant is calculated as

$$\nu_{\lambda} = \ell_{\lambda} \kappa_{\lambda} \quad \text{mod } 2, \quad (118)$$

where ℓ_{λ} and κ_{λ} are the first Chern number and the vorticity in the mirror subsector λ . The former characterizes the bulk topology and $\ell_{\lambda=\pm i} = \pm 1$. The latter is given by $\kappa_{\lambda} = \kappa - nM$ for the bulk component M in the λ subsector. In the case of the isolated HQVs, $(\nu_{+i}, \nu_{-i}) = (0, -1)$ $[(+1, 0)]$ for $(\kappa, n) = (1/2, +1/4)$ $[(1/2, -1/4)]$. The two HQVs host Majorana fermions in different mirror sectors, and thus the \mathbb{Z}_2 invariant of the molecule state is given by $(\nu_{+i}, \nu_{-i}) = (+1, -1)$. The \mathbb{Z}_2 invariant of the o vortex has the same one, and the pairwise Majorana fermions are localized at the same core Masaki et al. (2020).

The zero energy state bound in each HQV core is protected by the two topological invariants based on the mirror reflection symmetry and the chiral symmetry, and it is identified as non-Abelian (Ising) anyon of the Majorana fermion. Therefore, the HQV in the D_4 -BN state has two fold non-Abelian nature: one from the non-Abelian Ising anyon, and the other from non-Abelian first homotopy group.

6. Summary

We have presented various types of non-Abelian anyons in topological SCs/SFs and other systems. Non-Abelian anyons are attracting a great attention because of possible applications to topological quantum computations, where quantum computations are realized by braiding of non-Abelian anyons. The simplest non-Abelian anyons are Ising anyons realized by Majorana fermions hosted by vortices (or edges) of topological superconductors, $\nu = 5/2$ quantum Hall states, spin liquids, and high density quark matter. These are, however, insufficient for universal quantum computations. The other anyons which can be used for universal quantum computations is given by Fibonacci anyons which exist in $\nu = 12/5$ quantum Hall states. There are also Yang-Lee anyons which are non-unitary counterparts of Fibonacci anyons. Another class of non-Abelian anyons of the bosonic origin can be given by non-Abelian vortex anyons realized by non-Abelian vortices supported by a non-Abelian first homotopy group. These vortex anyons exist in BN liquid crystals, cholesteric liquid crystals, spin-2 spinor BECs, and high density quark matter. There is a unique system simultaneously admitting two kinds of non-Abelian anyons, which is the Majorana fermions (Ising anyons) and non-Abelian vortex anyons. That is 3P_2 SFs, spin-triplet, p -wave pairing of neutrons, expected to exist in neutron star interiors as the largest topological quantum matter in universe.

Acknowledgements

This work was supported by a Grant-in-Aid for Scientific Research on Innovative Areas “Quantum Liquid Crystals” (Grant No. JP22H04480) from JSPS of Japan and JSPS KAKENHI (Grants No. JP18H01217, No. JP19K14662, No. JP20K03860, No. JP20H01857, No. JP21H01039, and No. JP22H01221), and the WPI program “Sustainability with Knotted Chiral Meta Matter (SKCM²)” at Hiroshima University.

References

- Akhmerov, A. R., Dahlhaus, J. P., Hassler, F., Wimmer, M. & Beenakker, C. W. J. (2011), ‘Quantized Conductance at the Majorana Phase Transition in a Disordered Superconducting Wire’, *Phys. Rev. Lett.* **106**, 057001.
URL: <https://link.aps.org/doi/10.1103/PhysRevLett.106.057001>
- Alford, M. G., Benson, K., Coleman, S. R., March-Russell, J. & Wilczek, F. (1990), ‘The Interactions and Excitations of Nonabelian Vortices’, *Phys. Rev. Lett.* **64**, 1632. [Erratum: *Phys. Rev. Lett.* **65**, 668 (1990)].
- Alford, M. G., Benson, K., Coleman, S. R., March-Russell, J. & Wilczek, F. (1991), ‘Zero modes of nonabelian vortices’, *Nucl. Phys. B* **349**, 414–438.
- Alford, M. G., Lee, K.-M., March-Russell, J. & Preskill, J. (1992), ‘Quantum field theory of non-abelian strings and vortices’, *Nucl. Phys. B* **384**, 251–317.
- Alford, M. G., Schmitt, A., Rajagopal, K. & Schäfer, T. (2008), ‘Color superconductivity in dense quark matter’, *Rev. Mod. Phys.* **80**, 1455–1515.
- Alicea, J. (2012), ‘New directions in the pursuit of Majorana fermions in solid state systems’, *Rep. Prog. Phys.* **75**(7), 76501.
- Alicea, J., Oreg, Y., Refael, G., von Oppen, F. & Fisher, M. P. A. (2011), ‘Non-Abelian statistics and topological quantum information processing in 1D wire networks’, *Nat. Phys.* **7**, 412.
URL: <https://doi.org/10.1038/nphys1915>
- Ambegaokar, V., deGennes, P. G. & Rainer, D. (1974), ‘Landau-Ginsburg equations for an anisotropic superfluid’, *Phys. Rev. A* **9**, 2676–2685.
URL: <https://link.aps.org/doi/10.1103/PhysRevA.9.2676>
- Andersen, T. I. et al. (2022), ‘Observation of non-Abelian exchange statistics on a superconducting processor’, *arXiv:2210.10255*.
- Anderson, P. W. & Brinkman, W. F. (1973), ‘Anisotropic superfluidity in ³He: A possible interpretation of its stability as a spin-fluctuation effect’, *Phys. Rev. Lett.* **30**, 1108–1111.
URL: <https://link.aps.org/doi/10.1103/PhysRevLett.30.1108>
- Anderson, P. W. & Morel, P. (1961), ‘Generalized bardeen-cooper-schrieffer states and the proposed low-temperature phase of liquid he³’, *Phys. Rev.* **123**, 1911–1934.
URL: <https://link.aps.org/doi/10.1103/PhysRev.123.1911>
- Anderson, P. W. & Toulouse, G. (1977), ‘Phase slippage without vortex cores: Vortex textures in superfluid ³He’, *Phys. Rev. Lett.* **38**, 508–511.
URL: <https://link.aps.org/doi/10.1103/PhysRevLett.38.508>
- Ardonne, E., Gukelberger, J., Ludwig, A. W. W., Trebst, S. & Troyer, M. (2011), ‘Microscopic models of interacting Yang-Lee anyons’, *New J. Phys.* **13**(4), 045006.
URL: <https://dx.doi.org/10.1088/1367-2630/13/4/045006>
- Arovas, D., Schrieffer, J. R. & Wilczek, F. (1984), ‘Fractional Statistics and the Quantum Hall Effect’, *Phys. Rev. Lett.* **53**, 722–723.
- Autti, S., Dmitriev, V. V., Mäkinen, J. T., Soldatov, A. A., Volovik, G. E., Yudin, A. N., Zavjalov, V. V. & Eltsov, V. B. (2016), ‘Observation of Half-Quantum Vortices in Topological Superfluid ³He’, *Phys. Rev. Lett.* **117**(25), 255301.
- Auzzi, R., Bolognesi, S., Evslin, J., Konishi, K. & Yung, A. (2003), ‘Non-Abelian superconductors: Vortices and confinement in N=2 SQCD’, *Nucl. Phys. B* **673**, 187–216.
- Awoga, O. A., Cayao, J. & Black-Schaffer, A. M. (2019), ‘Supercurrent Detection of Topologically Trivial Zero-Energy States in Nanowire Junctions’, *Phys. Rev. Lett.* **123**, 117001.
URL: <https://link.aps.org/doi/10.1103/PhysRevLett.123.117001>
- Bais, F. A. (1980), ‘Flux Metamorphosis’, *Nucl. Phys. B* **170**, 32–43.
- Balachandran, A. P., Dikal, S. & Matsuura, T. (2006), ‘Semi-superfluid strings in high density QCD’, *Phys. Rev. D* **73**, 074009.
- Balachandran, A. P., Lizzi, F. & Rodgers, V. G. J. (1984), ‘Topological Symmetry Breakdown in Cholesterics, Nematics, and ³He’, *Phys. Rev. Lett.* **52**, 1818–1821.
- Bartolomei, H., Kumar, M., Bisognin, R., Marguerite, A., Berroir, J.-M., Bocquillon, E., Plaças, B., Cavanna, A., Dong, Q., Gennser, U., Jin, Y. & Fève, G. (2020), ‘Fractional statistics in anyon collisions’, *Science* **368**(6487), 173–177.
URL: <https://www.science.org/doi/abs/10.1126/science.aaz5601>
- Beenakker, C. (2013), ‘Search for Majorana Fermions in Superconductors’, *Annu. Rev. Condens. Matter Phys.* **4**(1), 113–136.
URL: <http://dx.doi.org/10.1146/annurev-conmatphys-030212-184337>
- Beenakker, C. W. J. (2020), ‘Search for non-Abelian Majorana braiding statistics in superconductors’, *SciPost Phys. Lect. Notes* **15**, 15.
URL: <https://scipost.org/10.21468/SciPostPhysLectNotes.15>
- Bonderson, P., Freedman, M. & Nayak, C. (2008), ‘Measurement-Only Topological Quantum Computation’, *Phys. Rev. Lett.* **101**, 010501.
URL: <https://link.aps.org/doi/10.1103/PhysRevLett.101.010501>
- Bonderson, P., Freedman, M. & Nayak, C. (2009), ‘Measurement-only topological quantum computation via anyonic interferometry’, *Annals of Physics* **324**(4), 787–826.
- Bonesteel, N. E., Hormozi, L., Zikos, G. & Simon, S. H. (2005), ‘Braid topologies for quantum computation’, *Phys. Rev. Lett.* **95**, 140503.
URL: <https://link.aps.org/doi/10.1103/PhysRevLett.95.140503>
- Borgh, M. O. & Ruostekoski, J. (2016), ‘Core Structure and Non-Abelian Reconnection of Defects in a Biaxial Nematic Spin-2 Bose-Einstein Condensate’, *Phys. Rev. Lett.* **117**(27), 275302. [Erratum: *Phys. Rev. Lett.* **118**, 129901 (2017)].
- Bravyi, S. (2006), ‘Universal quantum computation with the $\nu = 5/2$ fractional quantum Hall state’, *Phys. Rev. A* **73**, 042313.
URL: <https://link.aps.org/doi/10.1103/PhysRevA.73.042313>
- Brekke, L., Collins, S. J. & Imbo, T. D. (1997), ‘Non-abelian vortices on surfaces and their statistics’, *Nucl. Phys. B* **500**, 465–485.
- Brekke, L., Imbo, T. D., Dykstra, H. & Falk, A. F. (1993), ‘Novel spin and statistical properties of nonabelian vortices’, *Phys. Lett. B* **304**, 127–133.
- Bruin, J. A. N., Claus, R. R., Matsumoto, Y., Kurita, N., Tanaka, H. & Takagi, H. (2022), ‘Robustness of the thermal Hall effect close to half-quantization in α -RuCl₃’, *Nat. Phys.* **18**, 401.
URL: <https://doi.org/10.1038/s41567-021-01501-y>
- Bucher, M. (1991), ‘The Aharonov-Bohm effect and exotic statistics for nonabelian vortices’, *Nucl. Phys. B* **350**, 163–178.
- Bucher, M., Lee, K.-M. & Preskill, J. (1992), ‘On detecting discrete Cheshire charge’, *Nucl. Phys. B* **386**, 27–42.
- Cardy, J. L. (1985), ‘Conformal Invariance and the Yang-Lee Edge Singularity in Two Dimensions’, *Phys. Rev. Lett.* **54**, 1354–1356.
URL: <https://link.aps.org/doi/10.1103/PhysRevLett.54.1354>
- Cayao, J. & Buset, P. (2021), ‘Confinement-induced zero-bias peaks in conventional superconductor hybrids’, *Phys. Rev. B* **104**, 134507.
URL: <https://link.aps.org/doi/10.1103/PhysRevB.104.134507>
- Chen, W., Wang, J., Wu, Y., Qi, J., Liu, J. & Xie, X. C. (2022), ‘Non-Abelian statistics of Majorana zero modes in the presence of an Andreev bound state’, *Phys. Rev. B* **105**, 054507.
URL: <https://link.aps.org/doi/10.1103/PhysRevB.105.054507>
- Cheng, M., Lutchyn, R. M., Galitski, V. & Das Sarma, S. (2009), ‘Splitting of majorana-fermion modes due to intervortex tunneling in a $p_x + ip_y$ superconductor’, *Phys. Rev. Lett.* **103**, 107001.
URL: <https://link.aps.org/doi/10.1103/PhysRevLett.103.107001>
- Chung, S. B., Bluhm, H. & Kim, E.-A. (2007), ‘Stability of Half-quantum Vortices in $p_x + ip_y$ Superconductors’, *Phys. Rev. Lett.* **99**, 197002.
- Chung, S. B. & Kivelson, S. A. (2010), ‘Entropy-driven formation of a half-quantum vortex lattice’, *Phys. Rev. B* **82**, 214512.
URL: <https://link.aps.org/doi/10.1103/PhysRevB.82.214512>
- Chung, S. B. & Zhang, S.-C. (2009), ‘Detecting the Majorana Fermion Surface State of ³He–B through Spin Relaxation’, *Phys. Rev. Lett.* **103**(23), 235301.
URL: <https://link.aps.org/doi/10.1103/PhysRevLett.103.235301>

- Clarke, D. J., Sau, J. D. & Tewari, S. (2011), ‘Majorana fermion exchange in quasi-one-dimensional networks’, *Phys. Rev. B* **84**, 035120.
URL: <https://link.aps.org/doi/10.1103/PhysRevB.84.035120>
- De Gennes, P. (1973), ‘Long range distortions in an anisotropic superfluid’, *Phys. Lett. A* **44**(4), 271–272.
- Di Francesco, P. D., Mathieu, P. & Sénéchal (1997), *Conformal Field Theory*, Springer-Verlag, New York.
- Dmitriev, V. V., Senin, A. A., Soldatov, A. A. & Yudin, A. N. (2015), ‘Polar phase of superfluid ^3He in anisotropic aerogel’, *Phys. Rev. Lett.* **115**, 165304.
URL: <https://link.aps.org/doi/10.1103/PhysRevLett.115.165304>
- Elliott, S. R. & Franz, M. (2015), ‘Colloquium : Majorana fermions in nuclear, particle, and solid-state physics’, *Rev. Mod. Phys.* **87**(1), 137–163.
URL: <https://link.aps.org/doi/10.1103/RevModPhys.87.137>
- Eto, M., Hirono, Y., Nitta, M. & Yasui, S. (2014), ‘Vortices and Other Topological Solitons in Dense Quark Matter’, *PTEP* **2014**(1), 012D01.
URL: <https://doi.org/10.1093/ptep/ptt095>
- Eto, M., Isozumi, Y., Nitta, M., Ohashi, K. & Sakai, N. (2006), ‘Solitons in the Higgs phase: The Moduli matrix approach’, *J. Phys. A* **39**, R315–R392.
- Eto, M. & Nitta, M. (2009), ‘Color Magnetic Flux Tubes in Dense QCD’, *Phys. Rev. D* **80**, 125007.
- Eto, M. & Nitta, M. (2021), ‘Chiral non-Abelian vortices and their confinement in three flavor dense QCD’, *Phys. Rev. D* **104**(9), 094052.
- Fang, C., Gilbert, M. J. & Bernevig, B. A. (2014), ‘New class of topological superconductors protected by magnetic group symmetries’, *Phys. Rev. Lett.* **112**, 106401.
URL: <https://link.aps.org/doi/10.1103/PhysRevLett.112.106401>
- Field, B. & Simula, T. (2018), ‘Introduction to topological quantum computation with non-Abelian anyons’, *Quantum Sci. Technol.* **3**, 045004.
- Fisher, M. E. (1978), ‘Yang-Lee Edge Singularity and ϕ^3 Field Theory’, *Phys. Rev. Lett.* **40**, 1610–1613.
URL: <https://link.aps.org/doi/10.1103/PhysRevLett.40.1610>
- Freedman, M. H., Gukelberger, J., Hastings, M. B., Trebst, S., Troyer, M. & Wang, Z. (2012), ‘Galois conjugates of topological phases’, *Phys. Rev. B* **85**, 045414.
URL: <https://link.aps.org/doi/10.1103/PhysRevB.85.045414>
- Freedman, M., Hastings, M. B., Nayak, C. & Qi, X.-L. (2011), ‘Weakly coupled non-abelian anyons in three dimensions’, *Phys. Rev. B* **84**, 245119.
URL: <https://link.aps.org/doi/10.1103/PhysRevB.84.245119>
- Freedman, M., Hastings, M. B., Nayak, C., Qi, X.-L., Walker, K. & Wang, Z. (2011), ‘Projective ribbon permutation statistics: A remnant of non-abelian braiding in higher dimensions’, *Phys. Rev. B* **83**, 115132.
URL: <https://link.aps.org/doi/10.1103/PhysRevB.83.115132>
- Fu, L. & Kane, C. L. (2008), ‘Superconducting proximity effect and majorana fermions at the surface of a topological insulator’, *Phys. Rev. Lett.* **100**, 096407.
URL: <https://link.aps.org/doi/10.1103/PhysRevLett.100.096407>
- Fujimoto, Y. & Nitta, M. (2021a), ‘Non-Abelian Alice strings in two-flavor dense QCD’, *Phys. Rev. D* **103**, 054002.
- Fujimoto, Y. & Nitta, M. (2021b), ‘Topological confinement of vortices in two-flavor dense QCD’, *JHEP* **09**, 192.
- Fujimoto, Y. & Nitta, M. (2021c), ‘Vortices penetrating two-flavor quark-hadron continuity’, *Phys. Rev. D* **103**(11), 114003.
- Fujita, T. & Tsuneto, T. (1972), ‘The ginzburg-landau equation for 3p2 pairingsuperfluidity in neutron stars’, *Prog. Theor. Phys.* **48**(3), 766–782.
URL: <http://dx.doi.org/10.1143/PTP.48.766>
- Fujiwara, T., Fukui, T., Nitta, M. & Yasui, S. (2011), ‘Index theorem and Majorana zero modes along a non-Abelian vortex in a color superconductor’, *Phys. Rev. D* **84**, 076002.
- Fulga, I. C., Hassler, F., Akhmerov, A. R. & Beenakker, C. W. J. (2011), ‘Scattering formula for the topological quantum number of a disordered multimode wire’, *Phys. Rev. B* **83**, 155429.
URL: <https://link.aps.org/doi/10.1103/PhysRevB.83.155429>
- Gao, P., He, Y.-P. & Liu, X.-J. (2016), ‘Symmetry-protected non-abelian braiding of majorana kramers pairs’, *Phys. Rev. B* **94**, 224509.
URL: <https://link.aps.org/doi/10.1103/PhysRevB.94.224509>
- Génétay Johansen, E. & Simula, T. (2022), ‘Prime number factorization using a spinor Bose–Einstein condensate-inspired topological quantum computer’, *Quant. Inf. Proc.* **21**(1), 31.
- Haim, A. & Oreg, Y. (2019), ‘Time-reversal-invariant topological superconductivity in one and two dimensions’, *Physics Reports* **825**, 1–48. Time-reversal-invariant topological superconductivity in one and two dimensions.
- Halperin, B. I. (1984), ‘Statistics of quasiparticles and the hierarchy of fractional quantized Hall states’, *Phys. Rev. Lett.* **52**, 1583–1586. [Erratum: *Phys. Rev. Lett.* **52**, 2390 (1984)].
- Halperin, W. (2019), ‘Superfluid ^3He in aerogel’, *Annual Review of Condensed Matter Physics* **10**(1), 155–170.
URL: <https://doi.org/10.1146/annurev-conmatphys-031218-013134>
- Hanany, A. & Tong, D. (2003), ‘Vortices, instantons and branes’, *JHEP* **07**, 037.
- Heeb, R. & Agterberg, D. F. (1999), ‘Ginzburg-Landau theory for a p -wave Sr_2RuO_4 superconductor: Vortex core structure and extended London theory’, *Phys. Rev. B* **59**(10), 7076–7082.
URL: <http://arxiv.org/abs/cond-mat/9811190>
<https://link.aps.org/doi/10.1103/PhysRevB.59.7076>
- Hirono, Y., Yasui, S., Itakura, K. & Nitta, M. (2012), ‘Non-Abelian statistics of vortices with multiple Majorana fermions’, *Phys. Rev. B* **86**, 014508.
- Hoffberg, M., Glassgold, A. E., Richardson, R. W. & Ruderman, M. (1970), ‘Anisotropic Superfluidity in Neutron Star Matter’, *Phys. Rev. Lett.* **24**(14), 775.
- Hong, J.-S., Poon, T.-F. J., Zhang, L. & Liu, X.-J. (2022), ‘Unitary symmetry-protected non-abelian statistics of majorana modes’, *Phys. Rev. B* **105**, 024503.
URL: <https://link.aps.org/doi/10.1103/PhysRevB.105.024503>
- Hormozi, L., Zikos, G., Bonesteel, N. E. & Simon, S. H. (2007), ‘Topological quantum compiling’, *Phys. Rev. B* **75**, 165310.
URL: <https://link.aps.org/doi/10.1103/PhysRevB.75.165310>
- Hosur, P., Ghaemi, P., Mong, R. S. K. & Vishwanath, A. (2011), ‘Majorana modes at the ends of superconductor vortices in doped topological insulators’, *Phys. Rev. Lett.* **107**, 097001.
URL: <https://link.aps.org/doi/10.1103/PhysRevLett.107.097001>
- Hu, Y. & Kane, C. L. (2018), ‘Fibonacci topological superconductor’, *Phys. Rev. Lett.* **120**, 066801.
URL: <https://link.aps.org/doi/10.1103/PhysRevLett.120.066801>
- Ikegaya, S., Suzuki, S.-I., Tanaka, Y. & Asano, Y. (2016), ‘Quantization of conductance minimum and index theorem’, *Phys. Rev. B* **94**, 054512.
URL: <https://link.aps.org/doi/10.1103/PhysRevB.94.054512>
- Ivanov, D. A. (2001), ‘Non-abelian statistics of half-quantum vortices in p -wave superconductors’, *Phys. Rev. Lett.* **86**(2), 268.
- Karzig, T., Knapp, C., Lutchny, R. M., Bonderson, P., Hastings, M. B., Nayak, C., Alicea, J., Flensberg, K., Plugge, S., Oreg, Y., Marcus, C. M. & Freedman, M. H. (2017), ‘Scalable designs for quasiparticle-poisoning-protected topological quantum computation with majorana zero modes’, *Phys. Rev. B* **95**, 235305.
URL: <https://link.aps.org/doi/10.1103/PhysRevB.95.235305>
- Karzig, T., Oreg, Y., Refael, G. & Freedman, M. H. (2016), ‘Universal geometric path to a robust majorana magic gate’, *Phys. Rev. X* **6**, 031019.
URL: <https://link.aps.org/doi/10.1103/PhysRevX.6.031019>
- Kasahara, Y., Ohnishi, T., Mizukami, Y., Tanaka, O., Ma, S., Sugii, K., Kurita, N., Tanaka, H., Nasu, J., Motome, Y., Shibauchi, T. & Matsuda, Y. (2018), ‘Majorana quantization and half-integer thermal quantum Hall effect in a Kitaev spin liquid’, *Nature* **559**, 227.
URL: <https://doi.org/10.1038/s41586-018-0274-0>
- Kasamatsu, K., Mizuno, R., Ohmi, T. & Nakahara, M. (2019), ‘Effects of a magnetic field on vortex states in superfluid $^3\text{He}-b$ ’, *Phys. Rev. B* **99**, 104513.
URL: <https://link.aps.org/doi/10.1103/PhysRevB.99.104513>
- Kashiwaya, S. & Tanaka, Y. (2000), ‘Tunnelling effects on surface bound states in unconventional superconductors’, *Rep. Prog. Phys.* **63**(10), 1641–1724.
URL: <https://doi.org/10.1088/0034-4885/63/10/202>
- Kashuba, O. & Timm, C. (2015), ‘Topological Kondo Effect in Transport through a Superconducting Wire with Multiple Majorana End States’,

- Phys. Rev. Lett.* **114**, 116801.
URL: <https://link.aps.org/doi/10.1103/PhysRevLett.114.116801>
- Kawaguchi, Y. & Ueda, M. (2012), ‘Spinor Bose-Einstein condensates’, *Phys. Rept.* **520**, 253–381.
- Kawakami, T. & Hu, X. (2015), ‘Evolution of density of states and a spin-resolved checkerboard-type pattern associated with the majorana bound state’, *Phys. Rev. Lett.* **115**, 177001.
URL: <https://link.aps.org/doi/10.1103/PhysRevLett.115.177001>
- Kawakami, T., Mizushima, T. & Machida, K. (2011), ‘Zero Energy Modes and Statistics of Vortices in Spinful Chiral p-Wave Superfluids’, *J. Phys. Soc. Jpn.* **80**(4), 044603.
URL: <http://journals.jps.jp/doi/10.1143/JPSJ.80.044603>
- Kawakami, T., Tsutsumi, Y. & Machida, K. (2009), ‘Stability of a half-quantum vortex in rotating superfluid ^3He —A between parallel plates’, *Phys. Rev. B* **79**(9), 092506.
URL: <https://link.aps.org/doi/10.1103/PhysRevB.79.092506>
- Kawakami, T., Tsutsumi, Y. & Machida, K. (2010), ‘Singular and Half-Quantum Vortices and Associated Majorana Particles in Superfluid ^3He -A between Parallel Plates’, *J. Phys. Soc. Jpn.* **79**(4), 044607.
URL: <http://journals.jps.jp/doi/abs/10.1143/JPSJ.79.044607>
- Kells, G., Meidan, D. & Brouwer, P. W. (2012), ‘Near-zero-energy end states in topologically trivial spin-orbit coupled superconducting nanowires with a smooth confinement’, *Phys. Rev. B* **86**, 100503.
URL: <https://link.aps.org/doi/10.1103/PhysRevB.86.100503>
- Kitaev, A. (2006), ‘Anyons in an exactly solved model and beyond’, *Ann. Phys. (N. Y.)* **321**(1), 2–111.
URL: <https://linkinghub.elsevier.com/retrieve/pii/S0003491605002381>
- Kitaev, A. & Laumann, C. (2008), *Topological phases and quantum computation*, Lecture Notes of the Les Houches Summer School. No.89., Oxford University Press.
- Kitaev, A. Y. (2001), ‘Unpaired Majorana fermions in quantum wires’, *Phys. Usp.* **44**(10S), 131–136.
- Kitaev, A. Y. (2003), ‘Fault tolerant quantum computation by anyons’, *Annals Phys.* **303**, 2–30.
- Knapp, C., Chew, A. & Alicea, J. (2020), ‘Fragility of the fractional josephson effect in time-reversal-invariant topological superconductors’, *Phys. Rev. Lett.* **125**, 207002.
URL: <https://link.aps.org/doi/10.1103/PhysRevLett.125.207002>
- Kobayashi, M., Kawaguchi, Y., Nitta, M. & Ueda, M. (2009), ‘Collision Dynamics and Rung Formation of Non-Abelian Vortices’, *Phys. Rev. Lett.* **103**, 115301.
- Kobayashi, M. & Nitta, M. (2022a), ‘Core structures of vortices in Ginzburg-Landau theory for neutron $^3\text{P}_2$ superfluids’, *Phys. Rev. C* **105**(3), 035807.
- Kobayashi, M. & Nitta, M. (2022b), ‘Proximity effects of vortices in neutron $^3\text{P}_2$ superfluids in neutron stars: Vortex core transitions and covalent bonding of vortex molecules’.
- Kobayashi, S., Kobayashi, M., Kawaguchi, Y., Nitta, M. & Ueda, M. (2012), ‘Abe homotopy classification of topological excitations under the topological influence of vortices’, *Nucl. Phys. B* **856**, 577–606.
- Koornwinder, T. H., Schroers, B. J., Slingerland, J. K. & Bais, F. A. (1999), ‘Fourier transform and the Verlinde formula for the quantum double of a finite group’, *J. Phys. A* **32**, 8539–8549.
- Kopnin, N. B. & Salomaa, M. M. (1991), ‘Mutual friction in superfluid ^3He : Effects of bound states in the vortex core’, *Phys. Rev. B* **44**, 9667–9677.
URL: <https://link.aps.org/doi/10.1103/PhysRevB.44.9667>
- Kortman, P. J. & Griffiths, R. B. (1971), ‘Density of Zeros on the Lee-Yang Circle for Two Ising Ferromagnets’, *Phys. Rev. Lett.* **27**, 1439–1442.
URL: <https://link.aps.org/doi/10.1103/PhysRevLett.27.1439>
- Lavrentovich, O. D. & Kleman, M. (2001), Cholesteric Liquid Crystals: Defects and Topology, in H.-S. Kitzerow & C. Bahr, eds, ‘Chirality in Liquid Crystals’, Springer New York, New York, NY, pp. 115–158.
- Lee, K.-M. (1994), ‘Vortices on higher genus surfaces’, *Phys. Rev. D* **49**, 2030–2040.
- Lee, T. D. & Yang, C. N. (1952), ‘Statistical Theory of Equations of State and Phase Transitions. II. Lattice Gas and Ising Model’, *Phys. Rev.* **87**, 410–419.
URL: <https://link.aps.org/doi/10.1103/PhysRev.87.410>
- Leggett, A. J. (1975), ‘A theoretical description of the new phases of liquid ^3He ’, *Rev. Mod. Phys.* **47**, 331–414.
URL: <https://link.aps.org/doi/10.1103/RevModPhys.47.331>
- Leijnse, M. & Flensberg, K. (2012), ‘Introduction to topological superconductivity and Majorana fermions’, *Semicond. Sci. Technol.* **27**(12), 124003.
URL: <http://stacks.iop.org/0268-1242/27/i=12/a=124003>
- Leinaas, J. M. & Myrheim, J. (1977), ‘On the theory of identical particles’, *Nuovo Cim. B* **37**, 1–23.
- Lesanovsky, I. & Katsura, H. (2012), ‘Interacting fibonacci anyons in a rydberg gas’, *Phys. Rev. A* **86**, 041601.
URL: <https://link.aps.org/doi/10.1103/PhysRevA.86.041601>
- Liu, C.-X., Sau, J. D. & Das Sarma, S. (2018), ‘Distinguishing topological Majorana bound states from trivial Andreev bound states: Proposed tests through differential tunneling conductance spectroscopy’, *Phys. Rev. B* **97**, 214502.
- Liu, C.-X., Sau, J. D., Stanescu, T. D. & Das Sarma, S. (2017), ‘Andreev bound states versus majorana bound states in quantum dot-nanowire-superconductor hybrid structures: Trivial versus topological zero-bias conductance peaks’, *Phys. Rev. B* **96**, 075161.
URL: <https://link.aps.org/doi/10.1103/PhysRevB.96.075161>
- Liu, D., Cao, Z., Liu, X., Zhang, H. & Liu, D. E. (2021), ‘Topological Kondo device for distinguishing quasi-Majorana and Majorana signatures’, *Phys. Rev. B* **104**, 205125.
URL: <https://link.aps.org/doi/10.1103/PhysRevB.104.205125>
- Liu, X.-J., Wong, C. L. M. & Law, K. T. (2014), ‘Non-Abelian Majorana Doublets in Time-Reversal-Invariant Topological Superconductors’, *Phys. Rev. X* **4**, 021018.
URL: <https://link.aps.org/doi/10.1103/PhysRevX.4.021018>
- Lo, H.-K. & Preskill, J. (1993), ‘Non-Abelian vortices and non-Abelian statistics’, *Phys. Rev. D* **48**, 4821–4834.
- Machida, T., Sun, Y., Pyon, S., Takeda, S., Kohsaka, Y., Hanaguri, T., Sasagawa, T. & Tamegai, T. (2019), ‘Zero-energy vortex bound state in the superconducting topological surface state of Fe(Se,Te)’, *Nat. Mater.* **18**, 811.
URL: <https://doi.org/10.1038/s41563-019-0397-1>
- Majorana, E. (1937), ‘Teoria simmetrica dell’elettrone e del positrone’, *Nuovo Cim.* **14**, 171–184.
- Makhlin, Y., Silaev, M. & Volovik, G. E. (2014), ‘Topology of the planar phase of superfluid ^3He and bulk-boundary correspondence for three-dimensional topological superconductors’, *Phys. Rev. B* **89**, 174502.
URL: <https://link.aps.org/doi/10.1103/PhysRevB.89.174502>
- Mäkinen, J. T., Dmitriev, V. V., Nissinen, J., Rysti, J., Volovik, G. E., Yudin, A. N., Zhang, K. & Eltsov, V. B. (2019), ‘Half-quantum vortices and walls bounded by strings in the polar-distorted phases of topological superfluid ^3He ’, *Nature Commun.* **10**(1), 237.
- Mäkinen, J. T., Zhang, K. & Eltsov, V. B. (2022), ‘Vortex-bound solitons in topological superfluid ^3He ’, *arXiv:2211.17117*.
- Marmorini, G., Yasui, S. & Nitta, M. (2020), ‘Pulsar glitches from quantum vortex networks’, *arXiv:2010.09032*.
- Marra, P. (2022), ‘Majorana nanowires for topological quantum computation’, *J. Appl. Phys.* **132**(23), 231101.
URL: <https://doi.org/10.1063/5.0102999>
- Masaki, Y., Mizushima, T. & Nitta, M. (2020), ‘Microscopic description of axisymmetric vortices in $^3\text{P}_2$ superfluids’, *Phys. Rev. Res.* **2**(1), 013193.
- Masaki, Y., Mizushima, T. & Nitta, M. (2022), ‘Non-Abelian half-quantum vortices in $^3\text{P}_2$ topological superfluids’, *Phys. Rev. B* **105**(22), L220503.
URL: <https://link.aps.org/doi/10.1103/PhysRevB.105.L220503>
- Masuda, K. & Nitta, M. (2016), ‘Magnetic Properties of Quantized Vortices in Neutron $^3\text{P}_2$ Superfluids in Neutron Stars’, *Phys. Rev. C* **93**(3), 035804.
- Masuda, K. & Nitta, M. (2020), ‘Half-quantized non-Abelian vortices in neutron $^3\text{P}_2$ superfluids inside magnetars’, *PTEP* **2020**(1), 013D01.
- Matsumoto, M. & Heeb, R. (2001), ‘Vortex charging effect in a chiral $p_x \pm ip_y$ -wave superconductor’, *Phys. Rev. B* **65**(1), 014504.
URL: <https://link.aps.org/doi/10.1103/PhysRevB.65.014504>
- Mawson, T., Petersen, T. C., Slingerland, J. K. & Simula, T. P. (2019), ‘Braiding and Fusion of Non-Abelian Vortex Anyons’, *Phys. Rev. Lett.*

- 123, 140404.
URL: <https://link.aps.org/doi/10.1103/PhysRevLett.123.140404>
- Mermin, N. D. (1974), 'd-wave pairing near the transition temperature', *Phys. Rev. A* **9**, 868–872.
- Mermin, N. D. (1979), 'The topological theory of defects in ordered media', *Rev. Mod. Phys.* **51**, 591–648.
- Mietke, A. & Dunkel, J. (2022), 'Anyonic Defect Braiding and Spontaneous Chiral Symmetry Breaking in Dihedral Liquid Crystals', *Phys. Rev. X* **12**(1), 011027.
- Mineev, V. P. (2014), 'Half-Quantum Vortices in Polar Phase of Superfluid ^3He ', *J. Low Temp. Phys.* **177**, 48.
URL: <https://doi.org/10.1007/s10909-014-1189-2>
- Mizushima, T. & Machida, K. (2010), 'Splitting and oscillation of majorana zero modes in the p-wave bcs-bec evolution with plural vortices', *Phys. Rev. A* **82**, 023624.
URL: <https://link.aps.org/doi/10.1103/PhysRevA.82.023624>
- Mizushima, T. & Machida, K. (2011), 'Effects of Majorana edge fermions on dynamical spin susceptibility in topological superfluid $^3\text{He-B}$ ', *J. Low Temp. Phys.* **162**(3-4), 204–211.
- Mizushima, T., Masuda, K. & Nitta, M. (2017), ' $^3\text{P}_2$ superfluids are topological', *Phys. Rev. B* **95**(14), 140503.
- Mizushima, T., Sato, M. & Machida, K. (2012), 'Symmetry Protected Topological Order and Spin Susceptibility in Superfluid $^3\text{He-B}$ ', *Phys. Rev. Lett.* **109**, 165301.
URL: <https://link.aps.org/doi/10.1103/PhysRevLett.109.165301>
- Mizushima, T., Tsutsumi, Y., Kawakami, T., Sato, M., Ichioka, M. & Machida, K. (2016), 'Symmetry-protected topological superfluids and superconductors—from the basics to ^3He ', *J. Phys. Soc. Jpn.* **85**(2), 022001.
- Mizushima, T., Yasui, S., Inotani, D. & Nitta, M. (2021), 'Spin-polarized phases of $^3\text{P}_2$ superfluids in neutron stars', *Phys. Rev. C* **104**(4), 045803.
URL: <https://link.aps.org/doi/10.1103/PhysRevC.104.045803>
- Mizushima, T., Yasui, S. & Nitta, M. (2020), 'Critical endpoint and universality class of neutron $^3\text{P}_2$ superfluids in neutron stars', *Phys. Rev. Res.* **2**, 013194.
URL: <https://link.aps.org/doi/10.1103/PhysRevResearch.2.013194>
- Mong, R. S. K., Clarke, D. J., Alicea, J., Lindner, N. H., Fendley, P., Nayak, C., Oreg, Y., Stern, A., Berg, E., Shtengel, K. & Fisher, M. P. A. (2014), 'Universal Topological Quantum Computation from a Superconductor-Abelian Quantum Hall Heterostructure', *Phys. Rev. X* **4**, 011036.
URL: <https://link.aps.org/doi/10.1103/PhysRevX.4.011036>
- Moore, C., Stanescu, T. D. & Tewari, S. (2018), 'Two-terminal charge tunneling: Disentangling majorana zero modes from partially separated andreev bound states in semiconductor-superconductor heterostructures', *Phys. Rev. B* **97**, 165302.
URL: <https://link.aps.org/doi/10.1103/PhysRevB.97.165302>
- Moore, C., Zeng, C., Stanescu, T. D. & Tewari, S. (2018), 'Quantized zero-bias conductance plateau in semiconductor-superconductor heterostructures without topological majorana zero modes', *Phys. Rev. B* **98**, 155314.
URL: <https://link.aps.org/doi/10.1103/PhysRevB.98.155314>
- Moore, G. W. & Read, N. (1991), 'Nonabelions in the fractional quantum Hall effect', *Nucl. Phys. B* **360**, 362–396.
- Motome, Y. & Nasu, J. (2020), 'Hunting Majorana Fermions in Kitaev Magnets', *J. Phys. Soc. Jpn.* **89**(1), 012002.
URL: <https://journals.jps.jp/doi/10.7566/JPSJ.89.012002>
- Muzikar, P., Sauls, J. A. & Serene, J. W. (1980), ' $^3\text{P}_2$ pairing in neutron star matter: magnetic field effects and vortices', *Phys. Rev. D* **21**, 1494–1502.
- Nagamura, N. & Ikeda, R. (2018), 'Stability of half-quantum vortices in equal-spin pairing states of ^3He ', *Phys. Rev. B* **98**(9), 094524.
URL: <https://link.aps.org/doi/10.1103/PhysRevB.98.094524>
- Nagato, Y., Higashitani, S. & Nagai, K. (2009), 'Strong Anisotropy in Spin Susceptibility of Superfluid $^3\text{He-B}$ Film Caused by Surface Bound States', *J. Phys. Soc. Jpn.* **78**(12), 123603.
URL: <http://journals.jps.jp/doi/10.1143/JPSJ.78.123603>
- Nakamura, J., Liang, S., Gardner, G. C. & Manfra, M. J. (2020), 'Direct observation of anyonic braiding statistics', *Nat. Phys.* **16**, 931–936.
URL: <http://dx.doi.org/10.1038/s41567-020-1019-1>
- Nakano, E., Nitta, M. & Matsuura, T. (2008), 'Non-Abelian strings in high density QCD: Zero modes and interactions', *Phys. Rev. D* **78**, 045002.
- Nayak, C., Simon, S. H., Stern, A., Freedman, M. & Das Sarma, S. (2008), 'Non-Abelian anyons and topological quantum computation', *Rev. Mod. Phys.* **80**, 1083–1159.
- Nayak, C. & Wilczek, F. (1996), ' 2^n -quasihole states realize 2^{n-1} -dimensional spinor braiding statistics in paired quantum Hall states', *Nucl. Phys. B* **479**(3), 529–553.
- Nielsen, M. & Chuang, I. (2010), *Quantum computation and quantum information*, Cambridge University Press.
- Oreg, Y. & von Oppen, F. (2020), 'Majorana Zero Modes in Networks of Cooper-Pair Boxes: Topologically Ordered States and Topological Quantum Computation', *Annu. Rev. Condens. Matter Phys.* **11**(1), 397–420.
URL: <https://doi.org/10.1146/annurev-conmatphys-031218-013618>
- Pachos, J. K. (2012), *Introduction to Topological Quantum Computation*, Cambridge University Press.
- Pan, H., Cole, W. S., Sau, J. D. & Das Sarma, S. (2020), 'Generic quantized zero-bias conductance peaks in superconductor-semiconductor hybrid structures', *Phys. Rev. B* **101**, 024506.
URL: <https://link.aps.org/doi/10.1103/PhysRevB.101.024506>
- Pan, H. & Das Sarma, S. (2020), 'Physical mechanisms for zero-bias conductance peaks in majorana nanowires', *Phys. Rev. Res.* **2**, 013377.
URL: <https://link.aps.org/doi/10.1103/PhysRevResearch.2.013377>
- Pan, H., Sau, J. D. & Das Sarma, S. (2021), 'Three-terminal nonlocal conductance in Majorana nanowires: Distinguishing topological and trivial in realistic systems with disorder and inhomogeneous potential', *Phys. Rev. B* **103**, 014513.
URL: <https://link.aps.org/doi/10.1103/PhysRevB.103.014513>
- Piroli, L. & Cirac, J. I. (2020), 'Quantum cellular automata, tensor networks, and area laws', *Phys. Rev. Lett.* **125**, 190402.
URL: <https://link.aps.org/doi/10.1103/PhysRevLett.125.190402>
- Plugge, S., Rasmussen, A., Egger, R. & Flensberg, K. (2017), 'Majorana box qubits', *New J. Phys.* **19**, 012001.
URL: <https://iopscience.iop.org/article/10.1088/1367-2630/aa54e1>
- Poenaru, V. & Toulouse, G. (1977), 'The crossing of defects in ordered media and the topology of 3-manifolds', *J. Phys. (Paris)* **38**, 887.
- Prada, E., San-Jose, P., de Moor, M. W. A., Geresdi, A., Lee, E. J. H., Klinovaja, J., Loss, D., Nygård, J., Aguado, R. & Kouwenhoven, L. P. (2020), 'From Andreev to Majorana bound states in hybrid superconductor-semiconductor nanowires', *Nat. Rev. Phys.* **2**, 575.
URL: <https://doi.org/10.1038/s42254-020-0228-y>
- Preskill, J. (2004), *Lecture notes for physics 219: Quantum computation.*
URL: http://www.theory.caltech.edu/~preskill/ph219/ph219_2004.html
- Preskill, J. & Krauss, L. M. (1990), 'Local Discrete Symmetry and Quantum Mechanical Hair', *Nucl. Phys. B* **341**, 50–100.
- Qi, X.-L., Hughes, T. L. & Zhang, S.-C. (2008), 'Topological field theory of time-reversal invariant insulators', *Phys. Rev. B* **78**, 195424.
URL: <https://link.aps.org/doi/10.1103/PhysRevB.78.195424>
- Read, N. & Green, D. (2000), 'Paired states of fermions in two-dimensions with breaking of parity and time reversal symmetries, and the fractional quantum Hall effect', *Phys. Rev. B* **61**, 10267.
- Read, N. & Rezayi, E. (1999), 'Beyond paired quantum Hall states: Parafermions and incompressible states in the first excited Landau level', *Phys. Rev. B* **59**, 8084–8092.
URL: <https://link.aps.org/doi/10.1103/PhysRevB.59.8084>
- Regan, R. C., Wiman, J. J. & Sauls, J. A. (2019), 'The Vortex Phase Diagram of Rotating Superfluid $^3\text{He-B}$ ', *Phys. Rev. B* **101**(2), 024517.
- Regan, R. C., Wiman, J. J. & Sauls, J. A. (2021), 'Half-quantum vortices in nematic and chiral phases of ^3He ', *Phys. Rev. B* **104**, 024513.
URL: <https://link.aps.org/doi/10.1103/PhysRevB.104.024513>
- Ricco, L. S., de Souza, M., Figueira, M. S., Shelykh, I. A. & Seridonio, A. C. (2019), 'Spin-dependent zero-bias peak in a hybrid nanowire-quantum dot system: Distinguishing isolated Majorana fermions from Andreev bound states', *Phys. Rev. B* **99**, 155159.
- Ricco, L. S., Sanches, J. E., Marques, Y., de Souza, M., Figueira, M. S., Shelykh, I. A. & Seridonio, A. C. (2021), 'Topological isoconductance

- signatures in Majorana nanowires', *Sci. Rep.* **11**, 17310.
 URL: <https://doi.org/10.1038/s41598-021-96415-3>
- Richardson, R. W. (1972), 'Ginzburg-landau theory of anisotropic superfluid neutron-star matter', *Phys. Rev. D* **5**, 1883–1896.
- Rysti, J., Mäkinen, J. T., Autti, S., Kamppinen, T., Volovik, G. E. & Eltsov, V. B. (2021), 'Suppressing the Kibble-Zurek Mechanism by a Symmetry-Violating Bias', *Phys. Rev. Lett.* **127**, 115702.
 URL: <https://link.aps.org/doi/10.1103/PhysRevLett.127.115702>
- Salomaa, M. M. & Volovik, G. E. (1985a), 'Half-quantum vortices in superfluid $^3\text{He}-a'$ ', *Phys. Rev. Lett.* **55**, 1184–1187.
 URL: <https://link.aps.org/doi/10.1103/PhysRevLett.55.1184>
- Salomaa, M. M. & Volovik, G. E. (1985b), 'Symmetry and structure of quantized vortices in superfluid ^3B ', *Phys. Rev. B* **31**, 203–227.
 URL: <https://link.aps.org/doi/10.1103/PhysRevB.31.203>
- Salomaa, M. M. & Volovik, G. E. (1986), 'Vortices with spontaneously broken axisymmetry in ^3B ', *Phys. Rev. Lett.* **56**(4), 363–366.
 URL: <https://link.aps.org/doi/10.1103/PhysRevLett.56.363>
- Salomaa, M. M. & Volovik, G. E. (1987), 'Quantized vortices in superfluid ^3He ', *Rev. Mod. Phys.* **59**, 533–613.
 URL: <https://link.aps.org/doi/10.1103/RevModPhys.59.533>
- Sanno, T., Yamada, M. G., Mizushima, T. & Fujimoto, S. (2022), 'Engineering Yang-Lee anyons via Majorana bound states', *Phys. Rev. B* **106**, 174517.
 URL: <https://link.aps.org/doi/10.1103/PhysRevB.106.174517>
- Sarma, S. D., Freedman, M. & Nayak, C. (2015), 'Majorana zero modes and topological quantum computation', *npj Quantum Inf.* **1**(1), 15001.
 URL: <http://www.nature.com/articles/npjqi20151>
- Sato, M. (2003), 'Non-Abelian statistics of axion strings', *Physics Letters B* **575**(1), 126–130.
- Sato, M. & Ando, Y. (2017), 'Topological superconductors: a review', *Reports on Progress in Physics* **80**(7), 076501.
 URL: <https://iopscience.iop.org/article/10.1088/1361-6633/aa6ac7>
- Sato, M. & Fujimoto, S. (2016), 'Majorana Fermions and Topology in Superconductors', *J. Phys. Soc. Jpn* **85**(7), 072001.
 URL: <http://journals.jps.jp/doi/10.7566/JPSJ.85.072001>
- Sato, M., Takahashi, Y. & Fujimoto, S. (2009), 'Non-Abelian Topological Order in s -Wave Superfluids of Ultracold Fermionic Atoms', *Phys. Rev. Lett.* **103**, 020401.
 URL: <https://link.aps.org/doi/10.1103/PhysRevLett.103.020401>
- Sato, M., Takahashi, Y. & Fujimoto, S. (2010), 'Non-Abelian topological orders and Majorana fermions in spin-singlet superconductors', *Phys. Rev. B* **82**, 134521.
 URL: <https://link.aps.org/doi/10.1103/PhysRevB.82.134521>
- Sato, M., Tanaka, Y., Yada, K. & Yokoyama, T. (2011), 'Topology of andreev bound states with flat dispersion', *Phys. Rev. B* **83**, 224511.
 URL: <https://link.aps.org/doi/10.1103/PhysRevB.83.224511>
- Sato, M., Yamakage, A. & Mizushima, T. (2014), 'Mirror Majorana zero modes in spinful superconductors/superfluids non-Abelian anyons in integer quantum vortices', *Physica E* **55**, 20.
- Sauls, J. A. (1980), Anisotropic superfluidity in neutron stars and strong coupling effect in superfluid ^3He , Ph.D Thesis, SUNY Stony Brook.
- Sauls, J. A. & Serene, J. W. (1978), ' $^3\text{P}_2$ pairing near the transition temperature in neutron-star matter', *Phys. Rev. D* **17**(6), 1524–1528.
- Sauls, J. A., Stein, D. L. & Serene, J. W. (1982), 'Magnetic vortices in a rotating $^3\text{P}_2$ neutron superfluid', *Phys. Rev. D* **25**, 967–975.
 URL: <https://link.aps.org/doi/10.1103/PhysRevD.25.967>
- Schnyder, A. P., Ryu, S., Furusaki, A. & Ludwig, A. W. W. (2008), 'Classification of topological insulators and superconductors in three spatial dimensions', *Phys. Rev. B* **78**(19), 195125.
- Schulenburg, J. & Flensberg, K. (2020), 'Absence of supercurrent sign reversal in a topological junction with a quantum dot', *Phys. Rev. B* **101**, 014512.
 URL: <https://link.aps.org/doi/10.1103/PhysRevB.101.014512>
- Schwarz, A. S. (1982), 'Field theories with no local conservation of the electric charge', *Nucl. Phys. B* **208**, 141–158.
- Sedrakian, A. & Clark, J. W. (2018), 'Superfluidity in nuclear systems and neutron stars'.
- Semenoff, G. W. & Zhou, F. (2007), 'Discrete symmetries and 1/3-quantum vortices in condensates of $F=2$ cold atoms', *Phys. Rev. Lett.* **98**, 100401.
- Shifman, M. & Yung, A. (2007), 'Supersymmetric Solitons and How They Help Us Understand Non-Abelian Gauge Theories', *Rev. Mod. Phys.* **79**, 1139.
- Shiozaki, K. & Sato, M. (2014), 'Topology of crystalline insulators and superconductors', *Phys. Rev. B* **90**, 165114.
 URL: <https://link.aps.org/doi/10.1103/PhysRevB.90.165114>
- Silaev, M. A. & Volovik, G. E. (2014), 'Andreev-Majorana bound states in superfluids', *J. Exp. Theor. Phys.* **119**(6), 1042–1057.
 URL: <http://link.springer.com/10.1134/S1063776114120097>
- Song, J. L., Semenoff, G. W. & Zhou, F. (2007), 'Quantum fluctuation-induced uniaxial and biaxial spin nematics', *Phys. Rev. Lett.* **98**, 160408.
- Sugeta, M., Mizushima, T. & Fujimoto, S. (2022), 'Enhanced 2π -periodic aharonov-bohm effect as a signature of majorana bound states probed by nonlocal measurements'.
 URL: <https://arxiv.org/abs/2205.07506>
- Takatsuka, T. (1972), 'Superfluid State in Neutron Star Matter. III Tensor Coupling Effect in 3P_2 Energy Gap', *Prog. Theor. Phys.* **47**(3), 1062–1064.
 URL: <http://dx.doi.org/10.1143/PTP.47.1062>
- Takatsuka, T. & Tamagaki, R. (1971), 'Superfluid State in Neutron Star Matter. II Properties of Anisotropic Energy Gap of 3P_2 Pairing', *Prog. Theor. Phys.* **46**(1), 114–134.
 URL: <http://dx.doi.org/10.1143/PTP.46.114>
- Tamagaki, R. (1970), 'Superfluid State in Neutron Star Matter. I Generalized Bogoliubov Transformation and Existence of 3P_2 Gap at High Density', *Prog. Theor. Phys.* **44**(4), 905–928.
 URL: <http://dx.doi.org/10.1143/PTP.44.905>
- Tanaka, Y. & Kashiwaya, S. (1995), 'Theory of tunneling spectroscopy of d -wave superconductors', *Phys. Rev. Lett.* **74**, 3451–3454.
 URL: <https://link.aps.org/doi/10.1103/PhysRevLett.74.3451>
- Tanaka, Y., Kashiwaya, S. & Yokoyama, T. (2005), 'Theory of enhanced proximity effect by midgap andreev resonant state in diffusive normal-metal/triplet superconductor junctions', *Phys. Rev. B* **71**, 094513.
 URL: <https://link.aps.org/doi/10.1103/PhysRevB.71.094513>
- Tanaka, Y., Nazarov, Y. V., Golubov, A. A. & Kashiwaya, S. (2004), 'Theory of charge transport in diffusive normal metal/unconventional singlet superconductor contacts', *Phys. Rev. B* **69**, 144519.
 URL: <https://link.aps.org/doi/10.1103/PhysRevB.69.144519>
- Tanaka, Y., Sanno, T., Mizushima, T. & Fujimoto, S. (2022), 'Manipulation of Majorana-Kramers qubit and its tolerance in time-reversal invariant topological superconductor', *Phys. Rev. B* **106**, 014522.
 URL: <https://link.aps.org/doi/10.1103/PhysRevB.106.014522>
- Teo, J. C. Y. & Kane, C. L. (2010a), 'Majorana fermions and non-abelian statistics in three dimensions', *Phys. Rev. Lett.* **104**, 046401.
 URL: <https://link.aps.org/doi/10.1103/PhysRevLett.104.046401>
- Teo, J. C. Y. & Kane, C. L. (2010b), 'Topological defects and gapless modes in insulators and superconductors', *Phys. Rev. B* **82**, 115120.
 URL: <https://link.aps.org/doi/10.1103/PhysRevB.82.115120>
- Terashima, H. & Ueda, M. (2005), 'Nonunitary quantum circuit', *Int. J. Quantum Inf.* **03**(04), 633.
 URL: <https://doi.org/10.1142/S0219749905001456>
- Thamm, M. & Rosenow, B. (2021), 'Transmission amplitude through a Coulomb blockaded Majorana wire', *Phys. Rev. Res.* **3**, 023221.
 URL: <https://link.aps.org/doi/10.1103/PhysRevResearch.3.023221>
- Thuneberg, E. V. (1986), 'Identification of vortices in superfluid ^3HeB ', *Phys. Rev. Lett.* **56**, 359–362.
 URL: <https://link.aps.org/doi/10.1103/PhysRevLett.56.359>
- Tojo, S., Hayashi, T., Tanabe, T., Hirano, T., Kawaguchi, Y., Saito, H. & Ueda, M. (2009), 'Spin-dependent inelastic collisions in spin-2 Bose-Einstein condensates', *Phys. Rev. A* **80**, 042704.
 URL: <https://link.aps.org/doi/10.1103/PhysRevA.80.042704>
- Trebst, S., Troyer, M., Wang, Z. & Ludwig, A. W. W. (2008), 'A Short Introduction to Fibonacci Anyon Models', *Progress of Theoretical Physics Supplement* **176**, 384–407.
 URL: <https://doi.org/10.1143/PTPS.176.384>
- Tsutsumi, Y., Ishikawa, M., Kawakami, T., Mizushima, T., Sato, M., Ichioka, M. & Machida, K. (2013), 'U $_3$ as a topological crystalline

- superconductor', *J. Phys. Soc. Jpn.* **82**(11), 113707.
URL: <http://dx.doi.org/10.7566/JPSJ.82.113707>
- Tsutsumi, Y., Kawakami, T., Shiozaki, K., Sato, M. & Machida, K. (2015), 'Symmetry-protected vortex bound state in superfluid $^3\text{He}-B$ phase', *Phys. Rev. B* **91**, 144504.
URL: <https://link.aps.org/doi/10.1103/PhysRevB.91.144504>
- Uchino, S., Kobayashi, M., Nitta, M. & Ueda, M. (2010), 'Quasi-Nambu-Goldstone Modes in Bose-Einstein Condensates', *Phys. Rev. Lett.* **105**, 230406.
URL: <https://link.aps.org/doi/10.1103/PhysRevLett.105.230406>
- Ueno, Y., Yamakage, A., Tanaka, Y. & Sato, M. (2013), 'Symmetry-Protected Majorana Fermions in Topological Crystalline Superconductors: Theory and Application to Sr_2RuO_4 ', *Phys. Rev. Lett.* **111**, 087002.
URL: <https://link.aps.org/doi/10.1103/PhysRevLett.111.087002>
- Usher, N., Hoban, M. J. & Browne, D. E. (2017), 'Nonunitary quantum computation in the ground space of local hamiltonians', *Phys. Rev. A* **96**, 032321.
URL: <https://link.aps.org/doi/10.1103/PhysRevA.96.032321>
- Vakaryuk, V. & Leggett, A. J. (2009), 'Spin polarization of half-quantum vortex in systems with equal spin pairing', *Phys. Rev. Lett.* **103**, 057003.
URL: <https://link.aps.org/doi/10.1103/PhysRevLett.103.057003>
- Valentini, M., Peñaranda, F., Hofmann, A., Brauns, M., Hauschild, R., Krogstrup, P., San-Jose, P., Prada, E., Aguado, R. & Katsaros, G. (2021), 'Nontopological zero-bias peaks in full-shell nanowires induced by flux-tunable Andreev states', *Science* **373**(6550), 82–88.
- Vinkler-Aviv, Y. & Rosch, A. (2018), 'Approximately Quantized Thermal Hall Effect of Chiral Liquids Coupled to Phonons', *Phys. Rev. X* **8**, 031032.
URL: <https://link.aps.org/doi/10.1103/PhysRevX.8.031032>
- Vollhardt, D. & Wölfle, P. (1990), *The Superfluid Phases of Helium 3*, Taylor & Francis, London.
URL: <https://books.google.co.jp/books?id=t0Rw75gMuwIC>
- Volovik, G. E. (1992), *Exotic Properties of Superfluid ^3He* , World Scientific, Singapore.
- Volovik, G. E. (1999), 'Fermion zero modes on vortices in chiral superconductors', *JETP Lett.* **70**, 609.
URL: <https://doi.org/10.1134/1.568223>
- Volovik, G. E. (2003), *The Universe in a Helium Droplet*, Clarendon, Oxford, U.K.
- Volovik, G. E. (2010), 'Topological superfluid $^3\text{He}-B$ in magnetic field and ising variable', *JETP Lett.* **91**(4), 201–205.
URL: <http://link.springer.com/10.1134/S0021364010040090>
- Volovik, G. E. & Mineev, V. P. (1977), 'Investigation of singularities in superfluid He_3 and in liquid crystals by the homotopic topology methods', *Zh. Eksp. Teor. Fiz* **72**, 2256. [Sov. Phys. JETP **45**, 1186 (1977)].
- Volovik, G. E. & Yakovenko, V. M. (1989), 'Fractional charge, spin and statistics of solitons in superfluid ^3He film', *J. Phys.: Condens. Matter* **1**(31), 5263.
URL: <https://dx.doi.org/10.1088/0953-8984/1/31/025>
- von Gehlen, G. (1991), 'Critical and off-critical conformal analysis of the Ising quantum chain in an imaginary field', *J. Phys. A: Math. Gen.* **24**(22), 5371.
URL: <https://dx.doi.org/10.1088/0305-4470/24/22/021>
- Vorontsov, A. B. & Sauls, J. A. (2003), 'Thermodynamic properties of thin films of superfluid $^3\text{He}-A$ ', *Phys. Rev. B* **68**, 064508.
URL: <https://link.aps.org/doi/10.1103/PhysRevB.68.064508>
- Wilczek, F. (1982), 'Quantum Mechanics of Fractional Spin Particles', *Phys. Rev. Lett.* **49**, 957–959.
- Wilczek, F. & Wu, Y.-S. (1990), 'Space-Time Approach To Holonomy Scattering', *Phys. Rev. Lett.* **65**, 13–16.
- Wölms, K., Stern, A. & Flensberg, K. (2014), 'Local adiabatic mixing of kramers pairs of majorana bound states', *Phys. Rev. Lett.* **113**, 246401.
URL: <https://link.aps.org/doi/10.1103/PhysRevLett.113.246401>
- Wölms, K., Stern, A. & Flensberg, K. (2016), 'Braiding properties of majorana kramers pairs', *Phys. Rev. B* **93**, 045417.
URL: <https://link.aps.org/doi/10.1103/PhysRevB.93.045417>
- Wong, C. L. M. & Law, K. T. (2012), 'Majorana Kramers doublets in $d_{x^2-y^2}$ -wave superconductors with Rashba spin-orbit coupling', *Phys. Rev. B* **86**, 184516.
URL: <https://link.aps.org/doi/10.1103/PhysRevB.86.184516>
- Wu, Y.-S. (1984), 'General theory for quantum statistics in two dimensions', *Phys. Rev. Lett.* **52**, 2103–2106.
URL: <https://link.aps.org/doi/10.1103/PhysRevLett.52.2103>
- Yamashita, M., Gouchi, J., Uwatoko, Y., Kurita, N. & Tanaka, H. (2020), 'Sample dependence of half-integer quantized thermal Hall effect in the Kitaev spin-liquid candidate $\alpha\text{-RuCl}_3$ ', *Phys. Rev. B* **102**, 220404.
- Yamashita, M., Izumina, K., Matsubara, A., Sasaki, Y., Ishikawa, O., Takagi, T., Kubota, M. & Mizusaki, T. (2008), 'Spin Wave and Vortex Excitations of Superfluid $^3\text{He}-A$ in Parallel-Plate Geometry', *Phys. Rev. Lett.* **101**, 025302.
URL: <https://link.aps.org/doi/10.1103/PhysRevLett.101.025302>
- Yasui, S., Chatterjee, C., Kobayashi, M. & Nitta, M. (2019), 'Reexamining Ginzburg-Landau theory for neutron 3P_2 superfluidity in neutron stars', *Phys. Rev. C* **100**(2), 025204.
- Yasui, S., Chatterjee, C. & Nitta, M. (2019), 'Phase structure of neutron 3P_2 superfluids in strong magnetic fields in neutron stars', *Phys. Rev. C* **99**(3), 035213.
- Yasui, S., Hirono, Y., Itakura, K. & Nitta, M. (2013), 'Non-Abelian statistics of vortices with non-Abelian Dirac fermions', *Phys. Rev. E* **87**(5), 052142.
- Yasui, S., Itakura, K. & Nitta, M. (2010), 'Fermion structure of non-Abelian vortices in high density QCD', *Phys. Rev. D* **81**, 105003.
- Yasui, S., Itakura, K. & Nitta, M. (2011), 'Majorana meets Coxeter: Non-Abelian Majorana Fermions and Non-Abelian Statistics', *Phys. Rev. B* **83**, 134518.
- Yasui, S., Itakura, K. & Nitta, M. (2012), 'Dirac returns: Non-abelian statistics of vortices with dirac fermions', *Nucl. Phys. B* **859**, 261.
- Yavilberg, K., Ginossar, E. & Grosfeld, E. (2019), 'Differentiating Majorana from Andreev bound states in a superconducting circuit', *Phys. Rev. B* **100**, 241408.
- Ye, M., Halász, G. B., Savary, L. & Balents, L. (2018), 'Quantization of the Thermal Hall Conductivity at Small Hall Angles', *Phys. Rev. Lett.* **121**, 147201.
URL: <https://link.aps.org/doi/10.1103/PhysRevLett.121.147201>
- Yokoi, T., Ma, S., Kasahara, Y., Kasahara, S., Shibauchi, T., Kurita, N., Tanaka, H., Nasu, J., Motome, Y., Hickey, C., Trebst, S. & Matsuda, Y. (2021), 'Half-integer quantized anomalous thermal Hall effect in the Kitaev material candidate $\alpha\text{-RuCl}_3$ ', *Science* **373**(6554), 568–572.
URL: <https://www.science.org/doi/abs/10.1126/science.aay5551>
- Yu, P., Chen, J., Gomanko, M., Badawy, G., Bakkars, E. P. A. M., Zuo, K., Mourik, V. & Frolov, S. M. (2021), 'Non-Majorana states yield nearly quantized conductance in proximatized nanowires', *Nat. Phys.* **17**, 482.
- Zhang, F., Kane, C. L. & Mele, E. J. (2013), 'Time-reversal-invariant topological superconductivity and majorana kramers pairs', *Phys. Rev. Lett.* **111**, 056402.
URL: <https://link.aps.org/doi/10.1103/PhysRevLett.111.056402>
- Zhang, G. & Spånslätt, C. (2020), 'Distinguishing between topological and quasi Majorana zero modes with a dissipative resonant level', *Phys. Rev. B* **102**, 045111.
URL: <https://link.aps.org/doi/10.1103/PhysRevB.102.045111>
- Zhang, H., de Moor, M. W. A., Bommer, J. D. S., Xu, D., Wang, G., van Loo, N., Liu, C.-X., Gazibegovic, S., Logan, J. A., Car, D., het Veld, R. L. M. O., van Veldhoven, P. J., Koelling, S., Verheijen, M. A., Pendharkar, M., Pennachio, D. J., Shojaei, B., Lee, J. S., Palmstrøm, C. J., Bakkars, E. P. A. M., Das Sarma, S. & Kouwenhoven, L. P. (2021), 'Large zero-bias peaks in insb-al hybrid semiconductor-superconductor nanowire devices', *arXiv:2101.11456*.
- Zhang, P., Yaji, K., Hashimoto, T., Ota, Y., Kondo, T., Okazaki, K., Wang, Z., Wen, J., Gu, G. D., Ding, H. & Shin, S. (2018), 'Observation of topological superconductivity on the surface of an iron-based superconductor', *Science* **360**(6385), 182.
URL: <https://www.science.org/doi/abs/10.1126/science.aan4596>
- Zheng, C. (2021), 'Universal quantum simulation of single-qubit nonunitary operators using duality quantum algorithm', *Sci. Rep.* **2021**, 3960.
URL: <https://doi.org/10.1038/s41598-021-83521-5>
- Zhu, S., Kong, L., Cao, L., Chen, H., Papaj, M., Du, S., Xing, Y., Liu, W., Wang, D., Shen, C., Yang, F., Schneeloch, J., Zhong, R., Gu, G., Fu,

L., Zhang, Y.-Y., Ding, H. & Gao, H.-J. (2020), 'Nearly quantized conductance plateau of vortex zero mode in an iron-based superconductor', *Science* **367**(6474), 189.

URL: <https://www.science.org/doi/abs/10.1126/science.aax0274>